XYLAN BASED COMPOSITE NANOPARTICLES AND BIOFOAMS FOR DRUG DELIVERY AND TISSUE ENGINEERING

A Thesis Progress Submitted to
the Graduate School of Engineering and Sciences of
İzmir Institute of Technology
in Partial Fulfillment of the Requirements for the Degree of

DOCTOR OF PHILOSOPHY

in Bioengineering

by
Nüket ZEYBEK

April 2022
İZMİR

ACKNOWLEDGEMENTS

Firstly, I would like to express my sincere gratitude to my supervisor, Assist. Prof. Dr. Ali Oğuz BÜYÜKKİLECİ for his expertise, guidance, encouragement, motivation, and support throughout my thesis. I have benefited greatly from his direction and valuable guidance in this study and I am deeply grateful for his support, caring, and confidence during my graduate education.

I would like to thank my deepest gratitude to Prof. Dr. Hürriyet POLAT, Prof. Dr. Mehmet POLAT, and Assist. Prof. Dr. Şükrü GÜLEÇ for their support, concern, and suggestions during this research, and I thank them for believing and supporting. Also, I would like to thank my thesis committee and jury members Prof. Dr. Gülşah ŞANLI MOHAMED, Assist. Prof. Dr. Yavuz OKTAY, Assist. Prof. Dr. Şükrü GÜLEÇ, Prof Dr. Hale AKPINAR, and Prof. Dr. Kadir Mehmet YURDAKOÇ for their valuable contributions.

I would like to appreciate the Integrated Research Centers of İzmir Institute of Technology for providing laboratory facilities and I am grateful to Yekta GÜNAY OĞUZ and Dr. Afife GÜLEÇ for their friendship and technical assistance.

I would like to thank my labmates and all friends, especially, Gülperi KARANFİL, Elif ÇAVDAROĞLU, Cansu ÖZEL, Pelin KAVUR, and Duygu BÜYÜKTAŞ for their support, contributions, and friendship.

Lastly, I would like to thank my deepest gratitude to my family, my parents İlknur and Mahmut POLAT for their endless support, love, and encouragement, in all conditions. Also, I would like to express sincere thanks to my spouse Sercan ZEYBEK who motivated and supported me all the time during my academic career.

ABSTRACT

XYLAN BASED COMPOSITE NANOPARTICLES AND BIOFOAMS FOR DRUG DELIVERY AND TISSUE ENGINEERING

Xylan is a hemicellulosic polysaccharide, which can be obtained from forest and agricultural wastes. Similar to some other polysaccharides, xylan can find application in drug delivery and tissue engineering due to its availability, structural diversity, biocompatibility, biodegradability, and low cost.

In the first part of the study, xylan-based nanoparticles were developed for colon-targeted oral drug delivery. Xylan is resistant to digestion and absorption in the upper GIT and is degraded by hydrolysis of glycosidic bonds by the colon microbiota; this makes it prominent in targeted drug delivery to the colon. The drug carrier was combined with a polymeric micelles system to increase the bioavailability of hydrophobic bioactive molecules in the colon targeting. The model hydrophobic molecule, curcumin, was loaded in the core of the triblock copolymer P-123 micelles by the thin-film hydration method. Curcumin-loaded micelles were coated with xylan supported by chitosan and tripolyphosphate using the ionic gelation method. In another approach, xylan was also used to coat curcumin-loaded mesoporous silica nanoparticles to prevent premature drug release in the upper GIT in colon-targeted delivery. In both approaches, the drug-containing structures were maintained up to the colon and the drug was released upon bacterial hydrolysis of xylan.

In the second part, xylan-based biofoams were synthesized by the oil in water emulsion templated method. Several physicochemical and mechanical tests have shown that at the optimal conditions foams with promising properties could be synthesized. Besides, to develop a more effective tissue therapy by utilizing the synergistic effect of the drug delivery and scaffold system, a model drug was successfully loaded into biofoams.

This study showed that xylan is a promising feedstock for the synthesis of stable and biocompatible materials in biomedical applications, which reveals its potential capability in drug carriers and scaffolds.

ÖZET

İLAÇ TAŞIMA VE DOKU MÜHENDİSLİĞİ İÇİN KSİLAN BAZLI KOMPOZİT NANOPARTİKÜLLER VE BİYOKÖPÜKLER

Ksilan, orman ve tarım atıklarından elde edilebilen hemiselülozik bir polisakkarittir. Diğer kimi polisakkaritlere benzer şekilde, ksilan bulunabilirliği, yapısal çeşitliliği, biyouyumluluğu, biyolojik olarak parçalanabilirliği ve düşük maliyeti nedeniyle ilaç dağıtımı ve doku mühendisliği uygulamalarında kendine yer bulabilir.

Çalışmanın ilk bölümünde, kolon hedefli oral ilaç dağıtımı için ksilan bazlı nanopartiküller geliştirildi. Ksilan, üst gastrointestinal sistemde sindirime ve absorpsiyona dirençlidir ve kolon mikrobiyotası tarafından glikozidik bağların hidrolizi ile parçalanır; bu da onun kolona hedeflenen ilaç dağıtımında öne çıkmasını sağlar. İlaç taşıyıcı, hidrofobik biyoaktif moleküllerinin kolon hedeflemede biyoyararlanımını arttırmak için, polimerik misel sistemi ile birleştirildi. Model hidrofobik molekül kurkumin, ince film hidrasyon yöntemiyle pluronik triblok kopolimer P-123 misellerinin çekirdeğine yüklendi. Kurkumin yüklü miseller, iyonik jelasyon yöntemi kullanılarak kitosan ve sodyumtripolifosfat destekli ksilan ile kaplandı. Diğer bir yaklaşımda ise ksilan, kolon hedefli taşıyıcılarda erken ilaç salımını önlemek için kurkumin yüklü mezogözenekli silika nanopartiküllerini kaplamak için kullanıldı. Her iki yaklaşımda da, ilaç içeren yapılar kolona kadar korunmuş ve ilaç, ksilanın bakteriyel hidrolizi sonucu salınmıştır.

İkinci bölümde, su içinde yağ emülsiyonu şablon yöntemi ile ksilan bazlı biyoköpükler sentezlendi. Çeşitli fizikokimyasal ve mekanik testler, optimal koşullarda umut verici özelliklere sahip köpüklerin sentezlenebileceğini göstermiştir. Ayrıca ilaç taşıma ve iskele sistemlerinin sinerjik etkisinden yararlanılarak daha etkili bir doku tedavisi geliştirmek için bir model ilaç başarıyla biyoköpüklere yüklendi.

Bu çalışma, ksilanın, ilaç taşıyıcıları ve yapı iskelelerindeki potansiyel kapasitesini ortaya çıkaran, biyomedial uygulamalarda kararlı ve biyouyumlu materyallerin sentezi için umut verici bir hammadde olduğunu göstermiştir.

TABLE OF CONTENTS

LIST OF FIGURES

Figure **Page**

Figure **Page**

LIST OF TABLE

CHAPTER 1

INTRODUCTION

Polysaccharides have remarkable physicochemical and physiological properties such as biocompatibility, biodegradability, and low immunogenicity, which are important for biomedical applications (Prasher et al. 2021). Natural polysaccharides have a considerable impact due to their structural diversity, wide availability, low cost, and ease of modification chemically and biochemically (Metaxa et al. 2021; Singh et al. 2020). Therefore, extensive scientific efforts have been given in recent years to develop polysaccharide-based biomaterials for tissue engineering and drug delivery systems. Natural polysaccharides have been combined with other organic and inorganic materials and synthetic polymers to enhance their functions (Hu, Li, and Xu 2017).

Drug delivery is the method or process of administering a pharmaceutical compound to achieve a therapeutic effect. The poor solubility, tissue damage on extravasation, rapid breakdown, poor biodistribution, and lack of selectivity for target tissues are some limitations of conventional (free) drugs or bioactive molecules. Such problems arising from free drug use can be overcome and improved using drug delivery systems (Tiwari et al. 2012; Inamuddin and Mohammad 2018). Colon-targeted drug delivery allows the topical treatment of colon diseases such as inflammatory bowel disease, ulcerative colitis, colon cancer, and Crohn's disease. In addition, the long residence time, low hydrolytic enzyme activity, and near-neutral pH of the colon provide important opportunities for systemic absorption of drugs (Sinha and Kumria 2001; Shimono et al. 2002). Traditional systems are hampered by various factors, such as reduced control over the rate of drug releases (eg. a burst release of drugs), failure of targeted delivery, or potential drug degradation in the upper gastrointestinal tract. In this context, various smart delivery approaches and strategies for colon-targeted drug delivery systems have been developed dependent on size, surface charge, pH, colonic microbiota, time, and redox (Sinha and Kumria 2001; Jeong et al. 2001, Hua et al. 2015).

Tissue engineering is an alternative and promising approach to developing biological substitutions that restore, maintain, or improve tissue function so that problems

like poor biocompatibility, low biological functionality, and immune rejection can be overcome. There are three main tools of tissue engineering: cell, scaffold, and cell signaling. To replace or repair damaged tissues, it is necessary to create an environment that supports the ability of cells to integrate, differentiate and proliferate (Jagur-Grodzinski 2009; Eltom, Zhong, and Muhammad 2019). Growth factors and extracellular matrix (ECM) components are used to induce the proliferation and differentiation of cells (Celikkin et al. 2017). The creation of the environment to hold this structure together is usually accomplished by the implantation of three-dimensional (3D) scaffolds. The scaffold provides a framework and assists in the proliferation, differentiation, and migration of the cell (Briquez and Hubbell 2020; Howard et al. 2008). Regardless of the type of tissue, several important matters like biocompatibility, biodegradability, proper mechanical properties, architecture, and physicochemical properties of scaffold surfaces should be considered to design and produce scaffolds.

Xylan is a promising natural hemicellulosic source for tissue engineering and drug delivery system. It is an abundant and cost-effective natural polysaccharide and is available in agricultural and forestry wastes. Although xylan structure varies according to the source and extraction method, it mainly comprises xylose units linked by β-(1→4) glycosidic linkage. Besides the great advantage of being a renewable material, xylan has several properties that make it a favorable material for pharmaceutical and biomedical applications. The different forms of xylan such as films, hydrogels, and particles have been used in biomedical applications (Melo-Silveira et al. 2012; Silva et al. 2013; Gao et al. 2016). Chitosan is one of the most widely used natural polymers in biomedical applications. It is composed of β-(1→4) linked linear copolymer, containing N-acetyl-D-glucosamine and D-glucosamine units with one amino (NH_2) group and two hydroxyls (OH) groups unit. Chitosan is obtained by deacetylation of chitin which is available in the shells of crustaceans, insects, and fungi. It displays attractive properties for drug delivery such as bioactivity, biodegradability, biocompatibility, toxicity, and antimicrobial properties (Sanyakamdhorn et al. 2013; Tang et al. 2014).

Natural polysaccharides are extensively used in biomedical applications for the development of functional materials due to their distinctive properties as described above. The ability of xylan to remain stable up to the colon and to be hydrolyzed by colon bacteria makes it advantageous and prominent compared to many other natural polymers in colon-targeted drug delivery systems. The objective of this thesis study was to develop a colon-targeted drug delivery system by utilizing xylan hydrolysis by colon bacteria as

a triggering mechanism. Besides, the stability of xylan in the upper GIT enables it to deliver drugs safely to the colon. To increase the bioavailability of hydrophobic molecules in the colon targeting, the drug carrier was combined with a polymeric micelles system. The model bioactive molecule, curcumin, was encapsulated into the core of P-123 micelles. These micelles could be improved the bioavailability of curcumin and serve as soft templates for subsequent particle formation. Since the micelles can easily be affected by the environmental conditions, they were coated with xylan to form shell and protect them until the colon. Additionally, silica nanoparticles were synthesized and coated with xylan to prevent premature drug release from the nanoparticles in the upper GIT. An additional application of natural polymers is their use as scaffold materials in tissue engineering. The second aim of this study was to investigate the suitability of a xylan-based biofoam as a scaffold by testing its physicochemical and mechanical properties and stability. Curcumin was used as a model hydrophobic bioactive molecule for the examination of the efficiency of drug loading and release.

This doctoral thesis study is designated to comprise of following four parts: 1) Curcumin loaded P-123 micelles to increase the bioavailability of a hydrophobic drug and serve as soft templates for subsequent particle formation; 2) Xylan/chitosan composite nanoparticles with a micellar core for microbially activated colon targeted delivery of curcumin loaded P-123 micelles; 3) Xylan/chitosan coated mesoporous silica nanoparticles for the efficient colon-targeted and microbially activated delivery of curcumin loaded silica nanoparticles; and 4) Curcumin loaded xylan based biofoams for tissue engineering applications.

CHAPTER 2

BACKGROUND INFORMATION

2.1. Drug Delivery

Drug delivery, as a general definition, is the method or process of administering a pharmaceutical compound to achieve a therapeutic effect. Free drugs and active ingredients have some unfavorable pharmacological properties such as poor solubility, tissue damage on extravasation, the rapid breakdown of the drug in vivo, poor biodistribution, and lack of selectivity for target tissues. Such problems arising from free drug use can be overcome and improved through the use of drug delivery systems (Tiwari et al. 2012; Inamuddin and Mohammad 2018). For example, hydrophobic drugs are difficult to obtain in a suitable pharmaceutical format because they tend to precipitate in aqueous media. Free drugs can lose activity at physiological pH and are cleared very quickly by the kidneys. Inadvertent extravasation of cytotoxic drugs leads to tissue damage and necrosis. In addition, drugs with a widespread distribution in the body can affect normal tissues, and cause dose limitations in practice. In this case, low drug concentrations in target tissues result in suboptimal therapeutic effects, making treatment difficult (Allen and Cullis 2004; Gundloori, Singam and Killi 2019).

There are alternative routes of administration of the drug to reach the target area most comfortably and efficiently, and in this way, a treatment opportunity can be offered according to the therapeutic area and the disease state. These are intranasal, buccal/sublingual, pulmonary, oral, and transdermal routes of administration. The drug can be delivered to the target by applying the best procedure and route, taking into account the advantages and limitations. For example, although, the transdermal route provides easy access, convenience to dose, and a large surface area for treatment; it has some limitations such as low dose delivery, and a tough barrier to penetrate. For the intranasal administration; highly permeable epithelia and well-perfused mucosa properties are advantages but also rapid mucociliary clearance and taste/sensory liability are disadvantages (Mathias and Hussain 2010). Each route of administration can be selected

according to the therapeutic area target and disease state, providing a synergistic effect. For example, there are approved examples of drugs using this synergistic effect: Intranasal administration of super-potent peptides enables therapeutic blood levels not achieved with oral administration; non-invasive insulin products improve patient compliance by reducing daily injections with inhalation administration; transdermal products eliminate gastrointestinal related adverse reactions.

2.2 Oral Drug Delivery and Colon Targeting

Oral delivery is the most widely used route for both systemic drug delivery in the gastrointestinal tract (GIT) and the treatment of local gastrointestinal diseases. It is the most convenient route for patients due to its non-invasiveness, ease of use, and self-administration. By oral administration, targeting both the upper parts of the GIT (mouth, pharynx, esophagus, stomach, first part of the small intestine) and the lower GIT (end of the small intestine and the large intestine) can be performed (Reinus and Simon 2014; Hua 2020).

There are three general main objectives for the oral route of gastrointestinal drug delivery: i) to treat a local gastrointestinal disease. In such a situation, the drug is usually not absorbed systemically or is poorly absorbed. Usually, the drug is taken by the mucous membrane; ii) for the drug to be absorbed by the GIT and pass into the systemic circulation; iii) to increase the dissolution rate of poorly soluble drugs. To meet one of these goals or sufficient drug absorption, formulations must be designed considering various factors in the GIT. These are the surface area and blood flow of the absorption region, the physicochemical properties, and the concentration of the drug (Martinez and Amidon 2002; Brunton, Knollmann, and Dandan 2018).

Recently, there is great interest in the development of new systems for the treatment of local colonic diseases by stably delivering therapeutic agents to the colon by using the oral route. In the treatment of local diseases of the colon, drug targeting can prevent possible systemic side effects and facilitate treatment by reducing the dose to be administered, as well as providing targeted therapy. However, despite the clear therapeutic advantages of colon-targeted drug delivery by the oral route, the GIT is complex and can be encountered with several physiological barriers that affect drug delivery, such as poor drug solubility, low metabolic stability, and low permeability across the mucosa. Therefore, the effects of GIT on the drug delivery system should be

considered during formulation design. Transition time, pH alteration, different enzymes, and giant microflora variation can be given as examples of these effects. Factors to be considered during the design of the drug delivery system are described in more detail.

i) Gastrointestinal Transit Time: A drug carrier that has taken by swallowing first encounters the stomach, and the time it takes to leave the stomach is highly variable. The gastric transit time can vary from 0 to 2 hours, depending on many physiological factors of the host (Kagan and Hoffman 2008). In general, the transit time in the small intestine is between about 2 and 4 h (Reinus and Simon 2014), while the colonic transit time has a highly variable range from 6 to 70 h (Rao 2004; Hua 2020).

ii) Gastrointestinal pH: While the lowest pH level in humans is 1.5-2.0 in the stomach (in the fasted state), the pH rises rapidly when it passes into the small intestine and reaches the highest pH level in the terminal ileum (pH 7.4). The pH drops to 6.4 when entering the colon. The pH is 6.6 in the middle colon and 7.0 in the left column. The decrease in pH upon entry to the colon is due to the production of short-chain fatty acids from bacterial fermentation of polysaccharides (Bratten and Jones 2006; Nugent, Rampton, and Evans 2001; Ibekwe et al. 2008)

iii) Gastrointestinal Mucus: Mucus consisting of water and mucin protein molecules coated with proteoglycans facilitates the passage of substances and provides mechanical protection to the epithelium. The small intestine has one type of mucus that is unbound and loose, while the stomach and colon have thicker, bilayered mucus. Mucus which is secreted by goblet cells has a negative charge due to proteoglycans (Homayun, Lin and Choi 2019; Johansson, Sjövall and Hansson 2013). Several studies have revealed that the cationic surface of drug carrier formulations has a great influence on its therapeutic efficacy. As the interaction between the cationic nanocarrier and the negatively charged intestinal mucosa promotes better contact with the mucosal surface, makes it a promising strategy for adhesion, cellular uptake, or drug release and an advantage for GIT targeting (Coco et al. 2013; Han, Shin and Ha 2012; Gradauer et al. 2013).

iv) Gastrointestinal Enzymes and Microbiome: The drug delivery systems can be enzymatically degraded in the stomach and small intestine, which is the site of action of the main enzymes involved in the digestion of food and disintegrated in the large intestine by microbial fermentation. Although these enzymes affect the stability of the drug delivery system, it can be turned into an advantage when designing the delivery system. The majority of the gut microbiome resides in the anaerobic colon and they ferment

indigestible polysaccharides. Non-digestible polysaccharides have been used as a coating material for drugs. Firmicutes, Bacteroidetes, Proteobacteria, Actinobacteria, and Fusobacteria constitute the majority of the colonic flora. In addition, although the microbiota is present in the small intestine compared to the colon, its density is much lower. They are species of *Clostridium*, *Escherichia*, *Turicibacter, Streptococcus*, and *Veillonella*.

There is great interest in the development of new systems for the delivery of active agents including drugs or supplements to the "colon" (large intestine) via the GIT. Because the colon provides an important opportunity for the absorption of bioactive molecules, with a long residence time (approximately 2-3 days), low hydrolytic enzyme activity, near-neutral pH, facilitating the treatment of local colon diseases, and much greater responsiveness to absorption enhancers (Sinha and Kumria 2001; Shimono et al. 2002). However, traditional delivery systems are hampered by various factors, such as reduced control over the rate of drug releases (eg. a burst release of drugs), failure of targeted delivery, or potential drug degradation in the upper GIT. In this context, various smart delivery approaches and strategies for colon-targeted drug delivery systems have been developed dependent on size, surface charge, PEGylation, pH, colonic microbiota, time, and redox (Sinha and Kumria 2001; Jeong et al. 2001, Hua et al. 2015).

For example, in the colon targeted pH-dependent systems, the coating polymer is resistant to low pH, whereas it dissolves at neutral or slightly alkaline pH in the distal part of the small intestine or colon. However, the formulation may begin to dissolve in the distal small intestine, or rapid transit through the ascending colon resulting in reduced site-specificity. Also, it has proven difficult as the pH of the GIT varies considerably within and between individuals. Despite this variability, it is commercially available as pH-sensitive oral tablets for colonic administration (McConnell, Short and Basit 2008; Brunton, Knollmann and Dandan 2018). The time-dependent delivery systems typically rely on relatively constant transit time through the small intestine for targeted drug release to the colon. This system assumes that it will spend about 6 h in the stomach and the small intestine in the fasting state, and the rate of drug release can be controlled by the reaction of the coating or matrix in contact with aqueous liquids. However, gastric emptying time is physiologically highly variable and differences can be observed with diet. Peristaltic movements or contractions in the stomach can change the transit time. Moreover, in diseases of the colon like diarrhea, ulcerative colitis, accelerated transit has been observed in some segments of the colon. For this reason, the drug has difficulty in reaching the

target region because the time of arrival in the colon cannot be predicted precisely (Caraballo 2010; Reinus and Simon 2014; Gazzaniga et al. 2006). Prodrugs are pharmacologically inactive derivatives of a parent molecule. The release of active drug moiety requires spontaneous or enzymatic transformation within the body. To optimize colon-specific drug delivery, natural polymers or azo conjugates that are stable in the upper GIT are used and the drug is released after hydrolysis of conjugates by enzymes in the colon. Although prodrugs provide site-specific distribution, they are new chemical entities and required detailed toxicological studies. The versatility of prodrugs is limited because their formation depends on functional groups on the drug moiety. Therefore, a drug specific carrier should be developed (Chourasia and Jain 2004; Hua 2020). The pressure-controlled system is based on the realization of drug release when the colon encounters higher pressures (luminal pressure) than the small intestine as a result of peristalsis (Philip and Philip 2010).

Colonic microbiota-dependent systems rely on the degradation of colon-specific polysaccharides by the microbiome residing in the colon. The colon has a huge variety of anaerobic bacteria which obtain their energy by fermenting the undigestible polysaccharides. *Bacteroides, Eubacteria, Clostridia, Enterococci,* and *Enterobacteria* are some examples of colon-specific species. Numerous enzymes such as glucuronidase, xylosidase, nitroreductase, and azoreductase are produced by them to ferment polysaccharides. As drug transported by undigested polysaccharides is digested only by these enzymes localized in the colon, this approach appears to be more promising for colon-specific delivery. Polymers can be chemically or physically modified or cross-linked, thereby, dose-controlled drug release can be achieved by varying the degree of enzymatic degradation. Examples of natural polysaccharides used for colon targeting include pectin, starch, alginate, guar gums, amylose, chitosan, dextran, chondroitin sulfate, inulin, xylan, and galactomannan (Awad et al. 2022). For example, pectin-hydroxypropyl methylcellulose tablets have been produced for successfully passing the proximal GIT and degrading in the colon (Hodges et al. 2009). Also, it has been produced as fluorouracil microspheres coated with Eudragit S100 (Paharia et al. 2007) and a microporous bilayer osmotic tablet with cellulose acetate and a layer of Eudragit L100 (Chaudhary et al. 2011). Another example guar gum is stable in the stomach and small intestine owing to its high viscosity; thence it has been studied for colon-specific drug delivery, both as a matrix polymer (Krishnaiah et al. 2003; Al-Saidan et al. 2005) and as a coating (Krishnaiah, Indira Muzib, and Bhaskar 2003). Resistant starch is not degraded

in the small intestine by pancreatic enzymes, making it an energy source for colonic bacteria (Basit, Short and McConnell 2009). Because amylose swells in the presence of water, it is often combined with a water-insoluble polymer such as ethylcellulose to prevent premature drug release (Tuleu et al. 2002; McConnell et al. 2006). McConnell, Short and Basit (2008) compared two colonic drug delivery concepts, a pH-responsive system, and a bacterially-triggered approach to establish which physiological factor is the more reliable trigger in-vivo. They prepared the amylose/ethylcellulose coating and the pH-sensitive Eudragit S coating for colonic drug delivery. The pH-dependent system showed premature drug release in the small intestine, while the amylose/ethylcellulose coating only released the drug in the colon. Both systems had similar bioavailability, but the Eudragit S coating showed much higher variability, with no drug release in one patient. They concluded that the bacterially-triggered system has more reproducibly and reliably, and provides superior colonic targeting.

2.3. Tissue Engineering

When tissues or organs have been seriously diseased or lost as a result of cancer, trauma, etc; artificial organs/tissues or organ transplantation are preferred to reconstruct damaged structures. Transplantation can be performed in the same patient from one area to another (an autograft) or from one person to another (allograft) (Ikada 2006). Although artificial organs/tissues and transplantation treatments are life-saving, it has important difficulties as can be listed below:

- Anatomical limitations in autografts
- Shortage of organ donation because of the high difference between the number of patients requesting transplantation and the offered organs
- Risks of rejection by the patient's immune system
- Donor site morbidity
- Carrying infections from the donor.

Tissue engineering is an alternative and promising approach to overcome these problems. It is the use of a combination of cells, engineering, materials, methods, and suitable biochemical and physicochemical factors to improve or replace biological tissues (Atala 2004). Tissue engineering involves the use of a scaffold for the formation of new viable tissue for a medical purpose and aims to develop biological substitutions that restore, maintain, or improve the function of tissue; so that problems like poor

biocompatibility, low biological functionality, and immune rejection can be overcome. The cell, scaffold and cell signaling are three main tools of tissue engineering (Figure 2.1).

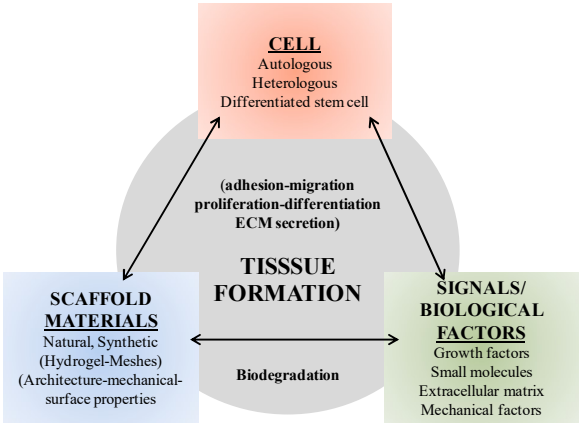

Figure 2.1. Three tools of tissue engineering and their relations.

Cells, primary constituents of biological tissues, can be considered as building units in tissue engineering (Briquez and Hubbell 2020). The source of cells can be classified as autologous (patient's own), allogenic (human other than the patient), and xenogenic (animal origin). Autologous cells are the most suitable for tissue engineering applications. Allogenic and xenogenic cells can cause immunogenic reactions, so immunosuppressive side therapy is needed. In addition, xenogeneic cells might have a risk of containing some infections (Ikada 2006; Fishman, Scobie and Takeuchi 2012). To replace or repair damaged/failed tissues with viable ones, it is necessary to create an environment that supports the ability of cells to integrate, differentiate and proliferate (Jagur-Grodzinski 2009; Eltom, Zhong and Muhammad 2019). Growth factors and extracellular matrix (ECM) components are used to induce the proliferation and differentiation of cells (Celikkin et al. 2017). The creation of the environment to hold this structure together is usually accomplished by the implantation of three-dimensional (3D) scaffolds. The scaffold is seeded with suitable living cells that secrete its extracellular matrix. The scaffold provides a framework and assists in the proliferation, differentiation, and migration of the cell (Briquez and Hubbell 2020; Howard et al. 2008). Regardless of the type of tissue, there are several important matters to consider to design and produce

scaffolds for tissue engineering applications. These are biocompatibility, biodegradability, proper mechanical properties, scaffold architecture, and physicochemical properties of scaffold surfaces:

i) Biocompatibility: The first criterion of any scaffold that will be used for tissue engineering applications is biocompatibility. This phenomenon is related to the interaction between cells and template material, and the need to develop the right micro-environment for the cells to create new tissue. Thus, cells can adhere, multiply, migrate and function normally (O'Brien 2011; Naahidi et al. 2017; Kohane and Langer 2010).

ii) Biodegradability: Implanted scaffolds are not designed as permanent implants. The body's cells are aimed to replace this structure over time. As the cells produce their extracellular matrix, the scaffold is biodegraded. By-products formed as a result of biodegradation should not be toxic to the body and should not harm other organs.

iii) Proper Mechanical properties: A scaffold must have mechanical properties suitable for the anatomical region where it will be implanted. In other words, it should mimic the structure of native parts of the body. The implanted scaffold must have enough mechanical integrity to function until the remodeling process is complete. Hence knowing the mechanical behaviour of the scaffold is important such as Young's modulus, compressive/tensile strength, breaking strain (elongation at break), etc. Even though many materials are produced with good mechanical properties, the composition and structural properties of scaffolds including porosity and pore size, also play fundamental roles in the success of the tissue engineering structure. In some of the studies conducted in this matter, it has been observed that in-vivo implanted materials fail when there is an absence of balance of mechanical properties and porosity of scaffolds (Hutmacher 2000; O'Brien 2011).

iv) Scaffold Architecture: The architecture of the scaffolds used for tissue engineering is critical. Desired features can be listed under three main captions: i) Pore size (average diameter of pores), ii) porosity (porosity volume/total volume), and iii) interconnectivity of pores (Declercq et al. 2014). The scaffolds should have an interconnected pore structure and high porosity to diffuse of sufficient nutrient and oxygen for cells, and removal of waste products (Causa, Netti and Ambrosio 2007). The porous and interconnected networks that necessary for tissue vascularisation and new tissue formation, are important in determining a cellular response (Hollister 2005; Loh and Choong 2013; Kang and Chang 2018). In addition, surface topography design plays an active role in cell and tissue organization, along with scaffold-cell interactions. It

affects the regulation of cell behaviors like adhesion, migration, proliferation, differentiation, and ECM secretion. Some researchers suggest that surface topography offers a new strategy to mimic the environment to be applied to the cells as much as possible. In this way, more effective results can be obtained by improving the interaction of cells with the microenvironment (Mansouri and SamiraBagheri 2016; Xiong et al. 2019).

v) Physico-chemical properties of scaffold surfaces: The contact of cells and ECM molecules with molecules on the physico-chemical properties of scaffold surfaces are critical for the applicability of scaffolds. As mentioned above, the scaffolding surface must support the functions of cells such as adhesion and migration. Unsuitable surface properties may prevent cell proliferation and cause the structure to fail (Bartis and Pongracz 2011; Katti, Vasita and Shanmugam 2008).

Bioactive Molecules Loaded Scaffolds:

Drug loaded foams, sheets or films were also produced as scaffold materials for different purposes like antimicrobial, antifungal, anti-inflammatory, and tissue repair. It is very exciting to be able to develop a more effective technique for tissue therapy by taking advantage of the synergistic effect of the drug delivery and scaffold system.

Bioactive molecules can be loaded on polymeric scaffolds in different ways. The appropriate method should be selected or designed according to the structure of the scaffold and the active molecules, the desired release rate, and the environment to be applied. Blend/soak loading; site-specific binding; drug-polymer conjugation; pre-loading in nono/microparticles are some methods to loading of bioactive molecules into scaffolds (Calori et al. 2020; Yang et al. 2020). In blend loading, which is one of the most common methods, polymers and drugs are prepared by blending before fabrication. Soak loading consists of two stages; the scaffold is prefabricated and then immersed in a solution containing the drug (Sriamornsak et al. 2010; Zhu and Mao 2019). Site-specific binding loading can be used to overcome unfavourable solvent or drug-polymer interaction problems. More specific and stronger drug-polymer interaction can be achieved by covalent binding of active molecules to the polymer or site-specific binding of active molecules via surface functional groups. In the encapsulation loading method, firstly the drug is encapsulated in nano- or micro-sized particles and then incorporated into the scaffold material. In this way, while undesired drug and polymer interactions can be prevented, more suitable molecule-polymer interactions can be achieved by changing

the particle surfaces according to the application (Calori et al. 2020; Polat and Polat 2020).

Controlled bioactive molecule release from scaffolds, the purpose of which is to provide effective tissue therapy comes into prominence with its advantages in many aspects. The release of active ingredient from scaffolds is dependent on a variety of factors, including the environment and the structural features of the scaffold. In order to modulate this system in accordance with the purpose, it is necessary to determine and evaluate these factors well. The release of active materials can be controlled by the structural features of the scaffolds (pore sizes and interconnectivity), the chemical structures of drugs, physicochemical properties of scaffolds, active material-scaffolds interaction, and environment.

When producing drug-loaded scaffolds, the structure should be designed considering the release kinetics, otherwise the drug release may remain at low levels. For example, drug molecules in the core of non/difficultly degradable scaffold or scaffolds with inadequate pores will be much more difficult to release. This problem in porous structures can also occur in the mesh size of hydrogels. The mesh size, which is critical in the release of the drug to be used, should be considered during the production phase and the ratios of polymer cross-linking agents should be determined accordingly (Schneider et al. 2004). Another factor is the physical and chemical interactions between polymers (matrix) and active molecules, which should also be considered in the drug loading process. Besides, drug release can be achieved by biological or external stimuli such as pH (Anna and Katarina 2018), light (Vivero-Escoto et al. 2009), reducing agent, temperature (Coughlan, Quilty and Corrigan 2004; Lindner et al. 2008), ultrasound, electrical (Pierce 2010) and magnetic fields (Pirmoradi et al. 2011). Polymeric scaffolds that can on-demand respond to such stimuli can be produced by different approaches such as surface modifications, coating, forming composite structures with alternative sensitive materials, or introducing nanoparticles (Davoodi et al. 2018). Many different natural and synthetic polymers are used as a potential scaffold material with controlled drug release that increases tissue regeneration (Prabaharan and Jayakumar 2009; Prabaharan et al. 2007).

2.4. Polysaccharides in Drug Delivery and Tissue Engineering

Polysaccharides have considerable physicochemical and physiological properties such as biocompatibility, biodegradability, and low immunogenicity (Prasher et al. 2021). Additionally, natural polysaccharides have a considerable impact due to their structural diversity, wide availability, low cost, and ease of modification chemically and biochemically (Metaxa et al. 2021; Singh et al. 2020). Therefore, researchers have shown an increased interest in developing polysaccharide-based biomaterials for biomedical applications (Sood, Gupta, and Agrawal 2021). Besides, natural polysaccharides have been combined with synthetic polymers due to their unique properties to develop functional materials (Hu, Li, and Xu 2017).

They are included in the "generally safe" category and easily available from plants (guar gum, inulin, and xylan), animals (chitosan, chondroitin sulfate), algal (alginates), and microbes (dextran). Given the increased concern about the environment and sustainability in recent times, it is clear that the use of renewable material resources has an important circumstance. In this regard, the use of natural polysaccharides is promising in biomedical applications (Zheng et al. 2020; Sun et al. 2020).

2.4.1. Xylan

Xylan, the most common hemicellulose, comprises xylose units linked by β-(1→4) glycosidic linkage. It can be readily found in forest/pulping and agricultural industry debris and side streams (Cartaxo da Costa Urtiga et al. 2020). It is one of the most abundant biopolymers in residues produced by the agricultural industry (Ebringerová and Heinze 2000). Depending on their source and extraction method, the backbone can be substituted by α-D-glucuronic acid, 4-O-methyl-α-D-glucuronic acid, α-L-arabinose, α-D-xylose, and α-D-galactose. Generally, xylans are classified based on their substituents. The α-L-arabinofuranose units are attached to the backbone as side chains of arabinoxylan that is found in the cell wall of the starchy endosperm and outer layer of cereals. Glucuronoxylan which is found in hardwood species like beech and birch wood is substituted with 4-O-methyl glucuronyl groups (Scheller and Ulskov 2010; Ebringerova 2006). Heteroxylans are present in cereal bran and seed. They consist of various mono-oligosaccharide residues. The chemical structure of beechwood xylan substituted with 4-O-methylated glucuronic acid (GlcAOMe) is shown in Figure 2.2.

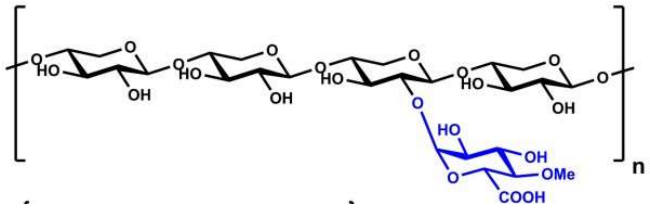

Figure 2.2. Chemical strucrure of beechwood xylan.

Xylan is resistant the digestion and absorption in the human small intestine and is fermented in the large intestine by microbiota in the colon, especially *Bacteroides* species. (Hopkins et al. 2003; Hughes et al. 2007). Utilization of polysaccharides depends on the structural properties of the carbohydrates and the ability of the bacteria to act on them (Flint et al. 2012). The xylan degradation mechanism depends on the degree of polymerization, cross-linking and branching (Hughes et al. 2007; Rose, Inglett and Liu 2010). Besides, the degradation of the xylan requires the activity of different bacterial enzymes, like endo-xylanases, beta-xylosidases, reducing end xylose-releasing exo-oligoxylanases and alpha-l-arabinofuranosidases (Pollet et al. 2012).

Xylan can potentially be used in the food industry. It can be used as a food additive since it can act as a texturing and stabilizing agent (Rosa-Sibakov et al. 2016). Due to their film-forming capacity xylans can be used in the preparation of edible food packing materials (Hansen and Plackett 2008). It can influence the rheological behavior of dough and texture in bakery products (Izydorczyk and Biliaderis 1992). Besides the great advantage of being a renewable material, xylan has several properties that make it a favorable material for pharmaceutical and biomedical applications (Melo-Silveira et al. 2012; Silva et al. 2013; Gao et al. 2016; Noaman et al. 2008; Oliveira et al. 2010). The different forms of xylan such as films and hydrogels (Sun et al. 2013; Gao et al. 2016; Cao et al. 2014; García-Uriostegui et al. 2018; Peng et al. 2011), prodrugs (Kumar et al. 2018; Sauraj et al. 2017, 2019, 2020; Daus and Heinze et al. 2010), micro and nanoparticles (Nagashima et al. 2008; Silva et al. 2013; Silva et al. 2007; Cartaxo da Costa Urtiga et al. 2017); Garcia et al. 2001; Araújo et al. 2015; Marcelino et al. 2015) have been used in drug delivery. The use of xylan in the pharmaceutical field is discussed in more detail in the following sections.

2.4.2. Chitosan

Chitosan is a biopolymer obtained by a deacetylated derivative of chitin (60%-100%), composed of β-(1→4) linked linear copolymer, containing N-acetyl-D-glucosamine and D-glucosamine units with one amino (NH_2) group and two hydroxyls (OH) groups in each repeating glycosidic units (Ali and Ahmed 2018). Chemical structure of chitosan is shown Figure 2.3.

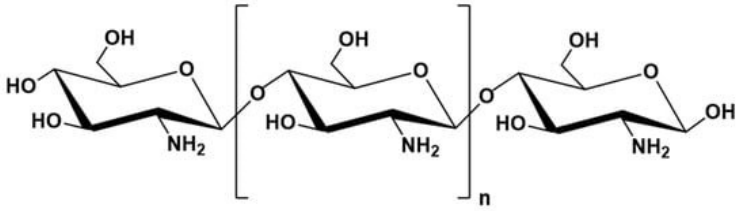

Figure 2.3. Chemical Structure of chitosan
(Source: Sami El-banna et al. 2019)

Chitin, the main source of chitosan is available in the cell walls of fungi, the exoskeletons of crustaceans, green algae, and insect cuticles (Croisier and Jérôme 2013; Ramos Berger et al. 2018; Kannan et al. 2010). The flexibility for chemical modification of chitosan caused by the reactive amino and hydroxyl group in the molecular chain, allows it to be applicable for pharmaceutical and biomedical applications (Ahmed et al. 2018). Owing to the advantage of chitosan being easily processable, it can be chemically or physically modified to manufacture tailor-made different functional forms such as gels, nanofibers, membranes, beads, nanofibrils, nanoparticles, microparticles, scaffolds, and sponge-like structure with desired properties. Further, chitin /chitosan have high bioactivity, biodegradability, biocompatibility, and antimicrobial properties. It can be also used in the food industry as food preservatives, as they have an antimicrobial activity that allows them to protect from microbial deterioration, and are used as a thickening and stabilizing agents. Moreover, it can be used as a carrier for cosmetic products to increase the penetration of active ingredients through the skin layer. It is used in skin, hair and oral care products in order to provide a permeability barrier on the skin surface and prevent the harmful effects of solar radiation responsible for ageing and wrinkles, and etc. Chitin/chitosan also used for enzymes-immobilization (wine, sugar, and wastewater

treatment for pollutant removal), biosensors manufacturing, biodegradable packaging (food wrapping), seeds-coating, dyes and chemicals removal from textile wastewaters (chelating agent), scavenge heavy metals from polluted water, acceleration of seeds germination.

2.5. Curcumin as a Model Bioactive Compound

Curcumin is a hydrophobic polyphenol with a broad spectrum of biological and pharmacological activity produced from the rhizome of the *Curcuma longa* plant (Figure 2.4). Curcumin is a bis-α, β-unsaturated β -diketone that shows keto-enol tautomerism having a predominant keto form in acidic and neutral solutions and stable enol form in alkaline medium. Commercial curcumin includes about 77% diferuloylmethane, 17% demethoxycurcumin, and 6% bisdemethoxycurcumin (Anand et al. 2007).

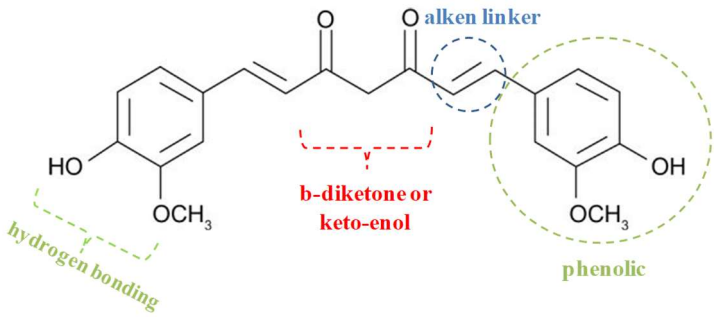

Figure 2.4. Chemical structure of curcumin.

Curcuma longa rhizomes have been used in local medicine for centuries in the treatment of various inflammations and other diseases, and today have preventive and therapeutic values against a wide range of diseases. These diseases include neurodegenerative diseases like Alzheimer's and Parkinson's disease, cancer (Anand et al. 2007; Sharma et al. 2004), asthma, bronchitis (Ram, Das, and Ghosh 2003), Crohn's disease, ulcerative colitis (Hanai et al. 2006) inflammatory bowel disease (Ukil et al. 2003), diabetes (Nishiyama et al. 2005). The anti-inflammatory and anti-cancer effect of curcumin has been known for many years and has been shown in several animal studies

(Dulbecco and Savarino 2013; Hatcher et al. 2008; Jurenka 2009; Aggarwal and Harikumar 2009; Aggarwal et al. 2003; Notarbartolo et al. 2005).

Despite its considerable therapeutic potential for the use of curcumin in various diseases, its rapid metabolism and poor water solubility have limited its use by the clinical area (Tønnesen, Másson and Loftsson 2002). Low bioavailability due to lipophilicity, degradation in alkaline pH and photodegradation are the main disadvantage of curcumin. Due to its lipophilic nature, it is difficult to achieve the desired therapeutic effect with the desired concentration. In the study on mice; after curcumin consumption, it was observed that approximately 75% of them were excreted in feces (Maheshwari et al. 2006) and this shows how poorly absorbed from the intestines. In another study, it was shown that curcumin was significantly excreted in feces in rats; the percentage absorbed was fixed independently of the dose and did not result in high absorption despite increased dose (Ravindranath and Chandrasekhara 1981). In addition, Yang et al. (2007) showed that the oral bioavailability of curcumin in the rats was 1%. In order to overcome these problems, to increase water solubility and bioavailability; liposome (Kunwar et al. 2006), polymeric nanoparticles (Bisht et al. 2007), lipid-based nanoparticles (Sou et al. 2008; Tiyaboonchai, Tungpradit, and Plianbangchang 2007), biodegradable microsphere, hydrogel (Vemula, Li and John 2006), and polymeric micelles (Zhu et al. 2016; Zhang et al. 2010; Bidkar, Sanpui, and Ghosh 2017) were developed to envelop curcumin.

CHAPTER 3

PRODUCTION OF CURCUMIN LOADED P-123 MICELLES

3.1. Introduction

The International Union of Pure and Applied Chemistry (IUPAC) defines micelles as “aggregates of surfactant molecules dispersed in solutions that is present in equilibrium with the molecules/ions from which they are formed” and forming a colloidal suspension. A polymeric micelle is defined as “a micelle developed in a peculiar solvent system employing one or more block and in some cases from graft copolymers” (Kapse et al. 2020). Polymeric micelles are formed by self-aggregation of amphiphilic polymers containing two or more blocks of different hydrophilicity. In micelle systems, hydrophobic blocks aggregate to form a core, while hydrophilic blocks form a corona (outer shell), which acts as the stabilizing interface between the hydrophobic core and the external environment. This self-organization of two or three blocks of amphiphilic polymers under favourable conditions is called micellization (Santos et al. 2016; Deshmukh et al. 2017).

Micelle formation occurs as a result of two main interactions; the attractive force which causes the association of the molecules and the repulsive force which prevents unlimited growth of the micelles into a distinct macroscopic phase. The minimum concentration required for the copolymers to self-assemble is called the critical micelle concentration (CMC). At concentration below CMC, amphiphilic copolymers accumulate at the air-water interface until the volume and the interface are saturated. Micelles at CMC and slightly higher concentrations are loose and contain a little water in their core. When the polymer concentration in the environment is increased, the micelle balance shifts towards the formation of the micelle and the micelles become more compact, durable and reduce their size. The CMC concentration is dependent on the composition and molecular structure of the amphiphilic polymer, as well as temperature,

pH and ionic composition, and co-surfactants (Owen, Chan, and Shoichet 2012; Mourya et al. 2011; Mondon, Gurny and Möller 2008).

Polymeric micelles have applications in various fields because they can be multi-functional and are convenient to modifications. The most important of these are applications in pharmaceutical fields such as medical diagnostic imaging (to receive a sufficient amount of contrast agents in the targeted area and to examine the blood-pool with computed tomography and evaluate the current blood flow status), regional drug targeting, immunology (as an immunological adjuvant for the modulation of the immune response and for the preparation of vaccines), gene therapy, and drug delivery (Trubetskoy 1996; Torchilin 1999; Torchilin 2002; Movassaghian, Merkel, and Torchilin 2015; Cormode, Naha, and Fayad 2014; Al Zaki et al. 2014). The widespread study and utilization of micelle systems in the many diverse fields mentioned above are due to their versatility, variable functionality, and ability to be produced in large quantities in an easy and reproducible manner (Deshmukh et al. 2017; Xu, Ling and Zhang 2013).

Especially in drug delivery systems, micelles have preferred because of their many advantages described as below:

- *Small diameter with narrow distribution:* The polymeric micelles have a significantly narrow distribution, between 10 and 100 nm, and their size can be easily controlled. Particles in this size range are not actively captured in the reticuloendothelial system (RES) and can maintain longer circulation in the bloodstream. At the same time, this controllable size of micelles can be an important tool for targeting the tumor site with their enhanced permeability and retention (EPR) effect.
- *High water solubility*: The polymeric micelle, which contains a large hydrophobic core, traps hydrophobic drugs there, indirectly imparting high water solubility to the drug. Also, through this large hydrophobic core, it may be possible to transport large amounts of drugs to one cell at a time. In a sense, it ensures that the toxic effect of the drug is avoided.
- *Separated functionality:* Polymeric micelles, consisting of an inner core and an outer shell, can play different roles in the drug delivery system. For example, the outer shell is responsible for interactions with biological components such as proteins and cells, while the inner core is independent of that and both can be responsible for different interactions for each step in drug delivery. While chemical modifications to the drug are not required to load the drug into the micelle, the shell part of the micelles can be modified

for active targeting purposes, e.g. modification with temperature, pH-sensitive agents or specific vector molecules.

Poly(ethylene oxide)-poly(propylene oxide)-poly(ethylene oxide) (PEO-PPO-PEO) block copolymers (called Pluronics or Poloxamers) are a famous family of widely studied amphiphilic block copolymers (He and Alexandridis 2017). PEO-PPO-PEO block copolymer are utilized widely in experimental medicine and pharmaceutical sciences because of its nontoxic, biocompatible, and biodegradable characteristics (Bruschi et al. 2017; Mayol et al. 2008; Dumortier et al. 2006; Kikuchi and Okano 2005). It has been shown in many studies that Pluronics increase the solubility and changes the pharmacokinetics of poorly soluble drugs safely (Batrakova and Kabanov 2008; Zhu et al. 2016; Fang et al. 2013; Zhang et al. 2010; Bidkar, Sanpui, and Ghosh 2017).

Micelles can be prepared by various methods, primarily depending on the physicochemical properties of the block copolymers and drug. Depending on the extent of the solubility of the block copolymer forming a micelle in an aqueous medium, simple dissolution, dialysis, oil in water emulsion, solvent evaporation and lyophilization can be used (Trivedi and Kompella 2010; Cholkar et al. 2012). Since the method chosen to prepare drug-loaded micelles would affect the physicochemical properties of the micelle and the drug-encapsulation efficiency, the most convenient method should be selected for both materials and the application area should be considered.

In pharmaceutical science, the dissolution ability of an active compound or drug in GI fluids is very crucial. Drugs must be dissolved for absorption to occur across the intestinal membrane. Therefore, hydrophobic drugs show low bioavailability due to their poor solubility in luminal fluids (Siew et al. 2012). Most of the drug candidates are relatively hydrophobic compounds because of their superior binding to receptor targets. Some degree of apolar character is considered important for drug absorption (Kesisoglou, Panmai, and Wu 2007; Stella and Nti-Addae 2007). However, poor water solubility hinders absorption. Chemical modifications, reduction in particle size, complexing with cyclodextrins, surfactants, and amphiphilic properties of polymers can be utilzed to improve the solubility of hydrophobic drugs (Tandya, Dehghani, and Foster 2006; Kayser 2003; Brewster and Loftsson; Szejtli 2004; Wong, Kellaway, and Murdan, 2006; Cheng 2006).

In this chapter curcumin (hydrophobic model drug) was encapsulated in the hydrophobic core of P-123 micelles by thin film hydration method. In this way, the bioavailability of a model drug and transporting large amounts of drugs to one cell at a

time can be increased. Also, curcumin loaded micelles can serve as soft templates for subsequent particle formation.

3.2. Materials and Methods

Sodium dodecyl sulfate (SDS), poly(ethylene glycol)-block-poly(propylene glycol)-block-poly(ethylene glycol) (P-123), cetyltrimethylammonium bromide (CTAB), and curcumin were of analytical grade and purchased from Merck (Darmstadt, Germany). Ultrapure water was used during all experiments.

3.2.1. Preparation of P-123 Micelles

P-123 micelles were prepared according to the thin-film hydration method (Fig. 3.1). Firstly, P-123 was dissolved in ethanol by using mechanical agitation. When ensuring the homogeneity of the solution, it was kept in the vacuum oven until the thin film formation at 42^{o}C. Then water was added to create micelle structures. Furthermore, the same method was applied to obtain curcumin loaded P-123 micelles (cur-P123). The only difference is that curcumin and P-123 molecules were simultaneously dissolved in ethanol and the following steps were applied. To separate unsolubilized curcumin, the curcumin micelle solution was ultracentrifuged for 5 min at 6000 rpm. Curcumin is known to remain stable at that temperature in an aqueous solution (Jagannathan et al. 2012). Figure 3.2 shows the different phases of cur-P123 formation.

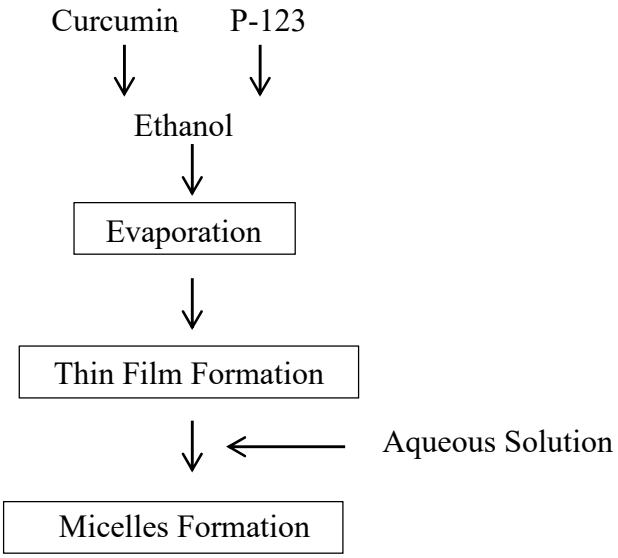

Figure 3.1. Production of curcumin loaded P-123 micelles by thin-film hydration method.

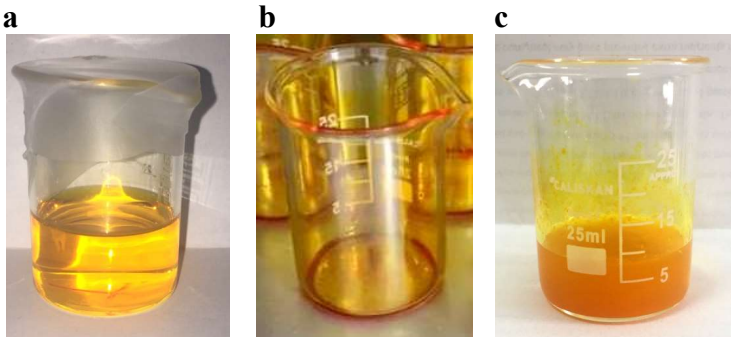

Figure 3.2. The phases of curcumin-loaded micelle formation. a) curcumin and P-123 dissolved in ethanol b) thin film c) curcumin micelles in a polymer solution.

3.2.2. Characterization of P-123 Micelles

To determination of particle size, distribution and zeta potential Zetasizer Nano ZS (Malvern, The United Kingdom) was used. The principle is based on the dynamic light scattering distribution of particles as a function of particle size. Before measurement, liquid and lyophilized samples were dispersed directly and in a buffer solution, respectively.

Scanning transmission electron microscopy (STEM) (Quanta 250FEG type 54 instrument) was used to examine the morphology of the micelles. The samples dispersed in water were dropped on EMR Carbon support film on copper 200 square mesh (Micro to Nano, Netherlands) and kept in a vacuum desiccator until completely dry. Carbon films on copper grids are electrically and thermally conductive under the electron beam. It provides image and specimen stability for high resolution imaging.

FTIR measurements were taken in the range of 450-4000 cm^{-1} using Perkin Elmer-UATR Two FT-IR spectrometer (UK).

3.2.3. Modification of P-123 Micelles with CTAB and SDS

To enhance the interaction of micelles and polymers in the further coating process, P-123 micelles were modified by an anionic surfactant sodium dodecyl sulfate (SDS) and cationic surfactant cetyl trimethyl ammonium bromide (CTAB). Curcumin, P-123, and CTAB or SDS were dissolved in ethanol together. The remaining steps were followed as in the thin-film hydration method (See 3.2.1). The characterization studies described above were applied.

3.3. Results and Discussion

3.3.1. P-123 Micelles with and without Curcumin

The presence of both hydrophilic and hydrophobic blocks in the same molecule leads to the self-assembly (also called spontaneous micellization process) of the block copolymers in solution due to the tendency to minimize the contact between the hydrophobic PPO moieties and the aqueous polar medium (Alexandridis 1997). The hydrophobic PPO groups of the micelles form a core structure that serves as a container for hydrophobic drugs or any active materials. Hydrophobic drugs can be encapsulated with the core of the micelles by different methods.

The thin film method is based on the formation of the drug-copolymer film. First both the copolymer and the drug are dissolved in a common solvent and evaporating the solvent under vacuum. When the film is reconstituted with an aqueous solution, the micelles form spontaneously and contain drugs in their core. By choosing a solvent that

can dissolve both the copolymer and the drug, phase separation is prevented during evaporation. The drug can be affected by the temperature during the evaporation process; therefore, the temperature should be determined according to the drug. The schematic representation of the molecular and micelle form of the P-123 block copolymer is given in Figure 3.3.

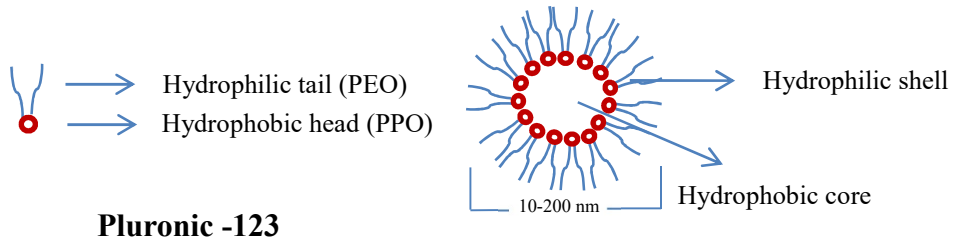

Figure 3.3. Schematic representations of the molecular and micelle form of the P-123 block copolymer.

After the hydration of thin-film, curcumin was encapsulated in P-123 micelles. The water solubility of free curcumin and cur-P123 at the same concentration is shown in Figure 3.4. While free curcumin showed very low solubility in water, it was completely soluble in the micelle formulation.

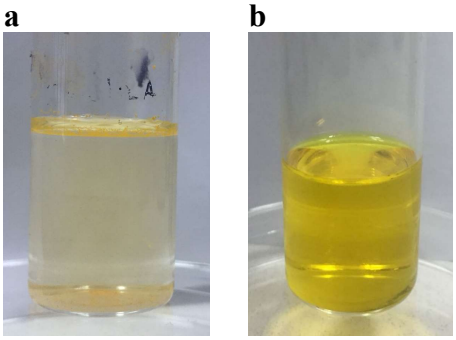

Figure 3.4. Solubility of two forms of curcumin in water a) free curcumin b) encapsulated curcumin.

3.3.2. Size Distribution and Zeta Potential

Figure 3.5 presents the three repeat size distributions of the free curcumin, P-123, and cur-P123 micelles by dynamic light scattering. The size of the curcumin molecules that dissolved in ethanol was difficult to measure because they were smaller than 2 nm (Fig. 3.5a). Although the d_{50} median size of P-123 micelles was around 20 nm, slightly expansion was observed in the distribution of cur-P123 (Fig. 3.5b-c). P-123 and cur-P123 micelles were slightly negatively charged, with a zeta potential of around -7.26 mV and - 4.28 mV, respectively (Fig. 3.6).

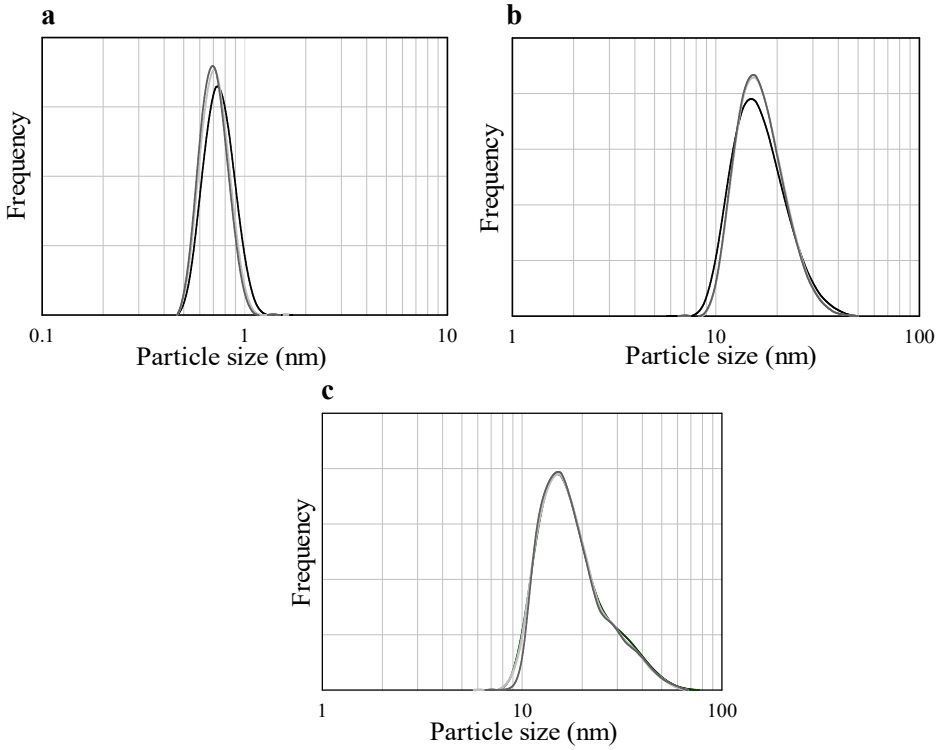

Figure 3.5. Size distribution of a) free curcumin; b) P-123; c) cur-P123 micelles.

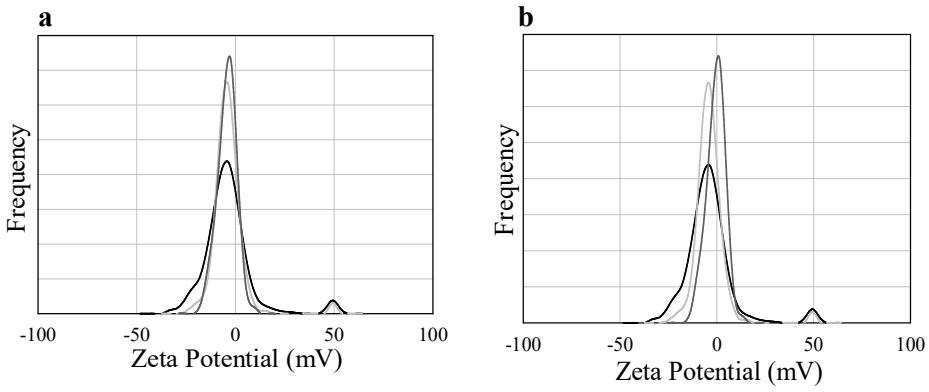

Figure 3.6. Zeta potential of a) P-123; b) cur-P123 micelles.

3.3.3. Morphology and Structure

The size and shape of the micelles were investigated by using STEM (Fig.3.7). The P-123 micelles were around 20 nm and a spherical shape. The size of the micelles increased when the curcumin was loaded, confirming the DLS spectra. This may have been caused by the retention of curcumin in the nucleus or an increase in the number of micelle aggregation due to hydrophobicity of the pluronic molecules in the presence of curcumin (Ganguly et al. 2017). It is necessary to calculate this number to determine which factor plays a dominant role. However, it is very difficult to determine the amount of curcumin in the core due to possible splitting between the core and the corona within the micelle.

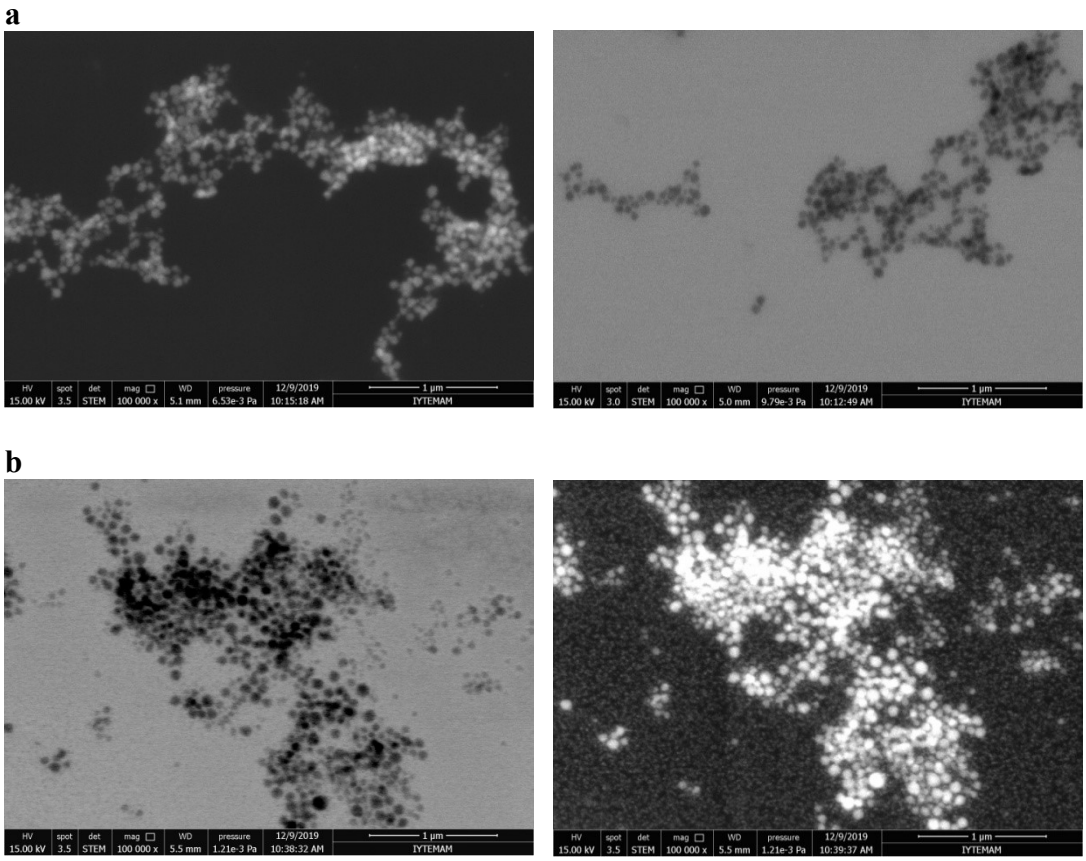

Figure 3.7. STEM images of a) P-123; b) cur-P123 micelles.

The FTIR spectrum of cur-P123 was compared with P123 micelles and free curcumin (Fig. 3.8). The characteristic bands of curcumin at 3510 cm^{-1} (stretching vibrations of the phenolic –OH group), 1605 cm^{-1} (stretching vibrations of benzene ring), 1502 cm^{-1}(C=O and C–C vibrations), and 1285 cm^{-1} (aromatic C–O stretching vibration) (Anitha et al. 2012) were hardly seen in cur-P123. This result suggested that curcumin was successfully entrapped into the hydrophobic core of pluronic micelles (Butt et al. 2012; Zhang et al. 2011).

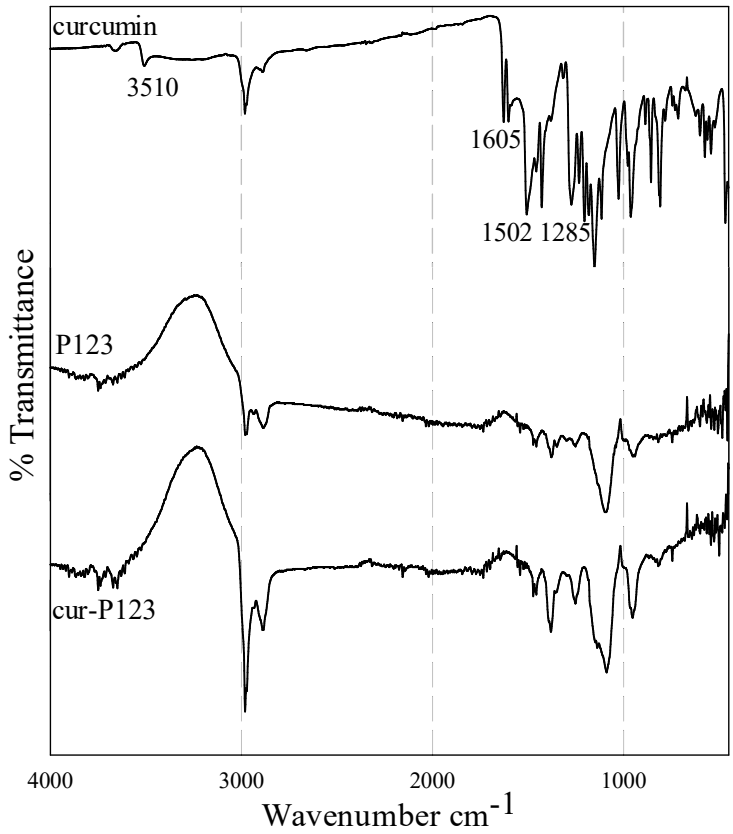

Figure 3.8. FT-IR spectra of curcumin, P-123, and cur-P123 micelles.

3.3.4. CTAB and SDS Modified P-123 Micelles

To enhance the interaction of micelles and polymers in the further coating process, P-123 micelles were modified by SDS and CTAB. The size of both modified cur-P123 micelles (around 5 nm) was smaller than P-123 micelles (Figure 3.9a). A bimodal distribution was not observed in modified micelles. This shows that SDS or CTAB did not exist as separate micelles and were incorporated in the P-123 micelle structure. The aggregation number of P-123 micelles is around 50 (Alexandridis and Alan Hatton 1995). Substitution of the P-123 constructs with smaller SDS and CTAB molecules altered the aggregation characteristic of P-123, resulting in compaction of the micelles (Foster, Cosgrove, and Hammouda 2009). In addition, it affected the charge of micelles. The P123-SDS micelles more negatively, P123-CTAB micelles more positively charged (Fig.3.9b-c).

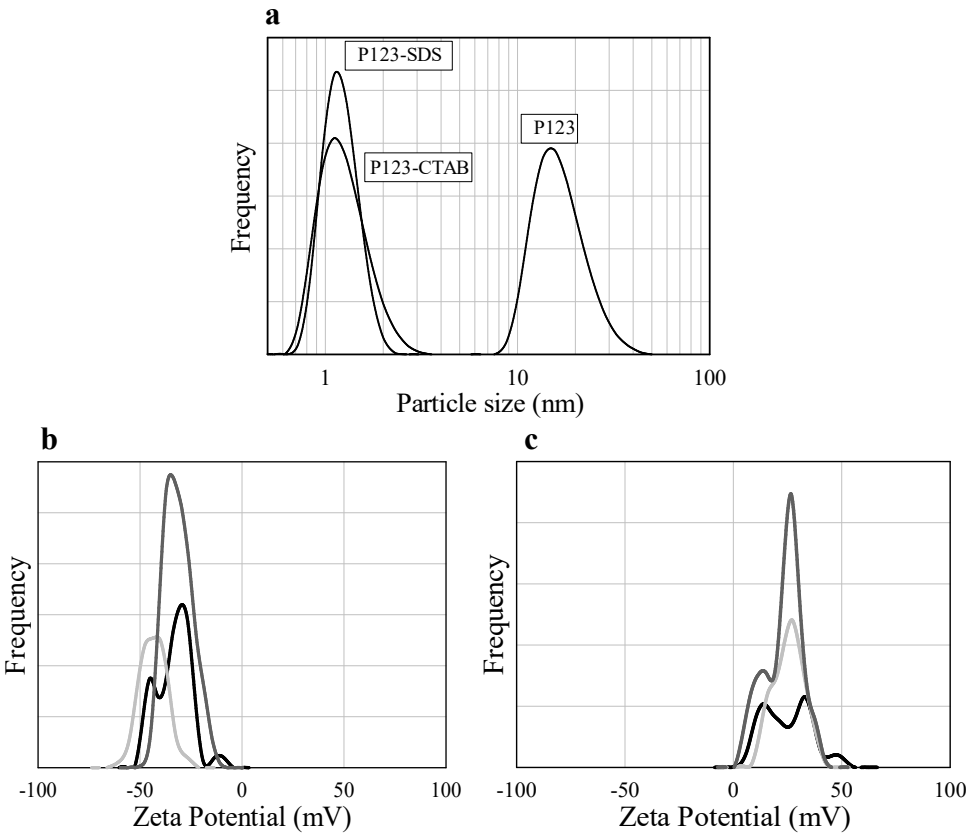

Figure 3.9. Size distribution of a) modified micelles and zeta potential of b) P123-SDS, and c) P123-CTAB micelles.

During the preparation CTAB modified P-123 micelles; a strong color change was observed (Figure 3.10). This might be a response of curcumin to pH changes. Curcumin appears yellow at pH values between 1.0 and 7.0 because most of the molecules are in neutral form. However, at a pH higher than 7.5 it exhibits an orange-red color (Lestari and Indrayanto 2014).

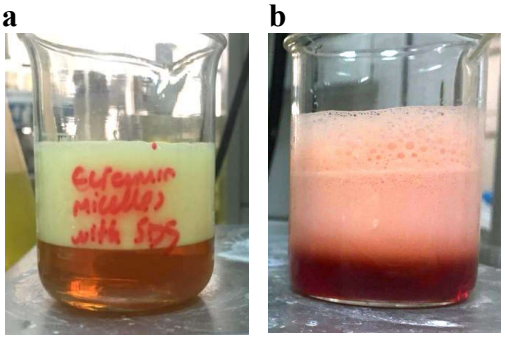

Figure 3.10. Color changes of curcumin loaded a) P123-SDS, b) P123-CTAB micelles.

Polymeric micelles have been developed to increase the therapeutic potential of different drugs such as paclitaxel (Wei et al. 2009), doxorubicin (Kabanov, Batrakova and Alakhov 2002), curcumin (Saxena and Hussain 2013), and gambogic acid (Hussain and Saxena 2012). However, the stability of polymeric micelles in aqueous environments is still controversial. Micelles are exposed to various environmental changes depending on their application. For example, after the intravenous injection, they can dilute in blood and decrease below their CMC. Their structures can deteriorate due to exposure to pH and salt changes. Also, they may contact various proteins and cells. Similarly, orally administered micelles are exposed to strong pH changes and enzymes (Owen, Chan, and Shoichet 2012; Sang et al. 2018; Hsu et al. 2018). For these reasons, different approaches have been developed to protect drug-loaded micelle structures from deleterious external factors. These are discussed in the following sections related to the polymer coating of P-123 micelles.

3.4. Conclusions

The solubility of an active compound or drug is crucial for its absorption through the intestinal membrane. The solubility and bioavailability of hydrophobic molecules can be improved by insertion in micelles. In this study, P-123 micelles carrying a model hydrophobic molecule, curcumin, were synthesized using thin-film hydration method. The characterization studies indicated that curcumin molecules were successfully entrapped in tight and spherical P-123 micelles (around 20 nm). The micelles could be modified by SDS and CTAB, which enhance the interaction between micelles and

polymers in coating with xylan in the following sections. Curcumin loaded P-123 micelles were small and had high drug loading capacity, therefore they are highly promising for increasing the therapeutic potential of hydrophobic molecules. In the following section of this study, these micelles were coated with natural polysaccharides to form nanoparticles for colon-taregeted derug delivery.

CHAPTER 4

PRODUCTION OF XYLAN/CHITOSAN COMPOSITE NANOPARTICLES WITH MICELLAR CORE

4.1. Introduction

Polymer-based particles have been extensively studied for their roles in drug delivery due to their biodegradability and biocompatibility. Polymeric drug carriers are considered as a safe way to deliver therapeutic agents to a specific target without presenting side effects. They can stabilize drugs, enhance drug solubility, improve circulation lifetime and provide dose-dependent drug release.

Oral drug intake is a widely used and easily accepted form of drug administration due to its ease of intake, pain avoidance, versatility, patient compliance, and low-cost (not requiring sterile conditions) (Sastry, Nyshadham and Fix 2000). Colon-targeted delivery through the oral route is desirable for topical treatment of diseases associated with the colon such as ulcerative colitis, Crohn's disease, colonic carcinomas. Also, the colon has more mild conditions and a higher retention time for drug release, compared to the upper gastrointestinal tract (GIT). However, before reaching the colon, the carriers should protect the drug from the harsh conditions of GIT such as low pH in the stomach and enzymatic degradation in the small intestine. Colon-targeted drug release can be managed with the different triggering mechanisms. Particularly, microbially activated polymeric systems are more colon-specific because they are less affected by physiological factors, such as GIT transit time, pH, osmotic pressure, or disease conditions.

In recent years, there has been an interest in using xylan in drug delivery systems. Xylan is the main hemicellulose found in hardwood and grass (Ebringerová and Heinze 2000). The great advantage of being a renewable material, xylan has several properties that makes it a favorable material for pharmaceutical and biomedical applications (Melo-Silveira et al. 2012; Silva et al. 2013; Gao et al. 2016; Noaman et al. 2008; Oliveira et al. 2010). The different forms of xylan such as films and hydrogels (Sun et al. 2013; Gao et

al. 2016; Cao et al. 2014; García-Uriostegui et al. 2018; Peng et al. 2011), micro and nanoparticles (Nagashima et al. 2008; Silva et al. 2013; Silva et al. 2007; Cartaxo da Costa Urtiga et al. 2017; Garcia et al. 2001; Araújo et al. 2015; Marcelino et al. 2015) have been used in drug delivery.

Xylan conjugated prodrugs have been synthesized to improve the bioavaibility and versatile drug releases kinetics. Drugs can be attached directly or through the linkers to xylan. Xylan based prodrugs were synthesis to delivery of ibuprofen (Daus and Heinze et al. 2010), curcumin (Kumar et al. 2018), 5-fluorouracil (Sauraj et al. 2019), and curcumin-5-fluorouracil (Sauraj et al. 2020) in cancer therapy. Additionally, xylan prodrugs have been synthesized for colon targeting. Xylan can maintain its structure through the physiological environment of the stomach and small intestine and can only be degraded by the extensive anaerobic microflora in the colon. Kumar and Negi synthesized xylan prodrugs of 5-aminosalicylic acid (5-ASA) by intermolecular covalent bond formation (2012a), and via activation of carboxylic acid with N,N-carbonyldiimidazole (2012b) to preventing drug release at upper GIT and minimizing the systemic side effects. Although they showed the stability of the prodrug in the upper GIT; assumed that the drug can be released in the lower part of GIT because of the presence of biodegradable enzymes only in the colon. Sauraj et al. (2017) synthesized xylan-5-fluorouracil-1-acetic acid conjugates as colon-specific prodrugs and evaluated by the in-vitro release of drug in the content of cecum and colon of rats. They showed that, the conjugates were stable in acidic (pH 1.2) and basic buffers (pH 7.4). The low amounts of drug 3-4% and 5-7% were released in gastric and small intestine contents respectively. The 53-61% of the drug was released in cecum and colonic contents. Although prodrugs provide site-specific delivery, these are new chemical entities and detailed toxicological studies need to be performed. The versatility of prodrugs is restricted due to their formation depending on functional groups on the drug moiety. A drug-specific carrier should be developed.

Xylan-based microparticles were produced by interfacial crosslinking polymerization using sodium trimetaphosphate (STMP) (Cartaxo da Costa Urtiga et al. 2017) and terephthaloyl chloride (TC) (Marcelino et al. 2015). The phosphate ester bonds were formed between STMP and xylan during the cross-linking process. The microparticles showed narrow monodisperse size distributions (3.5 and 12.5 mm). Xylan microparticles crosslinked with TC, the terephthalic esters bound were observed due to the reaction between TC and the xylan. The mean particle diameter was around 37-43

μm. In both studies, drug was not included in the microparticles, only the characterization and toxicity of xylan-based microparticles were investigated. The results showed that xylan-based microparticles crosslinked with STMP or TC were dose dependanlty safe systems for drug delivery applications. Silva et al. (2013) produced xylan based microparticles by interfacial cross-linking polymerisation and/or spray-drying technique in order to investigate feasibility and stability of the systems. The interfacial cross-linking polymerisation method was include a w/o emulsification (chloroform:cyclohexane containing sorbitan triesterate) and polymer cross-linking reaction with TC. The pH-dependent polymer Eudragit S-100 (ES100) was used as a coating material of xylan microparticles. 5-ASA was used as a model drug to investigate the interactions among drugs and excipients in pharmaceutical dosage forms. Both techniques successfully produced well-defined microparticles based on xylan and ES100 containing 5-ASA. The microparticles presented suitable physical characteristics and satisfactory yields. However, they suggested the spray-drying technique could be preferable to interfacial cross-linking polymerization. Because more stable microparticles regarding thermal behavior were produced by using spray-drying. Martínez-López et al. (2019) prepared insulin loaded arabinoxylans (AX) microspheres with different insulin/AX ratio for oral delivery of insulin. The spherical AX microspheres with smooth surface were produced an average diameter of 320 μm. The AX microspheres minimized the insulin loss in the upper GIT, high percentage (~75%) of insulin were retain in the microspheres. Significant hypoglycemic effects were registered in vivo on diabetic rat models. The efficacy of enzymatically crosslinked arabinoxylans microspheres demonstrated successful oral administration of insulin. Lastly, Silva et al. (2007) synthesized xylan coated superparamagnetic particles for protection of magnetic particles from gastric dissolution. An emulsification/cross-linking reaction was utilized to produce magnetic polymeric particles. In vitro dissolution tests at gastric pH demonstrated the xylan coating protected magnetite particles from gastric dissolution.

In this study, chitosan which is one of the most widely used natural polymers in drug delivery systems was used to produce xylan based nanoparticles due to its unique properties and particularly positive charge. It is composed of β-(1→4) linked linear copolymer, containing N-acetyl-D-glucosamine and D-glucosamine units with one amino (NH_2) group and two hydroxyls (OH) groups unit (Ali and Ahmet 2018). It displays attractive properties for drug delivery such as bioactivity, biodegradability, biocompatibility, toxicity and antimicrobial properties (Subramanian et al. 2005;

Sanyakamdhorn et al. 2013; Tang et al. 2014). Its adhesion ability, which leads to a prolonged residence time on mucosal surfaces and provides higher drug permeability, makes chitosan prominent in colon-targeted drug delivery (Takeuchi, Yamamoto, and Kawashima 2001). However, due to the high solubility of chitosan in gastric conditions, its successful use in colonic-specific delivery requires alternative approaches to protect it against gastric acidity. The combination or coating with a polymer that resist acidic conditions prevent premature drug release in upper gastrointestinal conditions. For example, chitosan has been combined with locust bean gum (Raghavan et al. 2002), pectin (Ofori-Kwakye et al. 2004), sodium cellulose sulfate (Wang et al. 2009) and hydroxypropyl methyl (Macleod et al. 1999) for colon-specific drug delivery. Xylan-chitosan composites were developed as a hydrogel (Gabrielii and Gatenholm 1998; Gabrielii et al. 2000; Meena, Lehnen and Saake 2013) and food preservative (Li et al. 2011; Gaoa et al. 2017) Altough xylan-chitosan blend has not been manifacture in a nanoparticle form for colon targeted delivery, chitosan-xylan polyelectrolyte complexes have been investigated (Mocchiutti et al. 2016). The polyelectrolyte complexes are good candidate for the design of different types of dosage forms.

Curcumin was used as a model hydrophobic therapeutic compound. In pharmaceutical science, the dissolution ability of an active compound or drug in GI fluids is very crucial. Drugs must be dissolved for absorption to occur across the intestinal membrane. Therefore, hydrophobic drugs show low bioavailability due to their poor solubility in luminal fluids (Siew et al. 2012). Chemical modifications, reduction in particle size, complexing with cyclodextrins, surfactants, and amphiphilic properties of polymers can be utilzed to improve the solubility of hydrophobic drugs (Tandya, Dehghani, and Foster 2006; Kayser 2003; Brewster and Loftsson; Szejtli 2004; Wong, Kellaway, and Murdan 2006; Cheng 2006). For the solubilization of curcumin, it was encapsulated in the hydrophobic core of P-123 micelles by the thin-film hydration method (See chapter 3). The P-123 micelles provided curcumin solubility and soft templates for subsequent particle formation. Polymeric micelles, which have advantages such as smaller particle size, higher drug loading capacity, and increased cellular uptake, have been developed to increase the therapeutic potential of different drugs such as paclitaxel (Wei et al. 2009), doxorubicin (Kabanov, Batrakova and Alakhov 2002), curcumin (Saxena and Hussain 2013), and gambogic acid (Hussain and Saxena 2012). However, the stability of polymeric micelles in aqueous environments is still controversial. Micelles are exposed to various environmental changes depending on their application. For

example, after the intravenous injection, they may be diluted in blood below their critical micelle concentration (CMC). Their structures can deteriorate due to exposure to pH and salt changes. Similarly, orally administered micelles are exposed to strong pH changes and enzymes (Owen, Chan, and Shoichet 2012; Sang et al. 2018; Hsu et al. 2018). Therefore, different approaches have been developed to protect drug-loaded micelle structures from deleterious external factors.

In this chapter, xylan/chitosan composite nanoparticles with micellar core which functions as a solvent for water-insoluble drugs were developed for a colon-targeted drug delivery. Xylan shows high stability in the upper GIT and it can be degraded by some colonic bacteria. Chitosan was included into the xylan-based nanoparticles production due to its unique properties and particularly positive charge. It has highly adhesion ability which leads to a prolonged residence time on mucosal surfaces and provides higher drug permeability in colon. Firstly, curcumin was encapsulated in the hydrophobic core of P-123 micelles. The curcumin-loaded P-123 micelles with a mean diameter of 20 nm were produced and characterized in the Chapter 3. This first stage provided curcumin solubility and soft templates for subsequent particle formation. Secondly, curcumin loaded P-123 micelles were coated with xylan and chitosan by ionic gelation method for the protect them from the upper digestive system and to activate them microbiologically in the colon. A *Bacteroides* species known to ferment xylan was used to test the microbial degradation of xylan for the release of drug from carriers. The general schematic illustration is given in Figure 4.1

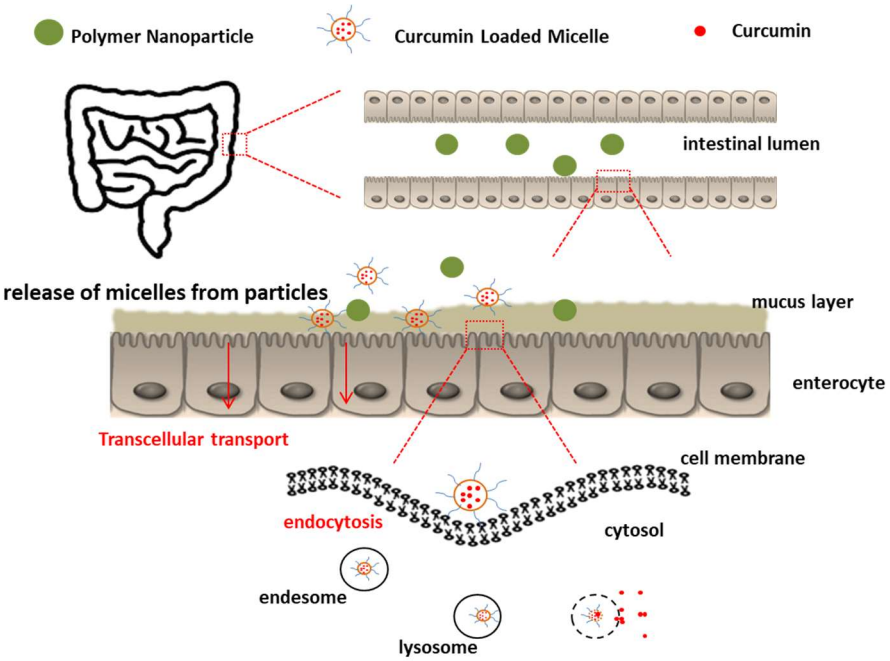

Figure 4.1. General schematic illustration of the proposed mechanism for oral delivery of xylan based polymeric nanoparticles.

4.2. Materials and Methods

Low molecular weight chitosan, sodium trimetaphosphate (STMP), sodium tripolyphosphate (TPP), poly(ethylene glycol)-block-poly(propylene glycol)-block-poly(ethylene glycol) (P-123), and curcumin were of analytical grade and purchased from Merck (Darmstadt, Germany). Beechwood xylan which composed of (w/ w) xylose ((80.8 %), glucuronic acid (11.4 %), other sugars (4.9 %), protein (0.3%), ash (2.4%), and moisture (2.4%) was purchased from Megazyme (Bray, Ireland). Xylooligosaccharide (XOS) (95.5 % of XOS has a degree of polymerization between 2 and 7) was a kind gift of Shandong Longlive (Yucheng, China).

Bacteroides ovatus DSM-1896 and *Bifidobacterium animalis* subsp. *lactis* DSM-10140 were purchased from Leibniz Institute DSMZ-German Collection of Microorganisms and Cell Cultures. For inoculum preparation and storage purposes, strains were grown anaerobically in Wilking Chalgren Medium (WCM) and Reinforced Clostridial Medium (RCM). The composition of WCM and RCM sre shown in Appendix A. Strains were stored at -80°C in the medium supplemented with 20% glycerol as a cryoprotectant.

The human colon cancer cell line Caco-2 (ATCC® HTB-37 ™) was purchased from American Type Culture Collection (ATCC) (Rockville, MA, USA).

4.2.1. Production of Curcumin Loaded Xylan Based Nanoparticles

For the synthesis of xylan based nanoparticles, the thin film which containing P-123 and curcumin was hydrated with polymer solutions to create curcumin loaded micelles. Then, the cross-linking agent was added and one h of stirring was applied. The nanoparticles were collected using a high-speed centrifuge and freeze-dried (Fig. 4.2). Different ratios of polymers and the cross-linking agent were tested. The schematic representation of curcumin loaded xylan based nanoparticles produced by thin film hydration coupled with ionic gelation method is given in Figure 4.3.

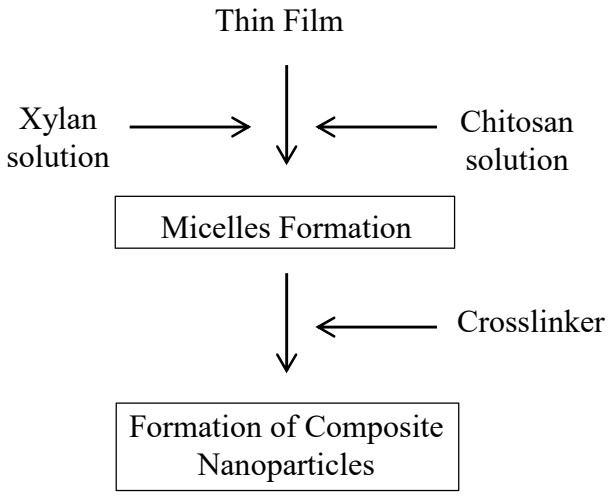

Figure 4.2. Curcumin loaded xylan/chitosan composite nanoparticles by ionic gelation method (see Fig. 3.1 for thin film formation).

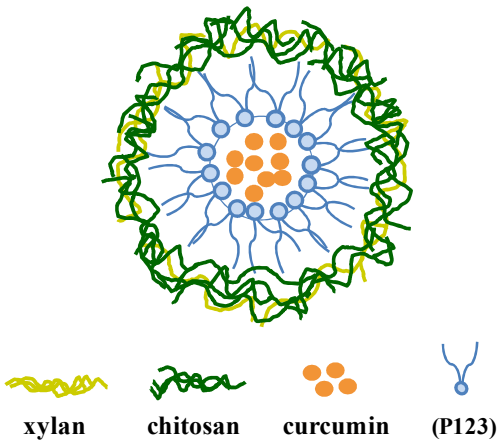

Figure 4.3. Schematic representation of curcumin loaded xylan-based nanoparticles.

4.2.2. Characterization Studies

Morphological Analysis: Scanning Electron Microscopy (SEM) (Philips, XL-30S FEG, Netherlands) was used to examine the surface morphology of particles. Samples were prepared from both powder and liquid suspensions. Liquid samples were dropped onto the aluminium sample holder, and stored in a moisture-free environment until dry at room temperature. Lyophilized particles were attached to the sample holder with aluminium tape. All samples were coated Au before analysis for the conductivity of the samples.

Structural Analysis: FT-IR spectra of pure materials and composite nanoparticles were obtained using an FT-IR spectrometer (Perkin Elmer-UATR Two, USA) at range of 400-4000 cm^{-1}.

Xylan Analysis: High-Performance Liquid Chromatography (HPLC) was used to determine concentrations of xylan incorporated in nanoparticle formation. The xylan were measured after hydrolyzing xylan into xylose using quantitative acid hydrolysis with 4% H_2SO_4 at 121°C for 1 h. After autoclaving, $CaCO_3$ was added to increase the pH to 5-6. Finally, samples were centrifugated and filtered by membrane filters (pore size 0.45 µm) before HPLC analysis. Xylan concentrations was calculated by multiplying the xylose concentrations by the anhydro correction factor (0.88) (NREL/TP-510-42623).

The operational conditions listed below;

HPLC system: Perkin Elmer, Series 200 (Shelton, USA)

Column: Rezex RPM-monosaccharides (Phenomenex, USA)

Mobile phase: Ultra-pure water

Injection volume: 20 μL

The flow rate of mobile phase: 0.6 mL min^{-1}

Column temperature: 80°C

Detector: Refractive index (RI)

Calibration curves are given in Appendix B were obtained using standard xylose solutions at a range of concentrations.

4.2.3. Determination of Curcumin Entrapment Efficiency

For entrapment efficiency of curcumin, nanoparticles were removed from the nanoparticle formation solution by centrifugation at 11.000 rpm for 5 min, followed by spectrophotometric analysis of the supernatant at 420 nm. Due to the differences in the absorbance of the free and encapsulated form of curcumin, the standard curve was also obtained with the cur-P123 micelles and SDS-modified cur-P123 micelles. The encapsulation efficiency and loading capacity were calculated by Eq.4.1 and 4.2.

$$\text{Encapsulation Efficiency \%} = \frac{\text{Curcumin Total - Curcumin free}}{\text{Curcumin Total}} \times 100 \quad (4.1)$$

$$\text{Loading Capacity \%} = \frac{\text{Total Entrapped curcumin}}{\text{Total Nanoparticle weight}} \times 100 \quad (4.2)$$

4.2.4. Effect of upper Digestive System pH on Nanoparticles

The effect of the digestive system pH on the nanoparticles was tested in simulated gastric and small intestinal fluid without enzymes. The simulated intestinal fluid at pH 7.4 was composed of KH_2PO_4 (6.8 g/L) and NaOH (0.9 g/L), while the simulated gastric fluid at pH 1.2 was composed of NaCl (2.0 g/L) and HCl (7 mL/L). Curcumin-loaded nanoparticles (10 g/L) were added into the simulated gastric fluid (pH 1.2) and incubated at 37 °C in a shaking incubator at 150 rpm. After 60 min, the nanoparticles were collected by centrifugation and transferred into simulated intestinal fluid and incubated at 37 °C for

an additional 2 h. Throughout the incubation, samples were taken for curcumin analysis and replaced by fresh medium.

4.2.5. Release Studies

Curcumin releasing as a result of bacterial digestion of polymers forming the outer shell of nanoparticles was tested. To test this, *Bacteroides ovatus* that a well-known xylan utilizer species was used. *Bacteroides ovatus* was pregrown in Wilkins-Chalgren Anaerobe Medium (Falony et al. 2009) and inoculated into the Basal medium (Palframan, Gibson, and Rastall 2003) containing nanoparticles for the release test. The composition of Basal Medium is shown Table A.3 in Appendix A.

The tubes containing 3 ml Basal medium at ph 6.8 except for heat-sensitive materials (haemin and vitamin K_1) were sealed with a layer of paraffin and incubated for at 90°C for 30 min creating an anaerobic environment (Hoseinifar et al. 2017). After the sterilization at 121°C for 15 min, the heat-sensitive materials, which were sterilized by membrane filter (pore size, 0.2 μm) were added in the sterile condition.

Nanoparticles (1.0% w/v) were added to the basal medium as a sole carbon source. After inoculation the organism (1.0 %), the tubes were incubated at 37ºC for 48 h. In the samples taken at intervals, curcumin released into the growth medium was measured by spectrophotometrically at 420 nm. The percentage of released curcumin was calculated using Eq. 4.3.

$$\text{Curcumin Release \%} = \frac{\text{Released curcumin}}{\text{Total curcumin}} \times 100 \tag{4.3}$$

Cur-P123 micelles released from nanoparticles into the growth medium can be utilized by organisms and that can cause misleading results. Therefore, the curcumin utilization ability of organisms was tested. Cur-P123 was prepared by the thin-film hydration method (See 3.2.1) and added into the growth medium as a sole carbon source. The tubes were incubated at 37°C for 48 h. The growth was quantified by measuring optical density at 600 nm in a spectrophotometer. Glucose was used as a positive control.

Organic Acid Production: For the analysis of organic acids, High-Performance Liquid Chromatography (HPLC) was used. The operational conditions and the procedure used for organic acid analysis in HPLC were listed:

HPLC system: Thermo Fisher Scientific

Column: BIORAD Aminex HPX-87H (300 x 7.8 mm)

Mobile phase, 5 mM H_2SO_4

Injection volume: 20 μL

Flow rate of mobile phase: 0.6 mL min^{-1}

Column temperature: 50°C

Detector: UV 210 nm.

Calibration curves given in Appendix C were obtained using standard organic acid solutions at certain concentrations.

4.2.6. In vitro cell culture

For in vitro cell culture studies human colon cancer cell line Caco-2 was used. The growth medium was Eagle's Minimum Essential Modified" medium containing 15% fetal bovine serum (FBS), 1% non-essential amino acid, 1% penicillin-streptomycin, and 1% sodium pyruvate. For the growth of the cell line, incubation was carried out 21 days in an oven with 95% humidity and 5% CO_2 at 37 °C. The procedure applied to thaw the Caco-2 cells stored in the freezer and to reach the appropriate form for the tests was as follows: Firstly, frozen cells were quickly thawed in a 37°C water bath. Then, it was transferred to a centrifuge tube containing MEM at the appropriate temperature (37°C). After centrifuging the cell suspension, the supernatant was removed. Pellet (cells) were resuspended in the growth medium and incubated in flasks. Cells were passaged when 80% confluent in the flask (2-3 times per week). Passage numbers were kept between 15-30 throughout the experiments.

Adherent cultures need to be passaged by transferring them to a new vessel a fresh growth medium while in the log phase before reaching confluence. Because cells stop growing due to contact inhibition and take longer to recover when reseeded, they do not provide a suitable cell suspension for further experiment. The procedure of passaging, which is the transfer of cells from a previous culture to a fresh growth medium, is as follows: After removing the old cell culture medium, the cells were gently washed to remove all traces of serum, calcium and magnesium that would inhibit the action of the

dissociation reagent. After the washing liquid was removed, adequate trypsin was added to cover the cell layer and incubated at 37°C for 2 min. After observing under the microscope that the cells were completely detached, MEM was added to terminate the reaction. The cell suspension diluted to the desired density was thoroughly pipetted, transferred to new flask.

Cytocompatibility of nanoparticles:

Cytocompatibility studies of the bare nanoparticles were evaluated by MTT assay. The cells were seeded in 96-well plates (4×10^3cells/well) and after reaching 50% confluency, the cells were treated with various concentrations of samples which were prepared by dilution with media. After the 24 h incubation, the growth medium was removed from each well and washed with the medium. The cells were incubated with MTT solution at 37 °C for 4 h and the resultant dark-blue formazan crystals were dissolved in DMSO. The absorbance of the solution at 570 nm was detected using a Multiskan go plate reader (Thermo Scientific, USA). The experiments were conducted in triplicate and the percent cell viability was determined by Eq. 4.4.

$$\text{Cell viability \%} = \frac{\text{Mean absorbance of the sample}}{\text{Mean absorbance of control}} \times 100 \quad (4.4)$$

4.3. Results and Discussion

4.3.1. Morphology and Structure of Nanoparticles

To preparation of composite nanoparticles, two physical interactions between the polysaccharides (xylan/chitosan) and the cross-linking agent (TPP/STMP) had been utilized. The relationship between polysaccharides consists of hydrogen bonds and electrostatic interactions between O–H, N–H groups in chitosan molecules and O–H groups in xylan molecules. Another interaction is caused by negatively charged oxygen on the cross-linking agent and positively charged amine groups on chitosan (Luo et al. 2014; Xu et al. 2012). Due to the negatively charged glucuronic acid groups on xylan, it could be included in the system owing to chitosan (Umemura and Kawai 2008). The

amount of xylan incorporated in the nanoparticles obtained using these interactions was analyzed using HPLC. To verify the total xylan added during the production of nanoparticles, both incorporated and not incorporated xylan were analyzed. The results confirmed each other. Different ratios of polysaccharides and crosslinking agents were tested. In addition to TPP as a cross-linker, STMP was also used as an alternative, or even used together.

Both crosslinking agents (STMP and TPP) were successful in inducing nanoparticle formation and the chitosan was able to keep the xylan in the system successfully (Table 4.1). The amount of xylan that can be incorporated into the nanoparticle depended mainly on chitosan and crosslinker. In all different conditions, xylan could be included in the system at very high rates, but small differences were observed depending on the amount of TPP in the particles using the same amount of polymer. For example, since the amount of TPP in CN-9 was quite low than the polymer ratio, less xylan incorporated xylan into the system. Using TPP as much as the total polymer concentration (CN-3) increased the xylan content. However, the polymer and crosslinking agent ratios should be designed considering the stability and release behaviours of the particles.

Table 4.1. The composition of composite nanoparticles and incorporated xylan into nanoparticles.

Code	P-123 (mM)	Xylan (g/L)	Chitosan (g/L)	TPP (g/L)	STMP (g/L)	Xylan Content (%)
CN-1	1.0	0.84	0.84	0.84	0	47.2
CN-2	1.0	1.67	1.67	1.67	0	49.4
CN-3	1.0	0.84	0.84	1.67	0	53.0
CN-6	1.0	1.67	1.67	0.84	0	48.0
CN-7	1.0	0.63	0.63	1.25	1.25	45.8
CN-8	3.3	1.67	1.67	0	1.67	42.1
CN-9	3.3	1.67	1.67	0.25	0	37.1

Morphological analysis of the composite nanoparticles was performed by SEM analysis (Fig. 4.4). The particles were spherical and nano-sized ranged from 80 to 450 nm. The relatively wide size distribution suggests that polymers may have precipitated around cur-P123 micelles at different rates. Also, some compact structures were observed

in SEM analysis. Aggregation may have occurred during the sample preparation stage for SEM analysis, which includes the drying process.

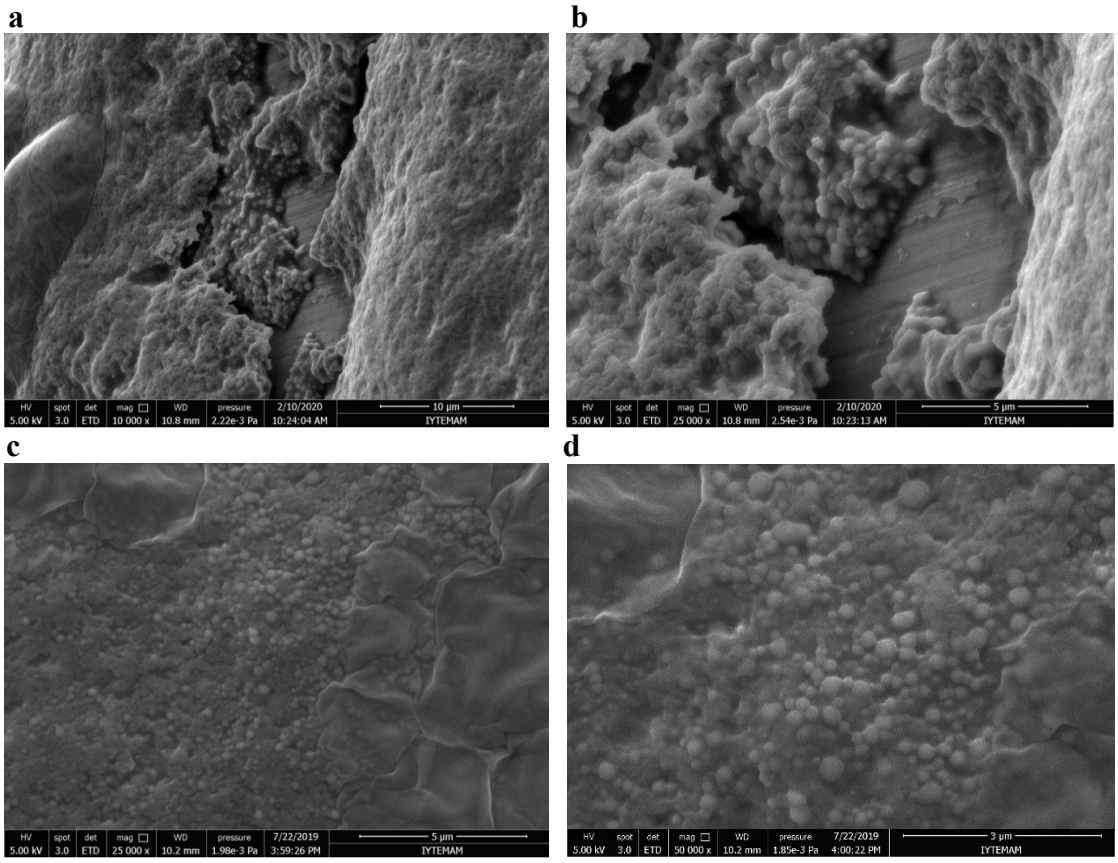

Figure 4.4. SEM images of composite nanoparticles a, b) CN-1 and c, d) CN-3

The FT-IR spectra of pure materials are shown in Figure 4.5. The beechwood xylan exhibited an absorption band at 890 cm^{-1} is attributed to the characteristic of β-glucosidic linkage between the xylose units. The band at 3420 cm^{-1} is attributed to the stretching of -OH group, and also the bands between 1465-1043 cm^{-1} arise from the stretching and bending vibration of C-O, C-C and C-OH groups (Kumar et al. 2018). The bands of COO- group from to glucuronic acid units were observed at 1620 and 1466 cm^{-1} (García-Uriostegui et al. 2018).

In the spectrum of the pure chitosan, the characteristic bands were observed at 3435 cm^{-1} (O-H stretching), 1651 cm^{-1} (amide linkages) and 1588 cm^{-1} (primary amine linkages). The bands at 1066 and 1028 cm^{-1} correspond to C-O stretching. The absorption

bands at around 2921 and 2877 cm^{-1} can be attributed to C-H stretching. These are characteristics band of polysaccharide and are found in other polysaccharides such as xylan, glucans (Antunes et al. 2015).

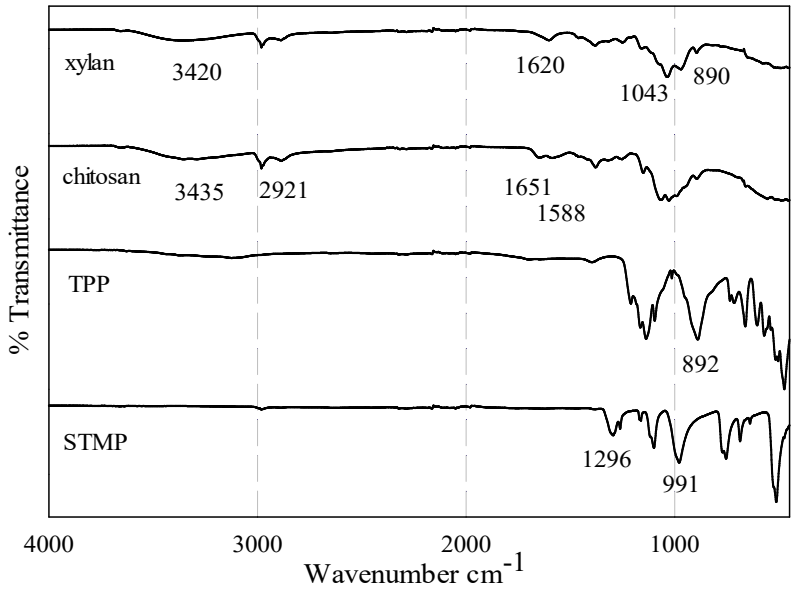

Figure 4.5. FT-IR spectra of pure materials.

The FT-IR spectrum of the composite nanoparticles is given in Figure 4.6. CN-1 and CN-3 were crosslinked with TPP, while CN-7 bound with TPP and STMP (See Table 4.1). Since other nanoparticles contain the same materials at different concentrations, the FT-IR result for each is not given separately. The band at 3450 cm^{-1} get sharper in the particles because of the presence of more -OH groups. Since, the entrapment of curcumin in micelles, the characteristic bands of curcumin at 1605 cm^{-1}, 1502 cm^{-1}, and 1285 cm^{-1} were hardly seen in nanoparticles. The characteristic bands shift was observed in the composite nanoparticles because of the potential interaction of protonated amine and/or amide groups and a negatively charged cross-linking agent. The amine band at 1588 cm^{-1} shifted to 1545 cm^{-1} and similarly, the amide band shifted from 1648 cm to 1637 cm^{-1}. The band at 2988 cm^{-1} were also sharper which could be based on the presence of more number of C–H groups in the nanoparticles. Additionally, TPP and STMP had a very sharp characteristic bands for the P-O-P band at 892 cm^{-1} and 991 cm^{-1}, respectively (See Fig. 4.5). The intensity of this band decreased significantly after polymerization, it

indicates cross-linking between the negatively charged oxygen and the positively charged ammonium groups. All these facts suggest that curcumin loaded xylan/chitosan composite nanoparticles were successfully obtained.

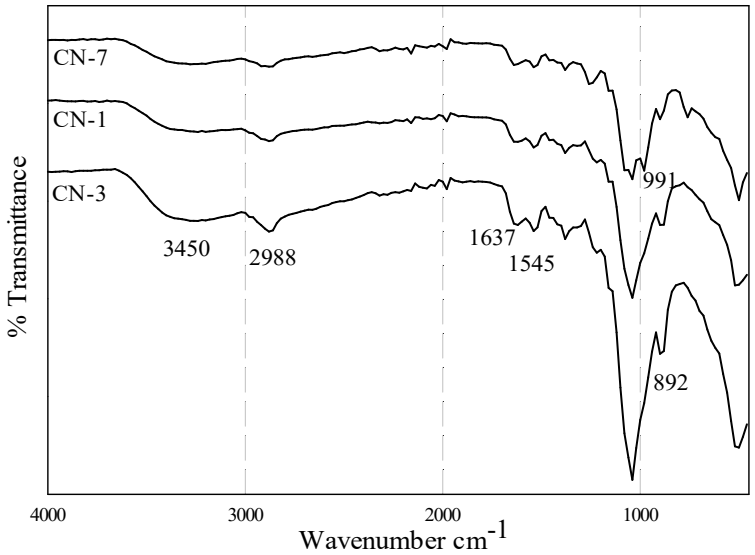

Figure 4.6. FT-IR spectra of cur-P123 micelle loaded composite nanoparticles.

To strengthen the interaction between curcumin-loaded micelles and polysaccharides, curcumin was encapsulated in SDS-modified P-123 micelles (see section 3.2.3). The ionic interaction between positive groups of chitosan with SDS could be more stable loaded nanoparticles. Both STMP and TPP were successful in inducing nanoparticle formation and the chitosan was able to keep the xylan in the system successfully (Table 4.2). In all different conditions xylan could be incorporated in the system and xyan content of composite particles reached 39.0%.

Table 4.2. The composition of composite nanoparticles and incorporated xylan into SDS modified cur-P123 micelles loaded nanoparticles.

Code	P-123 (mM)	SDS (mM)	Xylan (g/L)	Chitosan (g/L)	TPP (g/L)	STMP (g/L)	Xylan content (%)
CN-11	1.0	1.0	0.84	0.84	1.67	1.67	37.8
CN-12	1.0	3.3	0.84	0.84	1.67	0	39.0
CN-13	1.0	10.0	0.84	0.84	1.67	X	38.9
CD-14	1.0	3.3	0.84	0.84	0.84	0.84	37.0

SEM images of composite nanoparticles produced with SDS modified cur-P123 micelles are given in Figure 4.7. Particles were with a range of diameter of approximately 130-260 nm, but it was difficult to separate individual nanoparticles in SEM images due to the dense structure and agglomeration. The phase separation was observed during the preperation of CN-11 particle (contained 1.0 mM SDS). This might be due to the SDS concentration which was much below the critical micelle concentration (CMC of SDS: 8 mM).

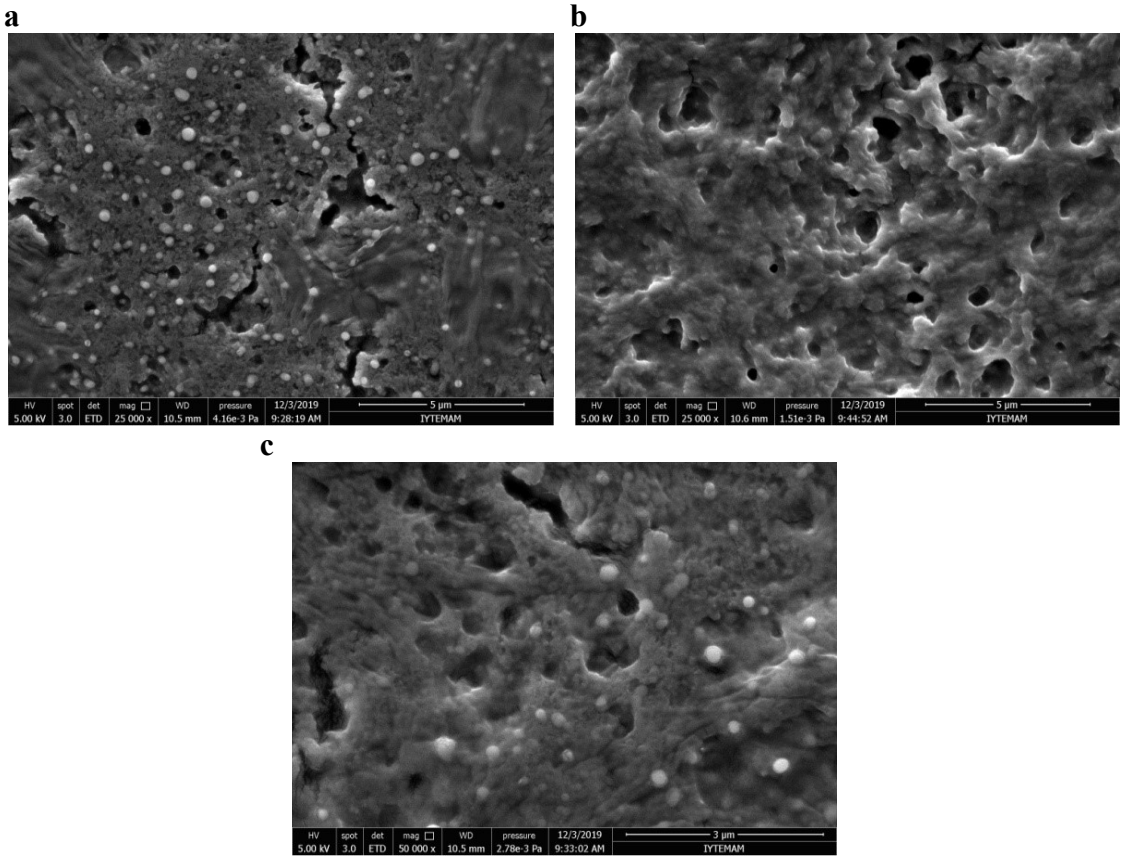

Figure 4.7. SEM images of composite nanoparticles a) CN-12; b) CN-11; c) CN-13.

The FT-IR spectrum of the cur-P123-SDS loaded nanoparticles and pure SDS are given in Figure 4.8. In the spectrum of the pure SDS, the characteristic bands were observed at 1216 and 1080 cm^{-1} for asymmetric and symmetric stretching of the S=O, and at 995 cm^{-1} shows the asymmetrical stretching vibration of C–O–S. The absorption bands at 1469 and 1380 cm^{-1} correspond to the asymmetric and symmetric deformation vibrations of CH_3, respectively. The bands at 2952, 2916, and 2850 cm^{-1} represent the asymmetric stretching vibration of CH_3, asymmetric and symmetric stretching of CH_2, respectively (Ren and Zhang 2020).

In the specturum of composite nanoparticles, the typical characteristic bands, the asymmetric- symmetric stretching of S=O at 1216 and 1080 cm^{-1}, and the stretching vibration of S-O-C at 812 cm^{-1} belonging to SDS. The bands of the COO- group from glucuronic acid units belonging to xylan were observed at 1620 and 1460 cm^{-1} in the nanoparticles. The characteristic amide band shift from 1648 cm to 1637 cm^{-1} was observed in the composite nanoparticles because of the potential interaction of protonated

amide groups and a negatively charged cross-linking agent. The intensity of the P-O-P band at 892 cm-1decreased significantly after polymerization with TPP, it indicates cross-linking between the negatively charged oxygen and the positively charged ammonium groups. (García-Uriostegui et al. 2018; Amri, Husseinsyah, and Hussin 2011).

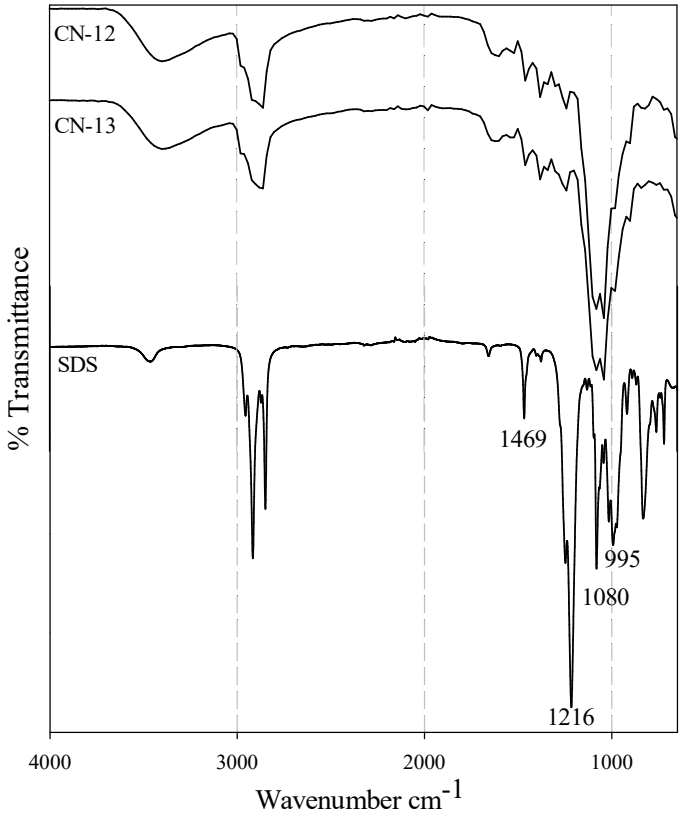

Figure 4.8. FT-IR spectra of cur-P123-SDS micelles loaded composite nanoparticles.

4.3.2. Curcumin Entrapment Efficiency

The entrapment efficiency of curcumin was calculated using data obtained by UV spectrophotometer as described in section 4.2.3. To accurately measure curcumin spectrophotometrically, calibration curves of free curcumin, cur-P123 micelle and cur-P123-SDS micelles were obtained. The calibration curves were presented in Appendix D.

One of the most important parameters in the evaluation of drug delivery systems is entrapment efficiency of drug. The percentage of drugs successfully entrapped in the carrier (EE %) and the mass fraction of the drug in the nanoparticle (LC %) are shown in

Table 4.3. The EE % was reached 90 in the CN 1-7 particles that 1 mM P-123 used, regardless of polysaccharide or crosslinking agent concentrations. The EE % of CN 8-10 particles that 3.3 mM P-123 used decreased to 20%, dramatically. P-123 molecules are aggregated as micelles at a concentration of approximately 0.1 mM, and the transition from spherical to cylindrical form begins at 10 mM (Cihan et al 2017; Petrov et al. 2008). Tight and spherical micelles were obtained with the 1 mM P-123 (See Fig. 1d-g). On the other hand, the 3.3 mM P-123, probably caused the shape of the micelles to change and the formation of a viscous structure during the thin film formation. Hence, the solubility of curcumin decreased in the micelles, resulting in a low EE %. As a result, when there were enough polysaccharides and crosslinking agents in the system, the EE % could be related to the ability of P-123 micelles to capture curcumin in their core.

LC % depends on the nanoparticle entrapment capacity of the curcumin micelles and the ability of the crosslinking agent to keep the system together. The very low LC% of the CN 8-10 particles could be attributed to the low EE%. The CN 11-13 nanoparticles that containing SDS modified micelles showed relatively lower EE % and LC% than un-modified ones. Therefore, SDS was not used in further studies. The CN 1-6 nanoparticles had very promising LC % and EE %. They can have great potential as a drug carrier. Due to its high loading capacity, low quantities of carriers would be required to deliver the drug to the site of interest, thus minimizing potential toxicity and immune reactions.

Table 4.3. Composition, encapsulation efficiency, and loading capacity of composite nanoparticles.

Code	P-123 (mM)	SDS (mM)	Cur (mM)	Xyl (g/L)	Cs (g/L)	Tpp (g/L)	Stmp (g/L)	EE (%)	LC (%)
CN-1	1.0	0	0.045	0.84	0.84	0.84	0	93	10.0
CN-2	1.0	0	0.045	1.67	1.67	1.67	0	93	6.0
CN-3	1.0	0	0.045	0.84	0.84	1.67	0	92	9.8
CN-4	1.0	0	0.9	1.67	1.67	1.67	0	91.1	11.0
CN-5	1.0	0	0.9	0.84	0.84	0.84	0	93.4	19.0
CN-6	1.0	0	0.9	1.67	1.67	0.84	0	93	10.0
CN-7	1.0	0	0.9	0.63	0.63	1.25	1.25	77	5.1
CN-8	3.3	0	0.9	1.67	1.67	0	1.67	47	1.0
CN-9	3.3	0	0.9	1.67	1.67	0.25	0	20	0.3
CN-10	3.3	0	0.9	1.67	1.67	1.67	0	20	0.3
CN-11	1.0	1.0	0.045	0.84	0.84	1.67	1.67	76	1.0
CN-12	1.0	3.3	0.045	0.84	0.84	1.67	0	57	5.6
CN-13	1.0	10.0	0.045	0.84	0.84	1.67	0	82	5.0

Cur: Curcumin, **Xyl:** Xylan, **Cs:** Chitosan, **EE:** Encapsulation efficiency, **LC:** Loading capacity.

4.3.3. Effect of upper Digestive System pH on Nanoparticles

The first biological barrier against any delivery system that is administered orally and is targeted to the colon is the harsh acidic conditions in the stomach (pH 1-2.5). Then the pH rises rapidly in the small intestine and reaches its highest pH level (pH 7.4) in the terminal ileum (Bratten and Jones 2006; Nugent, Rampton, and Evans 2001; Ibekwe et al. 2008). In both of these pH conditions, the carrier system is expected to protect the drug and prevent the burst release of drug.

The release of curcumin (also it can be called loss) over time was presented in Figure 4.9. The major burst curcumin release was not observed in the first 60 min at pH 1.2. A maximum release of 9% was observed in CD-17. The loss of curcumin in the early stage might have resulted from curcumin condensed in the outer region of the particles. The release of curcumin slowly increased throughout the incubation (pH 7.4). A maximum curcumin loss of 19% was observed in CD-17.

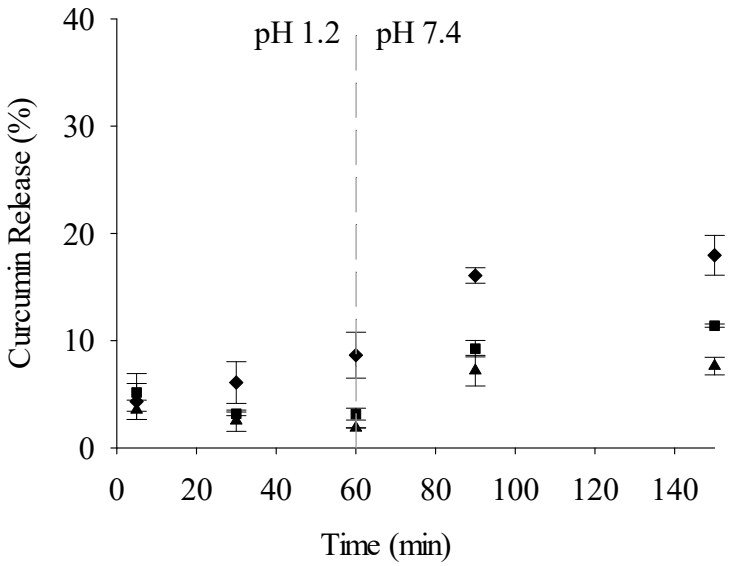

Figure 4.9. The effect of the GIT pH on the micelle embedded xylan/chitosan nanoparticles. (diamond: CD17; square: CD 16; triangle: CD15)

Composition of nanoparticles:

Code	XYL (g/L)	CS (g/L)	TPP (g/L)
CD15	0.84	0.42	0.42
CD16	1.67	0.42	0.42
CD17	2.52	0.42	0.84

Curcumin release in the upper GIT pH can vary depending on the mainly polymers and crosslinking agent concentration. The effects of polymer ratio and crosslinker on curcumin loss are shown in Figure 4.10. Release was monitored for 60 minutes at pH 1.2, followed by 90 minutes at pH 7.4 These graphs were generated by taking the highest release of curcumin at upper GIT pH (after 140 min). The xylan concentration was increased while the concentration of TPP and chitosan was kept constant at 0.84 g/L. The use of 1:1 polysaccharides ratio has the lowest curcumin release (~5.0%). As the xylan/chitosan ratio increased, drug release increased in parallel. However, this is not originated the inability of xylan to withstand these conditions. Because it is known that xylan can reach the last parts of the large intestine without being affected by the upper GIT (Hopkins et al. 2003). The factor here can be attributed to the low ratio of chitosan, which allows keeps xylan in the system with electrostatic interactions.

Furthermore, the response to pH conditions in the upper digestive tract is also highly dependent on the concentration of the crosslinking agent. In different studies, increasing cross-linking agent concentration has been successful in increasing the stability of particles or films structures and minimizing drug loss (McConnell, Murdan

and Basit 2008; Avadi et al. 2010). In order to test the TPP effect, six different composite nanoparticles with a constant polysaccharide ratio and gradually increased TPP concentration were produced. In line with other studies, increasing TPP concentration reduces curcumin loss (Fig. 4.10b). However, the effect of cross-linking agent and polysaccharides ratios on the stability of nanoparticles should be interpreted together with the release of curcumin in the colon (See section 4.3.4).

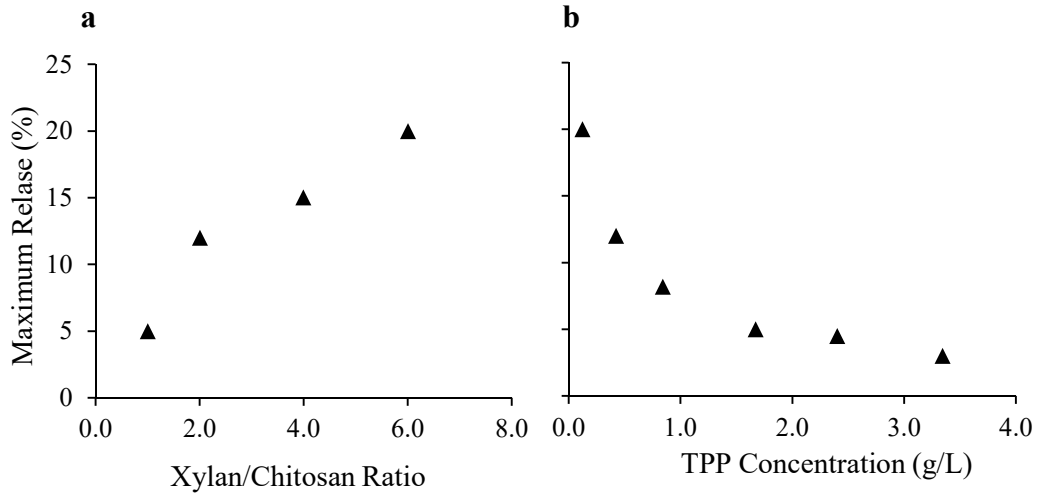

Figure 4.10. Effect of a) xylan to chitosan ratio and b) cross-linking agent (TPP) on curcumin release in upper GIT pH.
(in a: TPP and chitosan concentration was constant at 0.84 g/L, in b: xylan and chitosan concentrations were kept constant at 0.84 g/L).

4.3.4. Curcumin Release from Nanoparticles

Microbiologically activated polysaccharide-based drug delivery systems carry the drug along the upper digestive tract and arrive the colon. Then, in the colon, the glycosidic bonds in the drug-coating polysaccharides are hydrolyzed by the major saccharolytic species like *Bacteroides* and *Bifidobacterium* (Sinha and Kumria 2001). Thus, the drug can be released at the targeted site. When the produced composite nanoparticles reach the colon, they can be fermented by the microbial community and release drugs. To monitor curcumin micelles, release by microbiologically digesting xylan, *B. ovatus* species, which is known to ferment xylan and is included in a critical xylanolytic group in the human colon microbiota, was preferred. However, curcumin micelles released from the carrier

system can be digested by *B. ovatus* as a carbon source and give false negative results during curcumin measurement. Therefore, curcumin micelles were produced as described in section 3.2.1 and tested for degradation by *B. ovatus.* Glucose-containing medium was used as a positive control. The result showed that *B. ovatus* did not degrade or utilize curcumin loaded in the micelles (Fig. 4.11).

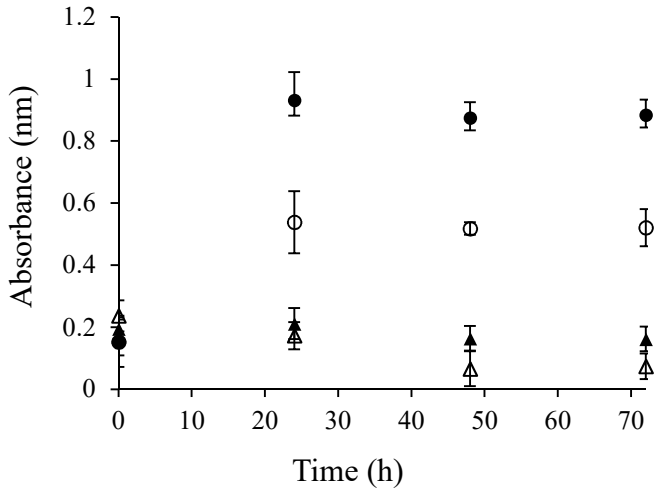

Figure 4.11. The growth of *B. ovatus* and *B.lactis* on glucose and cur-P123 micelles. (closed: *B. ovatus*; open: *B.lactis*; triangle: cur-P123 micelle; circle: glucose)

The release of curcumin from the composite nanoparticles by bacterial activity was monitored. The Basal medium at pH 6.8 containing nanoparticles was inoculated by *B. ovatus*. The xylan in the nanoparticles was sole carbon source in the culture medium. Before the release test, nanoparticles were pre-imcubated at the upper GIT pH as described above. Spontaneous release of curcumin was also monitored, as the control. Three different nanoparticles were selected for release studies. The composition of the particles are given in the Figure 4.12 caption.

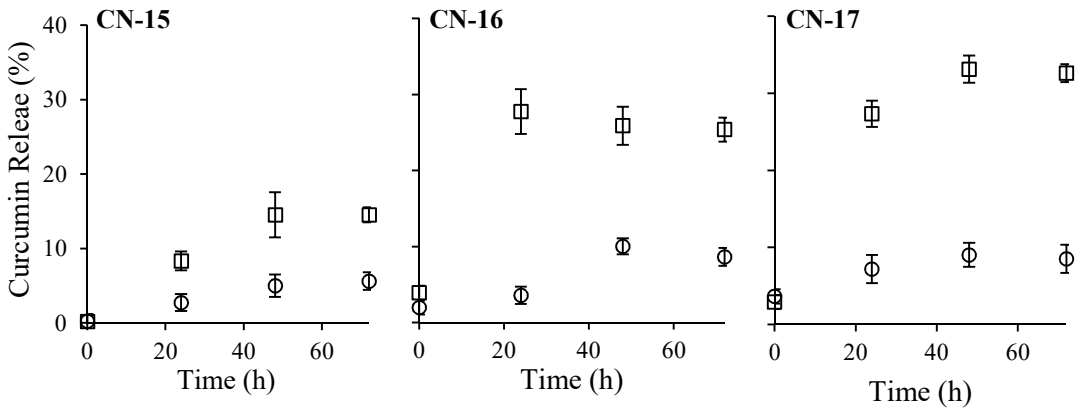

Figure 4.12. Curcumin release from composite nanoparticles with and without bacterial degradation. (square: with bacteria; circle: without bacteria)

Code	XYL (g/L)	CS (g/L)	TPP (g/L)
CN-15	0.84	0.42	0.42
CN-16	1.67	0.42	0.42
CN-17	2.52	0.42	0.84

The spontenous curcumin release from CN-15 which had the lowest xylan/chitosan ratio was 5.6%. The bacterial dependent release reached 14.5 % at 72 h. The spontenous curcumin release from CN-16 was higher than CN-15, reached maximum of 10.3%. In *B. ovatus* dependent curcumin release, while it was 3.5% in the first h, it increased rapidly and reached 27.8% at 24 h. The release within the first h was most likely due to non-bacterial release. CN-17, which had highest xylan ratio (6:1), showed the highest curcumin release. The release of non-bacterial curcumin was around 9.0%, quite similar to CN-16. The bacterial-dependent release reached 33.1% at 72h. As a result, the composite nanoparticles can release curcumin owing to the saccharolytic enzymes of a bacterial species localized in the colon. The increase in xylan concentration in composite nanoparticles increases the drug release in parallel.

Xylan can serve different roles in the drug delivery system developed in this study. Firstly, it protects the cur-P123 micelles from the upper GIT conditions due to its resistant to low pH (Ge et al. 2021). Secondly, it allows curcumin release in the colon, by its degradation by the colonic bacteria. Lastly, xylan degradation products, namely xylose and xylooligosaccharides are utilize by specific bacterial species as the carbon source. This prebiotic activity provides several health benefits to the host. The health-promoting effects of prebiotic substrates are generally attributed to the induction of beneficial species and the production of short-chain fatty acids (SCFA). Although xylan is mostly

not fermented by beneficial bacteria (e.g. *Bifidobacterium* species), the various in vitro and in vivo studies showed that it can induce an increase of beneficial species and SCFA production (Neyrinck et al. 2011; Nielsen et al. 2014; Van den Abbeele et al. 2011). This is associated with the substrate cross-feeding phenomenon between some species in the colon. An example of this is the cross-feeding of xylan between *B. ovatus* and *B. lactis* (Zeybek, Rastall and Buyukkileci 2020). While drug release occurs with the utilization of xylan by *B. ovatus*, *B. lactis* can increase their number owing to the cross-feeding interaction and contribute to organic acid production. In this study, when these two species were incubated together in the drug release medium, succinate, lactate, and acetate were released by the species (Table 4.4). It has been reported in previous studies that *Bacteroides* and *Bifidobacterium* could not produce succinate and lactate as end products, respectively (Chassard et al. 2008; Louis and Flint 2009; Macfarlane and Macfarlane 2003; Hughes et al. 2007). The presence of both lactate and succinate in addition to acetate indicated that the two species were actively growing and releasing respective organic acids as the end products of their fermentative metabolism.

Table 4.4. Organic acid production

Sample	Time (h)	Succunate (mM)	Lactate (mM)	Acetate (mM)
CN-16	24	0.685 ± 0.03	2.999 ± 0.11	7.118 ± 0.99
	48	0.242 ± 0.01	3.45 ± 0.35	7.305 ± 0.31
CN-17	24	0.637 ± 0.03	3.096 ± 0.08	6.518 ± 0.15
	48	0.465 ± 0.09	3.765 ± 0.14	7.478 ± 0.21

4.3.5. Cytocompatibility of Nanoparticles

The cytocompatibility of composite nanoparticles was measured through MTT assay with Caco-2 cells. The MTT assay is a colorimetric assay that measures cell metabolic activity. It based on the reduction of the tetrazolium dye MTT through the nicotinamide adenine dinucleotide phosphate (NADPH)-dependent cellular oxidoreductase enzyme of living cell mitochondria. MTT transforms into purple colored insoluble formazan crystals, and then the dissolved crystals are quantified by measuring

absorbance at 500-600 nanometers. MTT reduction, which is dependent on cellular metabolism, is low if cellular metabolism is low, and vice versa (Miri, Darroudi, and Sarani 2019; Berridge, Herst and Tan 2005).

The cell viability after the 24 h cultivation of cells in the sample-containing medium is shown in Figure 4.13a. The results did not show any significant cytotoxic ($p < 0.01$) effect for composite nanoparticles and micelles even for high concentrations (500 µg/mL). These results indicate the xylan and chitosan that cross-linked with TPP provide a non-toxic coating on the pluronic micelles. In addition, as shown in Figure 4.13b and c, the morphology of cells exposed to nanoparticles did not change significantly. The synthesized carrier can carry any active material entrapped therein without causing any cytotoxic effect and it can be used in biological applications.

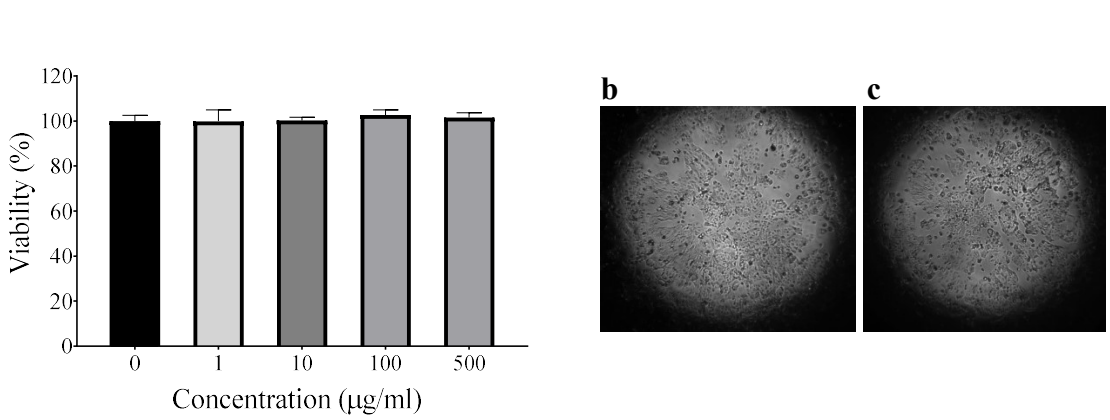

Figure 4.13. MTT cell viability assay of composite nanoparticles (a), morphology of cells before treatment (b), and after treatment with 500 µg/mL of composite nanoparticles (c).

4.4. Conclusions

In this study, xylan based composite nanoparticles with the micellar core were synthesized for effective delivery of the hydrophobic drug to the colon without deterioration or pre-releasing in the upper GIT. Xylan successfully precipitated on curcumin-loaded P-123 micelles owing to chitosan and TPP by ionic gelation technique, and spherical and nanosized xylan based nanoparticles were produced. In addition to the cross-linking of chitosan with TPP, xylan incorporated into nanoparticles owing to the

hydrogen bonds and electrostatic interactions between the hydroxyl and amine groups in the chitosan and the hydroxyl groups in the xylan molecules. Also, through chitosan, nanoparticles can improve drug permeability in the colon by providing long-term residence time on mucosal surfaces. The xylan based nanoparticles minimized the drug loss in the upper GIT pH, and released the drug as a result of xylan degradation. Although it has been observed that nanoparticles released drugs by *B. ovatus* activity, the in-ivo performance of nanoparticles should be investigated in clinical studies. Additionally, it was observed that polymer ratios and crosslinking agent concentration were important parameters in the drug release behaviors of carriers. In colon-targeted oral drug delivery systems, the optimizing of these compositions of nanoparticles should be considered to regulate drug protection and release. Besides the targeted delivery of hydrophobic drugs, the degradation of xylan could potentially contribute to colon health through prebiotic action.

Overall, xylan-based nanoparticles with a micelle core provide a promising and safe approach for colon-specific drug delivery. Since such a carrier is not drug-specific, it can be extended to the delivery of a broad range of hydrophobic drugs. Additionally, given the increased concern about the environment and sustainability in recent times, xylan a green biopolymer from a renewable source is promising for drug delivery applications.

CHAPTER 5

PRODUCTION OF XYLAN/CHITOSAN COATED MESOPOROUS SILICA NANOPARTICLES

5.1. Introduction

In recent years, there is great interest in developing new systems for more effective oral delivery of therapeutic agents through the gastrointestinal tract (GIT). The colon, last part of the GIT, long residence time, low hydrolytic enzyme activity, near-neutral pH, and much greater responsiveness to absorption enhancers provide an important opportunity for the absorption of drugs (Sinha and Kumria 2001; Shimono et al. 2002). In addition, colon-targeted delivery allows the treatment of various colon diseases like inflammatory bowel disease, ulcerative colitis, colon cancer and Crohn's disease. However, developing new formulations for efficient oral delivery of drugs with low permeability, low metabolic stability, poor water solubility, are still very challenging for the pharmaceutical industry. Further, traditional oral delivery systems are hampered by various factors, such as reduced control over the rate of drug releases (eg. an burst release of drugs), failure of targeted drug delivery, or potential drug degradation in the upper GIT (stomach and small intestine). In this context, various smart drug delivery approaches for targeted drug delivery systems have been considered. To overcome such various limitations, mesoporous silica nanoparticles (MSNs) have been proposed as promising candidates.

MSNs have been well recognized as potential carriers for drug delivery systems due to their hydrophilicity, biocompatibility, and non-toxicity, adjustable pore diameter, modifiable surface properties, and surface-area-to-volume ratio that allow them to keep significant cargo (Vallet-Regí et al. 2007; Rosenholm, Sahlgren, and Linden 2011; Baeza, Colilla, and Vallet-Regí 2014; Argyo et al. 2014). Monodisperse, spherical silica nanoparticles have been synthesized by the modified Stöber method, which uses the principles of sol-gel process (Stöber et al., 1968). Stöber et al. developed a synthesis based

on the hydrolysis and condensation of silicon alkoxides (TMOS, TEOS, etc.) in the ethanol-water mixture as solvent and ammonia as a base catalyst. Based on a Stöber-like approach, it is possible to synthesize mesoporous silica nanoparticles of uniform size by condensing the silicate source around this micelle template, using micelles formed by a cationic surfactant as the templating agent. Grün, Lauer and Unger (1997) first produced submicrometer-scale MCM-41 particles (Mobil Crystalline Material) using a modified Stober synthesis, and then mesoporous silica nanoparticles below 50 nm using a binary surfactant system or dialysis process.

Drug release mechanisms in MSNs are based on diffusion or erosion. The diffusion process can occur spontaneously without any control, or it can occur with a trigger mechanism. Although MSNs show excellent properties for enhancing the oral bioavailability of poorly water-soluble drugs, the pre-release or burst release of drugs into the targeted area is one of the well-documented disadvantages of MSNs (Popat et al. 2011; Rosenholm, Sahlgren, and Linden 2011; Popat et al. 2012). In this sense, the pores of MSNs can be capped by using stimuli-sensitive barriers or coating materials. Thus, the pores of MSNs exposed to external stimuli can be triggered to opening, allowing drug release. The stimuli-responsive drug release characteristic in MSNs can allow the drug release only at the target site and dose regulation. The trigger factors can be external such as magnet, light, temperature, and internal stimuli such as pH, redox, enzymes (Vallet-Regí et al. 2018; Bansal et al. 2020).

In colon-targeted drug delivery applications, with an inorganic-polymeric nanohybrid system based on MSNs, therapeutic agents can reach the colon while maintaining their stability throughout the gastrointestinal tract. In addition, they can acquire functional characteristics such as controlled release which is sensitive to stimuli such as pH, time, temperature, chemicals, and enzymes. (DeMuth et al. 2011; Muhammad et al. 2011; Aznar et al. 2009; Park, Lee, and Oh 2007; Vivero-Escoto et al. 2009; Coll et al. 2011). Because of these potential applications, hybrid systems are receiving widespread attention.

By using polymers that are especially biodegradable by colonic bacteria in the hybrid system, functional particles can be produced for colon targeting approaches. Fermentation of polysaccharides by colonic microflora is popular as a triggering mechanism to achieve colon-specific drug delivery (Amidon, Brown, and Dave 2015). This microbiologically activated delivery system has been developed as a variety of delivery strategies because it is independent of gastrointestinal transit time, pH, osmotic

pressure, or disease conditions and maintains its structure up to the target site. Therapeutic agents transported by biodegradable polymers can be released to the target site, colon, by degradation by microorganisms or digestion by an enzyme or degradation of the polymer backbone (Shimono et al. 2002). In addition to all these, it is remarkable to use low-cost, abundant in nature, chemically and biochemically changeable, stable, safe and non-toxic structures in a drug delivery system. Xylan, the most common hemicellulose and comprises xylose units linked by β-(1→4) glycosidic linkage, was one of the natural products used in the design of polymeric composite nanocarriers. It is found in the secondary cell walls of perennial plants and can be readily found in forest/pulping industry debris and side streams. It is one of the most abundant biopolymers in residues produced by the agricultural industry. Xylan-based films and hydrogels (Sun et al. 2013; Gao et al. 2016; Cao et al. 2014; García-Uriostegui et al. 2018; Peng et al. 2011), micro and nanoparticles (Nagashima et al. 2008; Silva et al., 2013; Silva et al. 2007; Cartaxo da Costa Urtiga et al. 2017; Garcia et al. 2001; Marcelino et al. 2015; Martínez-López et al. 2019), and prodrugs (Kumar et al. 2018; Sauraj et al. 2017, 2019, 2020; Daus and Heinze et al. 2010) have been studied for use in drug delivery systems.

Chitosan which is one of the most widely used natural polymers in drug delivery systems was used to produce xylan based nanoparticles due to its unique properties and particularly positive charge. Chitosan, obtained by deacetylation of chitin, composed of β-(1→4) linked linear copolymer, containing N-acetyl-D-glucosamine and D-glucosamine units with one amino (NH_2) group and two hydroxyls (OH) groups in each repeating glycosidic unit (Ali and Ahmet 2018). Chitosan is suitable for chemical modifications due to the presence of reactive amino and hydroxyl groups in the molecular chain. It can be easily processed in different functional forms such as gel, nanofiber, membrane, bead, nanofibril, nanoparticle, microparticle, scaffold, and exhibit bioactivity, biodegradability, biocompatibility, toxicity, and antimicrobial properties. (Subramanian et al. 2005; Sanyakamdhorn et al., 2013; Tang et al., 2014).

In this chapter, taking advantage of the stability of the xylan in the upper digestive system and its biological degradation, xylan and chitosan coated composite silica nanoparticles were developed for the efficient colon-targeted oral delivery of a hydrophobic active substance. Schematic representation of curcumin loaded polymer encapsulated silica nanoparticles is shown Figure 5.1. Firstly, porous silica nanoparticles were produced and loaded with soluble curcumin. The solubility of curcumin was achieved with the TX-100 surfactant. Curcumin loaded silica nanoparticles were coated

with xylan and chitosan to protect them from the upper digestive system, and to activate microbiologically in the colon. *Bacteroides* species known to ferment xylan was used for drug release test.

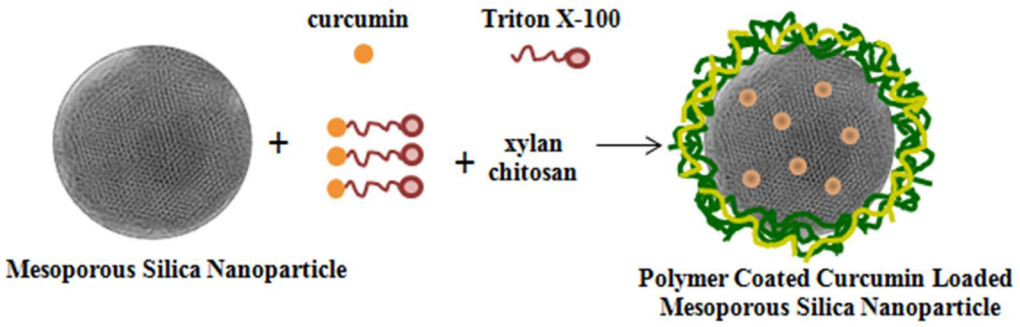

Figure 5.1. Schematic representation of curcumin loaded polymer encapsulated silica nanoparticles

5.2. Materials and Methods

Beechwood xylan from Megazyme (Bray, Ireland) was composed of (w/w) xylose (80.8 %), glucuronic acid (11.4 %), other sugars (4.9 %), protein (0.3%), ash (2.4%), and moisture (2.4%). Triton X-100 (TX-100), low molecular weight chitosan, tetraethyl orthosilicate (TEOS), curcumin, and sodium tripolyphosphate (TPP) were of analytical grade and purchased from Merck (Darmstadt, Germany).

Bacteroides ovatus DSM-1896 and *Bifidobacterium animalis* subsp. *lactis* DSM-10140 were purchased from Leibniz Institute DSMZ-German Collection of Microorganisms and Cell Cultures. For inoculum preparation and storage purposes, strains were grown anaerobically in Wilking Chalgren Medium (WCM) and Reinforced Clostridial Medium (RCM). The composition of WCM and RCM sre shown in Appendix A. Strains were stored at -80°C in the medium supplemented with 20% glycerol as a cryoprotectant.

Human colon cancer cell line Caco-2 (ATCC® HTB-37 ™) was purchased from American Type Culture Collection (ATCC) (Rockville, MA, USA).

5.2.1. Synthesis of Mesoporous Silica Nanoparticles (MSNs)

For the synthesis of mesoporous silica nanoparticles (MSNs); a cationic surfactant, CTAB (1mM), was dissolved in 50 ml of distilled water. Later, 4 ml of NH_4OH was added and mixing was continued for 5 min. Then 4 ml of TEOS was added to the solution by rapid addition. The solution was stirred on a magnetic stirrer for 2 h. The solution was centrifuged and the supernatant was removed. Finally, the pellets were calcined in an oven at 550ºC for 5 h. The flow sheet of the synthesis is presented in Figure 5.2.

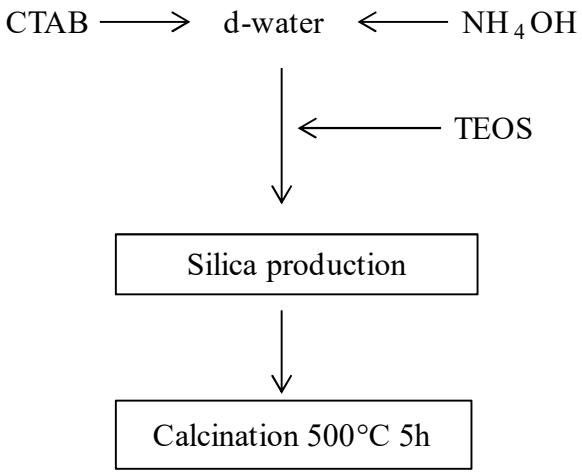

Figure 5.2. Production of mesoporous silica nanoparticles.

5.2.2. Curcumin loading in MSNs and coating with polymers

A non-ionic surfactant, TX-100, was used to make curcumin water-soluble. Drop by drop, 1.0 mM TX-100 was added into the aqueous curcumin solution to avoid micelle formation. After the proper amount of TX-100 addition, insoluble curcumin molecules were removed by centrifugation. To calculate the amount of soluble curcumin in the supernatant, the pellet was dissolved in ethanol homogeneously and the absorbance at 420 nm was measured spectrophotometrically. The amount of curcumin was subtracted from the initial amount of curcumin after being calculated from the standard curve, which was generated based on known curcumin concentrations.

Silica nanoparticles were soaked in a curcumin solution (30 mL) and the suspension was mixed on a magnetic stirrer for 3 h at room temperature to allow curcumin to enter the pores. The supernatant was analysed using UV-visible spectrophotometry at 420 nm to evaluate absorbed curcumin on the MSNs. After, chitosan (0.5% w/v) and xylan (0.5% w/v) solutions were added and stirring was continued for 1 more h. Finally, TPP (0.5% w/v) was added as a crosslinker and stirring was continued additional 30 min. Encapsulated silica nanoparticles were separated from the solution by centrifugation and particles were freeze-dried. A generalized flow sheet of the synthesis is presented in Figure 5.3.

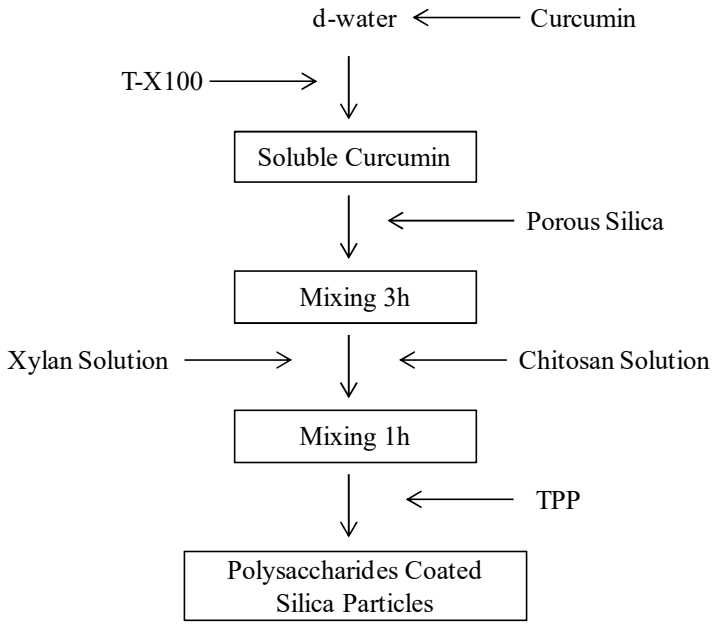

Figure 5.3. Production of curcumin loaded xylan/chitosan encapsulated MSNs.

5.2.3. Characterization

The surface morphology and size of particles was analyzed using Scanning Electron Microscopy (SEM) (Philips, XL-30S FEG, Netherlands). Samples for SEM analysis were prepared from both powder and liquid suspensions. Liquid samples were dropped onto the aluminium sample holder, and stored in a moisture-free environment at

room temperature. Lyophilized particles were attached to the sample holder. All samples were coated Au before analysis for the conductivity of the samples.

The zeta potential distribution of the MSNs was determined by the dynamic light scattering (DLS) technique using a Malvern Zetasizer Nano ZS instrument (Malvern Instruments, UK). Prior to the measurement, all samples were diluted with deionized water to obtain a suitable scattering intensity.

FTIR measurements were taken in the range of 450-4000 cm^{-1} using Perkin Elmer-UATR Two FT-IR spectrometer (UK).

The specific surface area and porosity measurement of the MSNs were performed by the Brunauer, Emmet and Teller (BET) method in liquid nitrogen environment at 77 K, based on nitrogen (N_2) gas adsorption technique.

5.2.4. Effect of Upper Digestive System pH on C-MSNs

The effect of the digestive system pH on the nanoparticles was tested in simulated gastric and small intestinal fluid without enzymes. The composition of the simulated intestinal fluid (pH 7.4) is KH_2PO_4 (6.8 g/L) and NaOH (0.9 g/L); the simulated gastric fluid (pH 1.2) is NaCl (2.0 g/L) and HCl (7 ml/L).

Curcumin-loaded MSNs (C-MSNs) with or without polymer-coating (10.0 g/L) were added into the simulated gastric fluid (pH 1.2) and incubated at 37 °C in a shaker at 150 rpm. After 60 min, the nanoparticles were collected by centrifugation and transferred into simulated intestinal fluid and incubated at 37 °C for an additional 2 h in a shaker. Throughout the incubation, samples were taken for curcumin analysis and replaced by fresh medium.

5.2.5. Curcumin Release from Polymer Coated C-MSNs

In this part of the study, curcumin releasing as a result of bacterial digestion of polymers forming the outer shell of MSNs was tested. To test this, *B. ovatus* was used. Basal Medium was used as a fermentation/release medium for growth of *Bacteroides* species (Palframan, Gibson, and Rastall 2003). The composition of Basal Medium is shown in Table A.3 in Appendix A.

The tubes containing 3 ml Basal medium at ph 6.8 except for heat-sensitive materials (haemin and vitamin K_1) were sealed with a layer of paraffin and incubated for at 90°C for 30 min creating an anaerobic environment (Hoseinifar et al. 2017). After the sterilization at 121°C for 15 min, the heat-sensitive materials, which were sterilized by membrane filter (pore size, 0.2 μm) were added in the sterile condition.

Nanoparticles (1.0% w/v) were added to the basal medium as a sole carbon source. After inoculation the organism (1.0 %), the tubes were incubated at 37°C for 48 h. In the samples taken at intervals, curcumin released into the growth medium was measured by spectrophotometrically at 420 nm. The percentage of released curcumin was calculated using Eq. 5.1.

$$\text{Curcumin Release \%} = \frac{\text{Released curcumin}}{\text{Total curcumin}} \times 100 \tag{5.1}$$

Organic acid production: For the analysis of organic acids, High-Performance Liquid Chromatography (HPLC) was used. Calibration curves given in Appendix C were obtained using standard organic acid solutions at certain concentrations. The operational conditions and the procedure used for organic acid analysis in HPLC are given section 4.2.5.

5.2.6. In vitro cell culture

For in vitro cell culture studies human colon cancer cell line Caco-2 was used. The growth medium was Eagle's Minimum Essential Modified" medium containing 15% fetal bovine serum (FBS), 1% non-essential amino acid, 1% penicillin-streptomycin, and 1% sodium pyruvate. For the growth of the cell line, incubation was carried out 21 days in an oven with 95% humidity and 5% CO_2 at 37 °C. The procedure applied to thaw the Caco-2 cells stored in the freezer and to reach the appropriate form for the tests was as follows: Firstly, frozen cells were quickly thawed in a 37°C water bath. Then, it was transferred to a centrifuge tube containing MEM at the appropriate temperature (37°C). After centrifuging the cell suspension, the supernatant was removed. Pellet (cells) were resuspended in the growth medium and incubated in flasks. Cells were passaged when 80% confluent in the flask (2-3 times per week). Passage numbers were kept between 15-

30 throughout the experiments. Adherent cultures need to be passaged by transferring them to a new vessel a fresh growth medium while in the log phase before reaching confluence. The procedure is given section 4.2.6.

Cytocompatibility of nanoparticles:

Cytocompatibility studies of the bare nanoparticles were evaluated by MTT assay. The cells were seeded in 96-well plates (4×10^3cells/well) and after reaching 50% confluency, the cells were treated with various concentrations of samples which were prepared by dilution with media. After the 24 h incubation, the growth medium was removed from each well and washed with the medium. The cells were incubated with MTT solution at 37 °C for 4 h and the resultant dark-blue formazan crystals were dissolved in DMSO. The absorbance of the solution at 570 nm was detected using a Multiskan go plate reader (Thermo Scientific, USA). The experiments were conducted in triplicate and the percent cell viability was determined by Eq. 5.2.

$$\text{Cell viability \%} = \frac{\text{Mean absorbance of the sample}}{\text{Mean absorbance of control}} \times 100 \quad (5.2)$$

5.3. Results and Discussion

5.3.1. Mesoporous Silica Nanoparticles (MSNs)

The SEM images of these MSNs are presented in Figure 5.4. The MSNs were synthesized using 1.0 mM CTAB at room temperature. The average particle sizes ranging from 200-230 nm and uniform spherical nanoparticles were produced. During the formation of mesoporous silica nanoparticles, the reaction temperature and surfactant concentration have significant effects on the particle size and shape. Based on previous studies in our laboratory, it has been observed that CTAB concentration rather than temperature affects the size and shape of the particles (Siretli 2012). It has been observed that the particles obtained with CTAB concentration between 50.0 mM-1.0 mM have spherical and smaller dimensions as the CTAB concentration decreases.

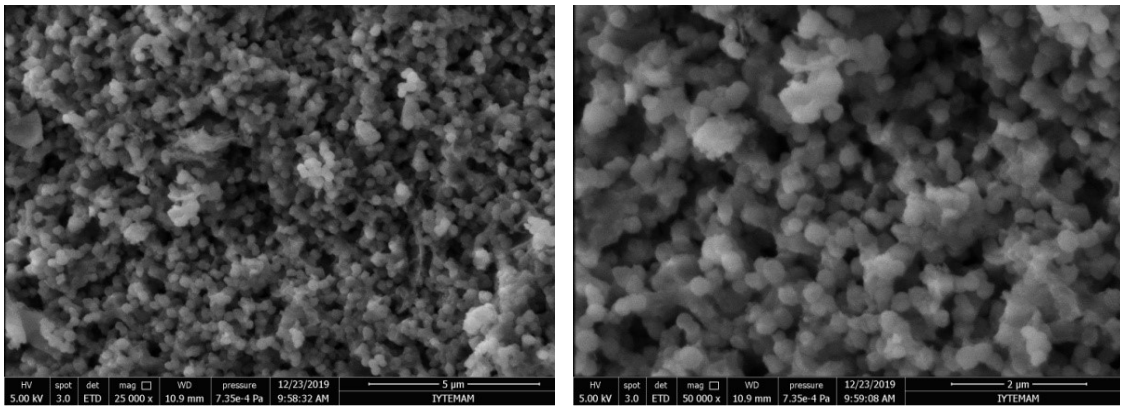

Figure 5.4. SEM images of MSNs.

5.3.2. Polymer Coated C-MSN

The dissolution of curcumin in water was achieved before loading into silica nanopores. For this purpose, a non-ionic surfactant T-X100 was preferred to larger surfactant molecules like P-123 considering the size of the silica pores (below 10 nm). The surfactants form micelles at CMC, but in order not to allow micelle formation, T-X100 concentration was kept below CMC and added dropwise to the curcumin-water mixture.

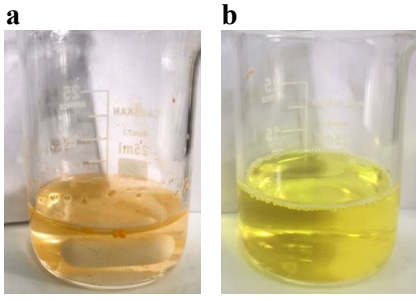

Figure 5.5. Solubility of curcumin a) free form and b) TX-100 molecules in water.

The loading efficiency of curcumin into the pores of silica nanoparticles was found to be as high as 85.7%. The entrapment efficiency of drugs is regarded as one of the most important parameters in the evaluation of drug delivery systems.

SEM images shows that, the curcumin loaded xylan/chitosan-coated MSNs were roughly spherical and non-uniform in size with a range of diameter of 250-400 nm (Fig. 5.6). The increase in the size of these particles suggests that the coating with xylan and chitosan was carried out successfully. The relatively wide range in the size distribution may have been due to the lack of homogeneity of polymers during. After coating with polymers, the nanoparticles tend to aggregate, due to the high density of polymers which results in coalescence. The presence of small and large fragments by the input of energy during nanoparticle synthesis can be another factor (Andreani et al. 2014).

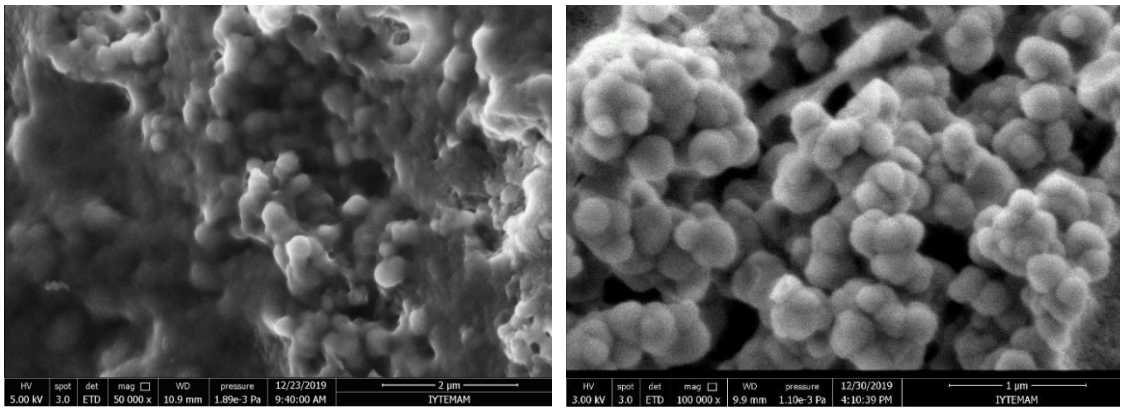

Figure 5.6. SEM images of curcumin loaded and xylan/chitosan-coated MSNs.

To coat MSNs, two physical interactions between the polymers (xylan/chitosan) and the cross-linking agent (TPP) had been utilized. The relationship between polymers consists of hydrogen bonds and electrostatic interactions between O–H, N–H groups in chitosan molecules and O–H groups in xylan molecules. Another interaction is caused by negatively charged oxygen on the cross-linking agent TPP and positively charged amine groups on chitosan (Luo et al. 2014; Xu et al. 2012).

The zeta potentials of the coated and uncoted MSNs were presented in Figure 5.7 Uncoated MSNs were charged negatively with a median zeta potential of around -22.53 mV. Whereas the zeta potential of the polymer coated MSNs increased to +5.14 mV due to the presence of abundant NH_2 groups on chitosan. The results confirmed that polymers were coated on the MSNs.

The cationic nature of chitosan may offer many advantages for colon-targeted delivery applications. Several studies have revealed that the cationic surface of nanocarriers has a great influence on its therapeutic efficacy. As the interaction between the cationic nanocarrier and the negatively charged intestinal mucosa promotes better contact with the mucosal surface, makes it a promising strategy for adhesion, cellular uptake or drug release and an advantage for GIT targeting (Coco et al. 2013; Han, Shin and Ha 2012; Gradauer et al. 2013).

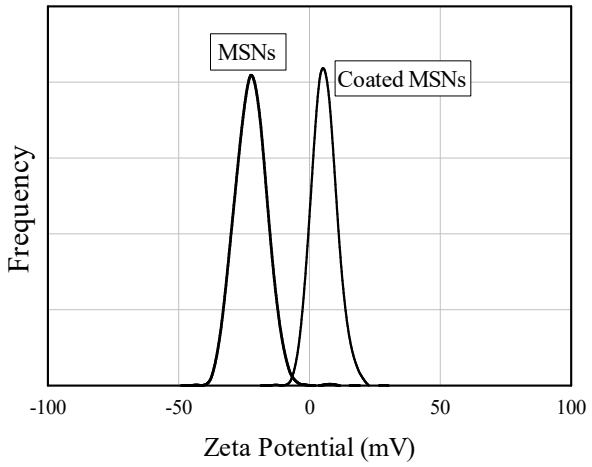

Figure 5.7. Zeta potential of coated and uncoated silica nanoparticles.

The FT-IR spectra for coated and uncoated MSNs display an absorption band at around 1080 cm^{-1} and 805 cm^{-1} which is assigned to the asymmetric vibration of the Si–Oi–O and symmetric vibration of the Si–O bond, respectively (Fig. 5.8). In the coated MSNs, the shifting of the characteristic band of chitosan was observed because of the potential interaction of protonated amine/amide groups and a negatively charged TPP. The amide band shifted from 1650 cm^{-1} to 1640 cm^{-1} and similarly, the amine band at 1588 cm^{-1} shifted to 1518 cm^{-1} (Azhary et al. 2019; Loutfy et al. 2016). The band at 898 cm^{-1} can be assigned to the asymmetric stretching vibration of the P−O−P bridge. The absorption bands at around 2921 and 2877 cm^{-1} can be attributed to C-H stretching which are characteristics band of polysaccharides. In addition, the bands of COO- group from to glucuronic acid units were observed at 1620 and 1466 cm^{-1} (García-Uriostegui et al. 2018). Furthermore, the bands at 1502 cm^{-1} (C=O and C–C vibrations), and 1265 cm^{-1}

(aromatic C–O stretching vibration) that are the characteristic bands of curcumin were observed (Anitha et al. 2012). All these facts suggest that xylan/chitosan-coated C-MSNs were successfully obtained.

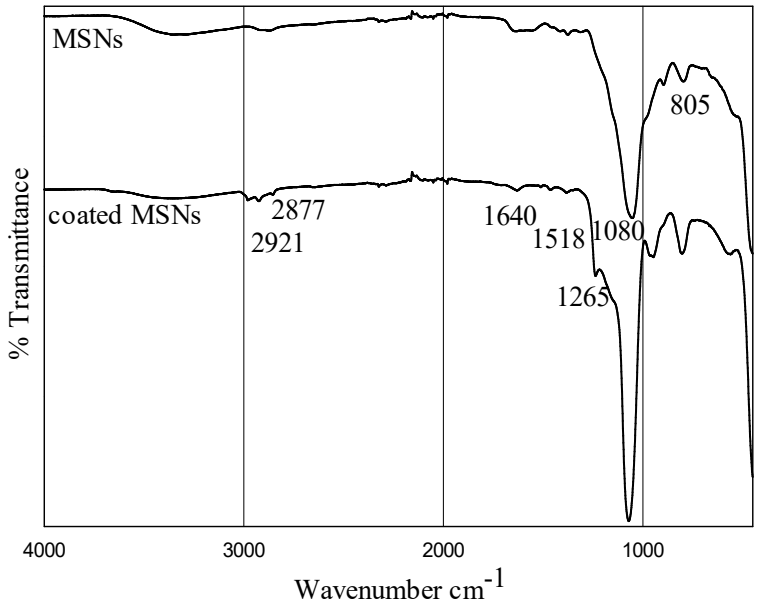

Figure 5.8. FT-IR spectra of pure materials, MSNs, and coated MSNs.

The nitrogen adsorption isotherms for the MSNs, C-MSNs and polymer coated C-MSNs are shown in Figure 5.9. According to the Brunauer-Deming-Deming-Teller classification, the MSNs had a type IV adsorption isotherm, characteristic of hexagonal ordered mesoporous silica with small pore width. On the other hand, C-MSNs and polymer-coated C-MSNs isotherms corresponded to type II due to their nonporous or some macroporous nature (Thommes et al. 2015; Sneddon, Ganin, and Yiu 2015). The low nitrogen adsorption after loading and coating with polymers affirmed that pores were mostly blocked. The specific surface area and the pore volume were calculated using the BET method (Table 1). The surface area, pore volume, and pore diameter of MSNs were 665.95 m^2/g, 0.48 cm^3/g, and 2.9 nm respectively. After curcumin loading or coating with polymers, the decrease in surface area and pore volume were prominent.

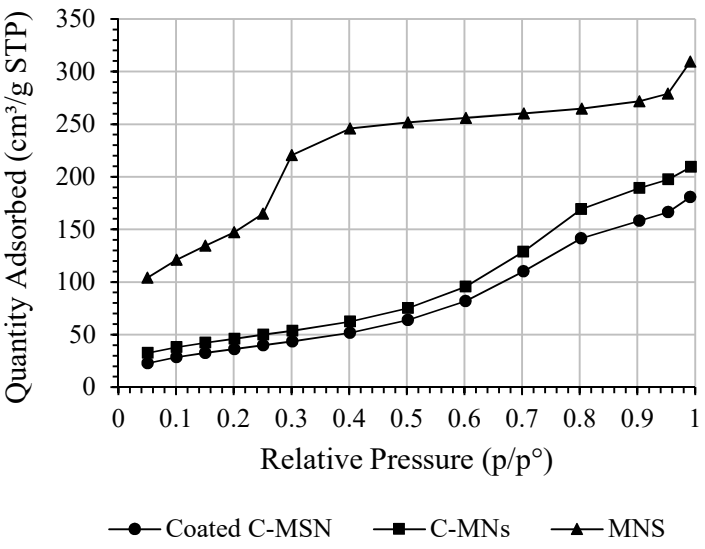

Figure 5.9. N_2 adsorption-desorption isotherms of nanoparticles.

Table 5.1. The surface area, pore volume, and pore size of nanoparticles.

Sample	Surface area (m^2/g)	Pore volume (cm^3/g)	Pore size (nm)
MSNs	665.95	0.48	2.87
C-MSNs	168.68	0.32	5.63
Coated C-MSNs	140.19	0.27	-

5.3.3. Stability of C-MSNs at Upper GIT pH

To simulate upper GIT transit following oral administration, the nanoparticles were tested at pH 1.2 (stomach) and pH 7.4 (small intestine), at 37 °C with stirring at 100 rpm (Fig. 5.10). At pH 1.2, a high amount of burst drug release was not observed in both particles at the end of the 30 min. Curcumin release of uncoated MSNs and coated MSNs was 29.88% and 10.01%, respectively. However, in the following 30 min, the difference was clearly observed. While a small increase was observed in the polymer-coated MSNs, the curcumin release reached 73.0% with a rapid increase in the uncoated MSNs. The drug release of uncoated MSNs increased steadily and at the end of the incubation, the almost all curcumin was released (99.5%). The release in polymer-coated MSNs at the

end of incubation was 17.8%. These results clearly demonstrate the effect of polymer coating of MSNs in inhibiting drug loss through the upper GIT pH.

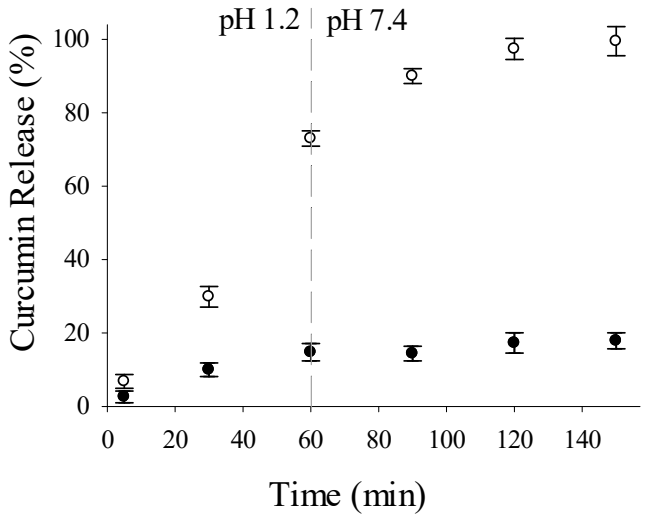

Figure 5.10. The effect of the upper GIT pH on curcumin release (open: uncoated C-MSNs, cloesed: coated C-MSNs).

In pharmaceutical technology, the protection of carrier materials from the harsh conditions of GIT (e.g., low pH in the stomach and enzymatic degradation in the small intestine) is a key issue. Some polysaccharides can maintain their structure through the physiological environment of the GIT and can only be degraded by bacterial polysaccharidases. Particularly, microbially activated polymeric systems are less affected by physiological factors, such as GIT transit time, pH, osmotic pressure, or disease conditions (Sinha and Kumria, 2001). Chitosan is widely used in drug delivery systems, however its utilization in colon-specific delivery requires modifications or alternative approaches. Since chitosan dissolves in dilute acid, chitosan based matrices are unstable in the stomach. The polymer-coated MSNs prepared in this study were resistant the low pH of the stomach so that, drug was protected. Thus, the stability can be attributed to the xylan component in the chitosan-xylan composite coating (Sinha and Kumria, 2001; McConnell, Murdan, and Basit 2008; Silva et al. 2007).

5.3.4. Curcumin Release

The release of curcumin from the polymer-coated C-MSNs by bacterial activity was monitored. The Basal medium at pH 6.8 containing nanoparticles was inoculated by *B. ovatus*. The xylan in the coating was sole carbon source in the culture medium. Before the release test, nanoparticles were pre-imcubated at the upper GIT pH as described above. Spontaneous release of curcumin was also monitored, as the control.

The non-bacterial curcumin release was an average of 7.45% in the first h, and increased slightly to 10.2% in 48 h (Fig. 5.11). *B. ovatus* dependent curcumin release, it was 7.5% in the first h, it increased rapidly over the 24 h to 46.1%. And at the end of the fermentation, 53.4 % of the curcumin was released. The results showed that nanoparticles can release drugs owing to the saccharolytic activity of bacterial species localized in the colon.

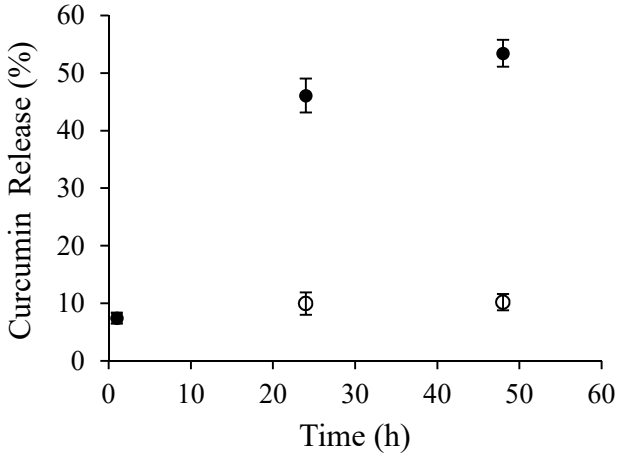

Figure 5.11. The release of the xylan/chitosan-coated C-MSNs
with and without bacterial degradation at pH 6.8 (closed: with; open: without).

Xylan-chitosan coated MSNs were prevented premature drug release in upper GIT pH and released curcumin by activating microbiologically. Besides the targeted delivery, coating material xylan can improve the colon health of the host by inducing the proliferation of beneficial bacteria. Xylan is considered an emerging prebiotic carbohydrate. The health-promoting effects of prebiotic substrates are generally attributed to the induction of beneficial species and the production of short-chain fatty acids

(SCFA). Although xylan is mostly not fermented by beneficial bacteria (e.g. *Bifidobacterium* species), the various in vitro and in vivo studies showed that it can induce an increase of beneficial species and SCFA production (Neyrinck et al. 2011; Nielsen et al. 2014; Van den Abbeele et al. 2011). This is associated with the substrate cross-feeding phenomenon between some species in the colon. An example of this is the cross-feeding of xylan between *Bact. ovatus* and *B. lactis*. While drug release occurs with the utilization of xylan by *Bact. ovatus*, *B. lactis* can increase their number owing to the cross-feeding interaction and contribute to organic acid production. When they were incubated together in the drug release medium, succinate (0.70 mM), lactate (2.99 mM), and acetate (6.90 mM) were produced (Table 5.2). It has been reported in previous studies that *Bacteroides* and *Bifidobacterium* could not produce succinate and lactate as end products, respectively (Chassard et al. 2008; Louis and Flint 2009; Macfarlane and Macfarlane 2003; Hughes et al. 2007). The presence of both lactate and succinate in addition to acetate indicated that the two species were actively growing and released as a result of their fermentative metabolism.

Table 5.2. Organic acid produciton

Sample	Time (h)	Succunate (mM)	Lactate (mM)	Acetate (mM)
Coated C-MSNs	24	0.38 ± 0.054	2.8 ± 0.13	5.3 ± 0.09
	48	0.70 ± 0.22	2.9 ± 0.44	6.9 ± 1.05

5.3.6. Cytocompatibility of Nanoparticles

In addition to the efficient delivery of therapeutic molecules, the biocompatibility of any carrier formulation is an important consideration for bio-applications. Silica-based materials are considered "generally safe (GRAS)" materials by the United States Food and Drug Administration (US-FDA). However, several factors affect the biocompatibility of MSNs, such as size, morphology, and surface chemistry. For example, the silanol groups in the outer layer, a negative zeta potential, particle sizes, and any coating materials of MSNs can affect biocompatibility while also affecting biological parameters (Chen, Chen and Shi 2013; Kankala et al. 2020; Niculescu 2020; Jafari et al. 2019; Manzano and Vallet-Regí 2020).

The cytocompatibility of the nanoparticles on $CaCo_2$ cells was examined by the MTT assay. The cell viability after the 24 h cultivation of cells in the nanoparticle-containing medium is shown in Figure 5.12. The results did not show any significant cytotoxic ($p< 0.01$) effect for MSNs and polymer-coated MSNs even for high concentrations (500 µg/mL). These results indicate the xylan and chitosan that cross-linked with TPP provide a non-toxic coating on the MSNs. Our results suggest that the synthesized carriers do not cause any cytotoxic effect and it can be used in biological applications.

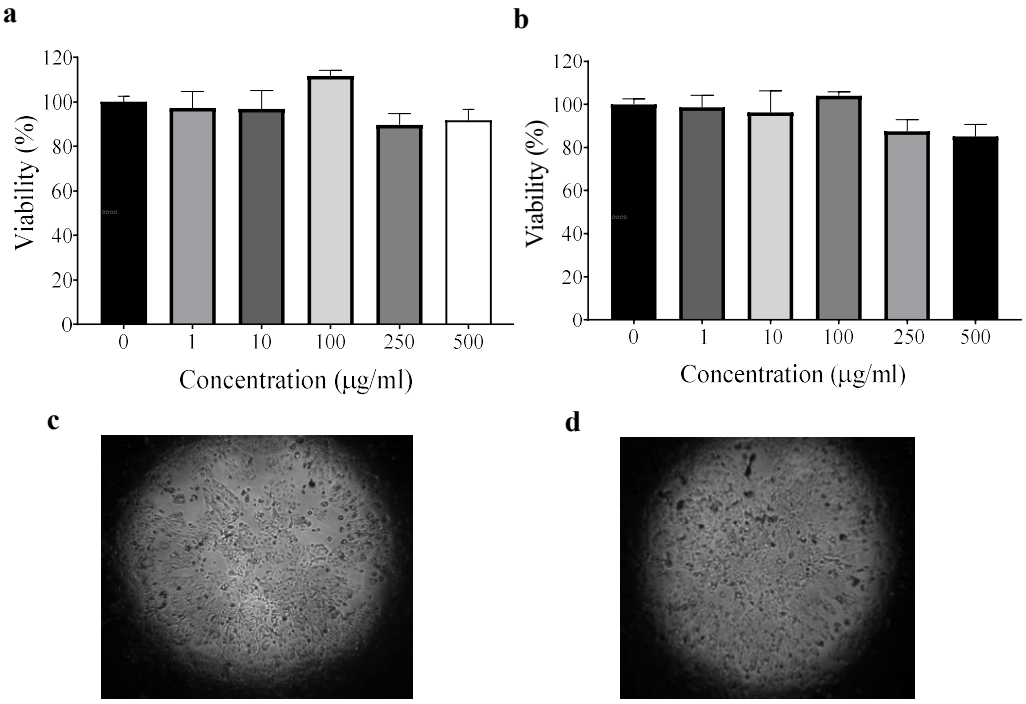

Figure 5.12. MTT assay for cytocompatibility of the MSNs (a) and polymer coated MSNs (b) with $CaCo_2$ cell line. Morphology of cells before treatment (c) and after treatment with 500 µg/mL of coated MSNs (d).
Results represent mean cell percent viability ± S.D. of triplicate determination.

5.4. Conclusions

In summary, this study demonstrated a facile strategy to a combination of an inorganic-polymeric nanohybrid system based on MSNs and xylan/chitosan for use in colon targeted drug delivery. Although MSNs have been preferred widely as drug carriers due to their hydrophilicity, biocompatibility, and modifiable properties premature release is one of the well-documented disadvantages. The coating of MSNs is a very rewarding oral administration approach that both protects them and allows drug release in the colon. This study was able to show that, xylan coating of curcumin-loaded MSNs as a shell prevented drug release from MSNs in the upper GIT pH, and bacterial degradation of xylan allowed the colon targeted curcumin delivery. In addition to demonstrating the usability of xylan as a natural, biodegradable, low-cost polymer in drug delivery systems, increasing the number of beneficial bacteria and SCFA production can provide a promising advantage to improve colon health.

CHAPTER 6

PRODUCTION OF CURCUMIN LOADED BIODEGRADABLE BIOFOAMS

6.1. Introduction

Tissue engineering is an alternative and promising approach to develop biological substitutions that restore, maintain, or improve the function of tissue or organ. To replace or repair damaged tissues, it is necessary to create an environment that supports the ability of cells to integrate, differentiate and proliferate (Jagur-Grodzinski 2009; Eltom, Zhong, and Muhammad 2019). Growth factors and extracellular matrix (ECM) components are used to induce the proliferation and differentiation of cells (Celikkin et al. 2017). The creation of the environment to hold this structure together is usually accomplished by the implantation of three-dimensional (3D) scaffolds. The scaffold provides a framework and assists in the proliferation, differentiation, and migration of the cell (Briquez and Hubbell 2020; Howard et al. 2008). Regardless of the type of tissue, several important matters like biocompatibility, biodegradability, proper mechanical properties, architecture, and physico-chemical properties of scaffold surfaces should be considered to design and produce scaffolds.

Bioactive material-loaded foams, sheets, or films have been produced as scaffold for different purposes like antimicrobial, antifungal, anti-inflammatory, and tissue repair. This approach is very exciting to be able to develop a more effective technique for tissue therapy by taking advantage of the synergistic effect of the drug delivery and scaffold system. Many types of active molecules can be loaded into synthetic or natural polymeric scaffolds by using different methods (Barroso et al. 2014; Yang et al. 2017; Tejada et al. 2017). The controlled drug release mechanism from scaffolds can maintain an effective treatment process around the tissue by keeping the drug concentration the therapeutically minimum effectiveness and preventing using a high dose of the drug. Many studies have been designed scaffolds for the controlled and sustained release of therapeutic agents (Zhang et al. 2017; Li et al. 2017; Ong et al. 2018; Álvarez et al. 2020; Wei et al. 2020;

Obayemi et al. 2020; Moradi Kashkooli, Soltani and Souri 2020). The release of active molecules from scaffolds is dependent on a variety of factors, including the environment and the structural features of the scaffold. In order to modulate this system in accordance with the purpose, it is necessary to determine and evaluate these factors well. The release of active materials can be controlled by the structural features of the scaffolds (pore sizes and interconnectivity), the chemical structures of drugs, the physicochemical properties of scaffolds, and environmental factors.

Scaffolds used in tissue engineering have been classified in different ways. Classifications can be made depending on the starting raw material, production method or the form of the resulting scaffolding structure (Dhandayuthapani et al. 2011). The most common forms of scaffolding structure are hydrogels scaffold, fibrillar scaffold, and porous matrix or foams. Hydrogels can be broadly defined as a three-dimensional network of hydrophilic polymers. Hydrogels, which have high swelling and water retention ability, are used in a wide variety of applications such as drug delivery, wound healing, cosmetology and tissue engineering. It is formed by chemical or physical cross-linking of hydrophilic amino, carboxyl and hydroxyl groups in polymer chains (Singh et al. 2016).

Three-dimensional polymeric or ceramic porous scaffolds or foams with interconnected pore networks create a very favourable attachment and proliferation environment for cells in tissue engineering applications (Zhang and Ma 1999). A porous matrix, including interconnected pores, provides a large surface for cells to form their own ECM. This network structure also acts as a channel for the transport of nutrients, oxygen and waste products. Moreover, they prevent the formation of very large clusters that can cause a necrotic centre (Dhandayuthapani et al. 2011). Polymeric porous or foam scaffolds can be produced by conventional techniques (solvent casting and particulate leaching, melt molding, emulsification polymerization/freeze-drying, gas foaming, thermally-induced phase separation) or advanced fabrication techniques (electro-spinning, rapid prototyping, 3D Printing) (Eltom, Zhong, and Muhammad 2019; Mabrouk, Beherei, and Das 2020; Li et al. 2014; Wang, Huang, and Zhou 2020). The template-polymerization route, which will also be used in our study, is one of the most common methods used to produce porous foams. While template materials can be chosen as gas, liquid or solid, polymerization can be achieved by freeze drying or evaporation of solvent or by use of a suitable cross-linking agent. In liquid templated method, a biphasic system is generated and then the continuous phase is polymerized (Silverstein 2014). The

volatile liquid phase is removed following polymerization to create porosity in the final polymeric material. Depending on the nature of emulsion, pore size can vary from nanaometer to micrometer.

Polysaccharides have remarkable physicochemical and physiological properties such as biocompatibility, biodegradability, and low immunogenicity, which are important for biomedical applications (Prasher et al. 2021). Therefore, they are receiving widespread attention for tissue engineering applications (Sood, Gupta and Agrawal 2021). The xylan containing scaffolds produced for different tissue applications are described below.

Xylan/chitosan/nano-hydroxyapatite composite matrix (Ali, Hasan, and Negi 2022) and xylan/chitosan/montmorillonite composite scaffold (Ali et al. 2019) were produced for bone tissue engineering application. Hydroxyapatite and montmorillonite (nano-clays) are most commonly used in hybrid structure for increasing mechanical properties of scaffold in the bone tissue applications. Bush et al. (2016) developed a composite hydrogel containing xylan and chitosan for the healing of bone fractures. This injectable hydrogel improved the response of animal host tissue and accelerated the healing of bone fractures compared to similar pure chitosan hydrogels in tissue engineering models. They concluded that, the successful application of xylan to fracture healing could reveal a new class of hemicellulose polymers. Additionally, xylan/polyvinyl alcohol (PVA) nanofibrous scaffolds cross-linked with glutaraldehyde were produced for myocardial infarction (Venugopal et al. 2013) and skin tissue engineering (Krishnan et al. 2012). Moreover, xylan has been incorporated into hydrogel production by blending with other natural or synthetic materials (Liu et al 2019; Ai et al. 2021; Köhnke et al. 2014). García-Uriostegui et al. (2018) produced a hybrid hydrogel based on spruce xylan, 2-hydroxyethyl methacrylate (HEMA), and mesoporous silica for the use of the fibroblast attachment and growth. They functionalized xylan with acryloyl chloride to introduce vinyl groups and was crosslinked by radical polymerization with HEMA in presence of mesoporous silica. The use of silica particles was increasing the mechanical properties of the hydrogel as well as to favor interconnected porous structure.

In this chapter, bioactive molecule loaded xylan and xylan-chitosan composite biofoams were produced for tissue engineering application. Curcumin was used as a model hydrophobic molecule. To produce curcumin-loaded biofoams, firstly, curcumin was encapsulated in the hydrophobic core of P-123 micelles by the thin-film hydration method (See Chapter 3) and then, the O/W emulsion templated method was used to

produce biofoams. While xylan foams were crosslinked with CTAB, composite biofoams were crosslinked with SDS and/or TPP, and the effects of the cross-linking agents were investigated. Curcumin release from biofoams was evaluated in physiologic buffer solutions. The fibroblast (3T3-L1) cell line was used to examine cell adhesion to biofoams.

6.2. Materials and Methods

Low molecular weight chitosan, poly(ethylene glycol)-block-poly(propylene glycol)-block-poly(ethylene glycol) (P-123), sodium dodecyl sulfate (SDS), cetyltrimethylammonium bromide (CTAB), sodium tripolyphosphate (TPP), and curcumin were of analytical grade and purchased from Merck (Darmstadt, Germany). Beechwood xylan which composed of (w/ w) xylose (80.8 %), glucuronic acid (11.4 %), other sugars (4.9 %), protein (0.3%), ash (2.4%), and moisture (2.4%) was purchased from Megazyme (Bray, Ireland).

The Mus musculus fibroblast cell line 3T3-L1 was purchased from American Type Culture Collection (ATCC) (Rockville, MA, USA).

6.2.1. Biofoam Production

To produce cur-P123 micelles loaded biofoams, two procedures were combined (Fig. 6.1). The thin-film hydration method was used for the entrapment of curcumin in P-123 micelles to increase its bioavailability (See 3.2.1). The oil in water (o/w) emulsion templated synthesis was used to create porous biofoams. In the first part, the thin film which curcumin and P123 contained was hydrated with the polymer solution. The aqueous phase forces the curcumin molecules energetically into the hydrophobic core of the P-123 micelles. To create an o/w emulsion, hexane (%12.0) was used as an oil phase and the ultrasonic probe was used to disperse oil droplets in the continuous phase. The polymerization was carried out by using TPP, SDS, or CTAB as a cross-linking agent. The matrix was poured into a mold with 9.5 mm thickness and 20 mm diameter. Freeze-drying was applied to remove hexane which creates the pores of the biofoams.

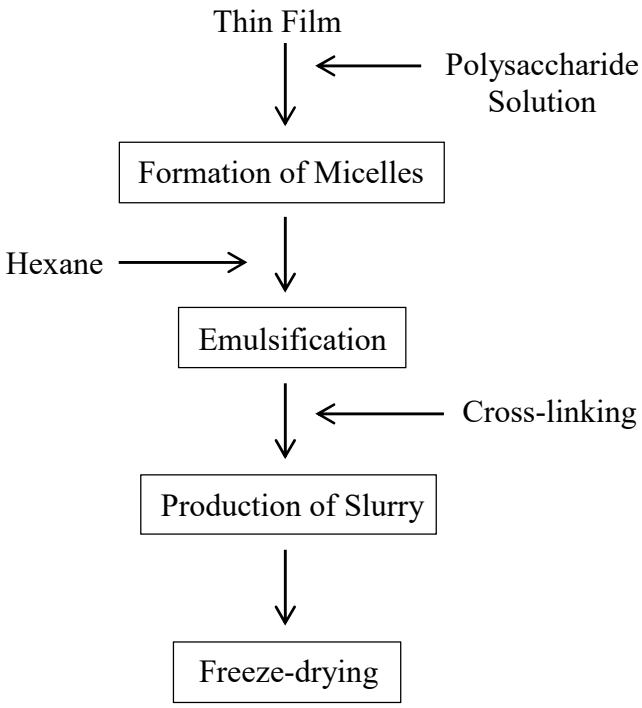

Figure 6.1. Production of cur-P123 micelles loaded biofoams (see Fig. 3.1 for thin film formation).

6.2.2. Characterization Studies

Morphology: The surface and internal microstructure of the biofoams were examined using scanning electron microscopy (SEM) (Philips, XL-30S FEG). The freeze-dried biofoams were sectioned into thin slices by razor blade were mounted on aluminium holders with aluminium tape. All samples were coated with a thin layer of Au before analysis for the conductivity of the samples.

Structure: FT-IR spectra of all pure materials and biofoams were obtained using an FT-IR spectrometer (Perkin Elmer-UATR Two, USA) at range of 400-4000 cm^{-1}.

Porosity: The porosity of the biofoams was measured by a liquid displacement method. Ethanol was used as the displacement liquid, which is generally preferred as it can easily penetrate into pores and does not cause shrinkage and swelling. The biofoams were immersed in a graduated cylinder filled with a known volume of ethanol V_1. The total volume after biofoam immersion was recorded as V_2. Then the biofoam was removed and the residual ethanol volume in the cylinder was measured as V_3. The percentage of porosity was determined using Eq. 6.1.

$$\text{Porosity}\ (\%) = \frac{V_1 - V_3}{V_2 - V_3} \times 100 \tag{6.1}$$

Swelling: For determining swelling behaviour, the dry weight of each biofoam was determined before immersion (W_d). Afterwards, the biofoams were immersed in phosphate buffer solution at pH 7.4 and kept at temperature of 37°C. After 4 and 24 h, the biofoam surface adsorbed water was removed by filter paper and wet weight (W_w) of the biofoam was determined using an electronic balance. The ratio of swelling was determined as per the Eq. 6.2.

$$\text{Swelling Ratio}\ (\%) = \frac{W_w - Wd}{W_d} \times 100 \tag{6.2}$$

The Specific Surface Area and Porosity: The specific surface area and porosity measurement of the biofoams was performed by the Brunauer, Emmet and Teller (BET) method in liquid nitrogen environment at 77 K, based on nitrogen (N_2) gas adsorption technique.

Mechanical Strength: For determination of mechanical properties, compressive tests were performed by TA.XTplus Texture Analyser (Surrey, UK). The biofoams with the dimension of approximately 9.5 mm thickness and 20 mm diameter were used. Across head speed of 0.5 mm/sec, with % 40 strain and 49.0 N load cell at room temperature was used. Each biofoam was repeated in four times to assure reproducibility.

6.2.3. Curcumin Release

In vitro release of cur-P23 micelles was evaluated in phosphate buffer solution at ph 7.4 and 5.5. Biofoams containing 0.3 mM curcumin were tested in 50 mL buffer solution and incubated in a shaking incubator at 37°C with 100 rpm. At regular time intervals, the samples were collected and replaced with the equivalent volume of fresh medium. The amount of curcumin released into the medium was analyzed by UV-vis spectroscopy at 420 nm. The percentage of released curcumin was determined by using Eq. 6.3.

$$\text{Curcumin Release \%} = \frac{\text{Released curcumin}}{\text{Total curcumin}} \times 100 \quad (6.3)$$

6.2.4. In-vitro Cell Culture

For in vitro cell culture studies 3T3 mouse embryonic fibroblasts was used. The growth medium was Dulbecco's Modified Eagle Medium (DMEM) containing 10% fetal bovine serum (FBS) and 1% penicillin-streptomycin. For the growth of the cell line, incubation was carried out 21 days in an oven with 95% humidity and 5% CO_2 at 37 °C. The procedure applied to thaw the 3T3 cells stored in the freezer and to reach the appropriate form for the tests was as follows: Firstly, frozen cells were quickly thawed in a 37°C water bath. Then, it was transferred to a centrifuge tube containing DMEM at the appropriate temperature (37°C). After centrifuging the cell suspension, the supernatant was removed. Pellet (cells) were resuspended in the growth medium and incubated in flasks. Cells were passaged when 80% confluent in the flask (2-3 times per week). Passage numbers were kept between 15-30 throughout the experiments.

Adherent cultures need to be passaged by transferring them to a new vessel a fresh growth medium while in the log phase before reaching confluence. Because cells stop growing due to contact inhibition and take longer to recover when reseeded, they do not provide a suitable cell suspension for further experiment. The procedure of passaging, which is the transfer of cells from a previous culture to a fresh growth medium, is as follows: After removing the old cell culture medium, the cells were gently washed to remove all traces of serum, calcium and magnesium that would inhibit the action of the dissociation reagent. After the washing liquid was removed, adequate trypsin was added to cover the cell layer and incubated at 37°C for 2 min. After observing under the microscope that the cells were completely detached, DMEM was added to terminate the reaction. The cell suspension diluted to the desired density was thoroughly pipetted, transferred to new flask.

Assessment of Attachment and Morphology of 3T3 Cells on Biofoams:

Biofoams of uniform size (15 mm diameter and 5 mm thickness) were sterilized by ultraviolet light (UV) for 30 min. Then, the biofoams were kept in a CO2 incubator in 24-well cell culture plates with a complete medium for 1 h to balance the system. Cells

that had reached 80% confluency were detached with trypsin, then diluted and seeded on the biofoam in each well. The cell-free biofoam was used as a control. Cells were allowed to attach on and in the biofoams in an oven with 95% humidity and 5% CO_2 at 37°C. For the examination of 1 day-old fibroblast morphology, the media was removed from cell culture wells and biofoams were washed three times with PBS buffer to remove unattached cells. After that, the samples were fixed in 2.5% glutaraldehyde for 2 h at 4°C. The biofoams were then rinsed with distilled water for 10 min and dehydrated in graded ethanol solution (50%, 70%, 90%, 95%, and 100% v/v) each for 5 min and freeze-dried. Cell morphology was observed by using SEM. For the sample preparation, lyophilized biofoams were attached to the sample holder with aluminium tape and coated with a thin layer of gold before analysis.

6.3. Results and Discussion

6.3.1. Curcumin Loaded Xylan Biofoams

To produce xylan biofoams, CTAB was used as the cross-linking agent. Beechwood xylan has a negative charge due to glucuronic acid substitutions. The electrostatic interaction was used between xylan and negatively charged CTAB to polymerization. The composition of xylan biofoams contained 0.3 mM curcumin is given in Table 6.1. The characterization studies of the xylan biofoams are shown in Figure 6.2.

Table 6.1. The composition of xylan biofoams.

Code	Xylan (%)	CTAB (mM)
XF-1	3.0	10.0
XF-2	4.0	10.0
XF-3	5.0	10.0

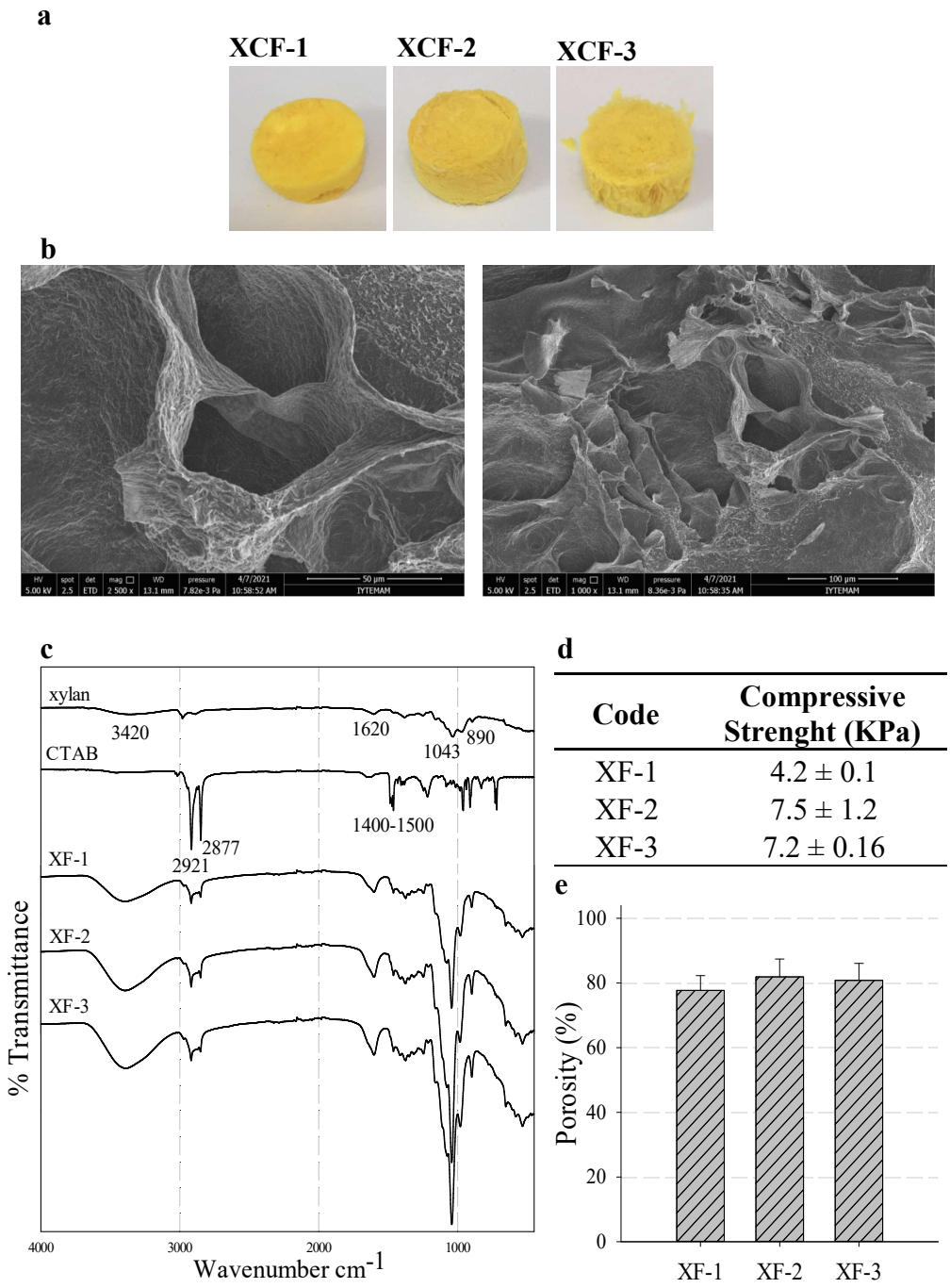

Figure 6.2. Characterization of curcumin loaded xylan biofoams. a) physical appearance; b) SEM images; c) FT-IR spectrum; d) mechanical properties; e) porosity.

The pore size and structure of biofoams were characterized by SEM (Fig. 6.2b). The xylan biofoam with pore diameters of 50-100 µm can be clearly observed. Porosity is one of the important parameters in scaffold production. Scaffolds should have sufficient porosity for nutrient and gas exchange, removal of metabolic waste products, cell

migration and vascularisation required for new tissue formation. It has been reported in different studies that an ideal scaffold should have more than 80 % porosity (Ikeda et al. 2014; She et al. 2018). The porosities of the all xylan biofoams reached to about 80% (Fig.6.2e). These results are consistent with the SEM analysis.

The FT-IR spectra of pure materials and xylan biofoams are shown in Figure 6.2c. The beechwood xylan exhibited an absorption band at 890 cm^{-1} is attributed to the characteristic of β-glucosidic linkage between the xylose units. The band at 3420 cm^{-1} is attributed to the stretching of -OH group, and also the bands between 1465-1043 cm^{-1} arise from the stretching and bending vibration of C-O, C-C and C-OH groups (Kumar et al. 2018). The bands of COO- group from to glucuronic acid units were observed at 1620 and 1466 cm^{-1} (García-Uriostegui et al. 2018). The absorption bands at around 2921 and 2877 cm^{-1} can be attributed to C-H stretching. These are characteristics band of polysaccharides (Antunes et al. 2015). In the spectrum of xylan biofoams, the strong and wide band in the biofoams at 3450 cm^{-1} arises from the stretching vibration of hydroxyl groups of the polymer. The strong absorption bands at 2920 and 2854 cm^{-1} are attributed to the C−H stretching vibration of methyl and methylene groups of CTAB. (Sornalatha and Murugakoothan 2013). The bands at the region of 1400−1500 cm^{-1} arise from the C−H bending. Since, the entrapment of curcumin in micelles, the characteristic bands of curcumin at 1605 cm^{-1} (stretching vibrations of benzene ring), 1502 cm^{-1} (C=O and C–C vibrations), and 1285 cm^{-1} (aromatic C–O stretching vibration) (See Fig. 3.8) were hardly seen in biofoams (Butt et al. 2012; Zhang et al. 2011; Anitha et al. 2012). All these facts suggest that cur-P123 micelles-loaded xylan biofoams were successfully obtained.

The scaffolds need to have sufficient mechanical stability to withstand the stress experienced during in vitro culturing and in vivo implantation and to provide adequate physical support to the cells. Many factors such as the natural mechanical properties of the scaffold components, their ratios, interactions to each other, and cross-linking characters can contribute to the mechanical response (Olad and Azhar 2014). The compressive strength of the xylan biofoams are given in Fig. 6.2d.

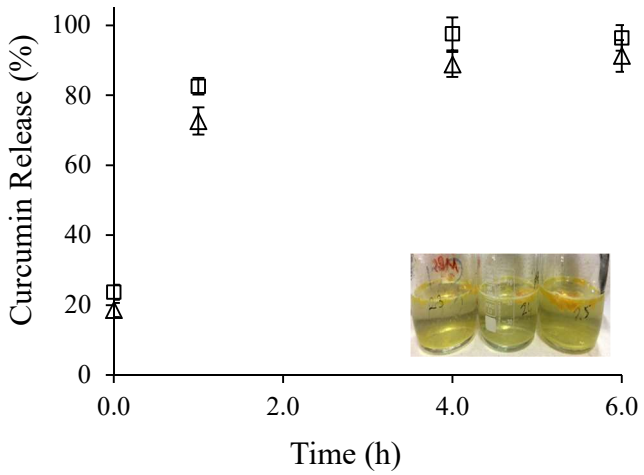

Figure 6.3. Curcumin release from xylan biofoams.
(triangle: XF-2, square: XF-3)

The curcumin release profile of xylan biofoams at pH 7.4 are presented in Figure 6.3. A significant amount of curcumin (70-80%) was released from xylan biofoams within the first h. In the following incubation, almost all curcumin was released and after 6 h the xylan biofoams were completely dissolved. The xylan biofoams in the phosphate buffer after 6 h can be seen in the figure.

Complete dissolution of xylan biofoams within 6 h is not suitable for use as scaffolds. Scaffolds need to maintain their structure longer for cells attachment, differentiation and migration. However, xylan biofoams that decompose in shorter times can be developed for alternative applications. It may be applicable for wound dressing applications containing active substances that affect wound healing after surgical procedures.

6.3.2. Curcumin Loaded Xylan-Chitosan Composite Biofoams

Crosslinking the polymeric chains of xylan with CTAB to form a 3D network did not provide adequate biostability. Xylan biofoams could not withstand the physiological environment to allow the differentiation of cells. Therefore, xylan was combined with another natural polymer, chitosan to produce more durable xylan-based biofoams.

Chitosan has been blended with collagen (Kaviani et al. 2019), hydroxyapatite, gelatin (Shen et al. 2015; Kuo et al. 2015), and silk fibroin (Li et al. 2019) to produce

composite materials for tissue engineering applications. Chitosan can provide many advantages for scaffold structure. It can mimic the extracellular matrix (ECM) environment due to its similarity with glycosaminoglycans. Its positively charged backbone allows cell attachment-proliferation and facilitates the formation of new tissue. Chitosan does not trigger the immune response because decomposition products are not toxic or carcinogenic. It has an antimicrobial activity that allows protection from microbial deterioration.

The mechanical strength and biostability of biofoams can be improved by the interconnection of polymeric chains with cross-linking agents. In composite biofoams, the cross-linking agent was used only for the polymerization of chitosan. Xylan was incorporated into the system by interacting with chitosan (described in the next section). Ionic (eg, triphosphate, hyaluronic acid, and alginate) or covalent crosslinking agents (glutaraldehyde and genipin) can be used for the polymerization of chitosan. The most commonly used negatively charged tripolyphosphate (TPP) can interact with positively charged chitosan by electrostatic forces. Additionally, negatively charged SDS was used as an alternative crosslinker because of the brittleness of composite biofoams crosslinked with TPP.

6.3.2.1. Cross-linking with TPP

To produce composite biofoams, two physical interactions between the polysaccharides (xylan/chitosan) and the cross-linking agent had been utilized. The relationship between polysaccharides consists of hydrogen bonds and electrostatic interactions between hydroxyl, amine groups in chitosan molecules and hydroxyl groups in xylan molecules (Umemura and Kawai 2008). Another interaction is caused by negatively charged oxygen on the TPP and positively charged amine groups on chitosan (Luo et al. 2014; Xu et al. 2012). The composition and physiochemical properties of composite biofoams contained 0.3 mM curcumin is given in Table 6.2. The mechanical strength of composite biofoams was quite low. The swelling ratios could not measure due to their high brittleness. Only the porosity of XCF-3 was measured and it was observed to have a highly porous structure (95.0%). The physical appearances are shown in Figure 6.4.

Table 6.2. Composition and physiochemical properties of composite biofoams cross-linked with TPP.

Code	Xylan (%)	Chitosan (%)	TPP (%)	Compressive Strenght	Porosity (%)	Swelling Ratio
XCF-1	1.5	1.5	1.5	Brittle	Nd	Nd
XCF-2	1.0	1.0	1.5	Brittle	Nd	Nd
XCF-3	1.5	1.5	2.0	Brittle	95.0	Nd

Nd: could not measured due to high britillness.

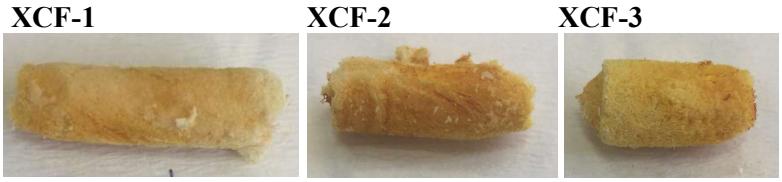

Figure 6.4. Curcumin loaded composite biofoams crosslinled with TPP.

The morphological properties of the biofoams were investigated by SEM (Fig. 6.5). Composite biofoams cross-linked with TPP actually had a highly porous structure. However, a complete pore form could not be observed by SEM due to their brittleness. During the sample preparation, biofoams were sectioned into thin slices and mounted on aluminum holders. This process caused the pore walls to mostly break.

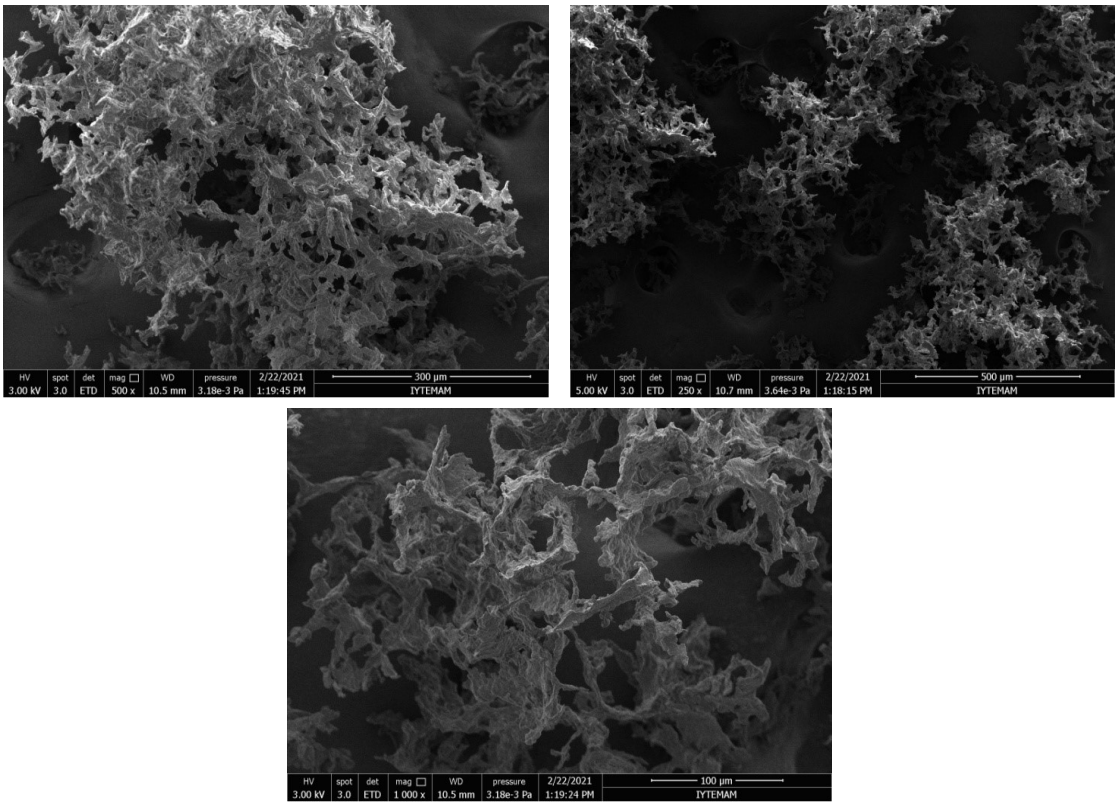

Figure 6.5. SEM images of XCF-2

The FT-IR spectra of pure materials and composite biofoams are shown in Figure 6.6. In the spectrum of pure chitosan and xylan, the absorption band at 3420 cm^{-1} was ascribed to deformation vibration of both O–H and N–H stretching vibrations. In the spectra of chitosan/xylan composite biofoams, the absorption bands of O–H and N–H became wider and stronger, and they shifted to the lower wavenumbers. This indicating that there might be strong hydrogen bonds and electrostatic interactions between the O–H, N–H groups in chitosan molecules and the O–H groups in xylan molecules (Umemura and Kawai 2008). The bands at 2882–2988 cm^{-1} were also sharper which could be based on the presence of more number of C–H groups in the biofoams. In the spectrum of the pure chitosan, the characteristic bands were observed at 3435 cm^{-1} (O-H stretching), 1651 cm^{-1} (amide linkages) and 1588 cm^{-1} (primary amine linkages). In the composite biofoams, shifting of these bands was observed because of the potential interaction of protonated amine and/or amide groups and a negatively charged cross-linking agent. The amine band at 1588 cm^{-1} shifted to 1545 cm^{-1} and similarly, the amide band shifted from 1648 cm to 1637 cm^{-1}. Since, the entrapment of curcumin in micelles, the characteristic

bands of curcumin at 1605 cm^{-1} (stretching vibrations of benzene ring), 1502 cm^{-1} (C=O and C–C vibrations), and 1285 cm^{-1} (aromatic C–O stretching vibration) (See Fig. 3.8) were hardly seen in biofoams (Butt et al. 2012; Zhang et al. 2011; Anitha et al. 2012). All these facts suggest that cur-P123 micelles-loaded xylan/chitosan composite biofoams were successfully obtained.

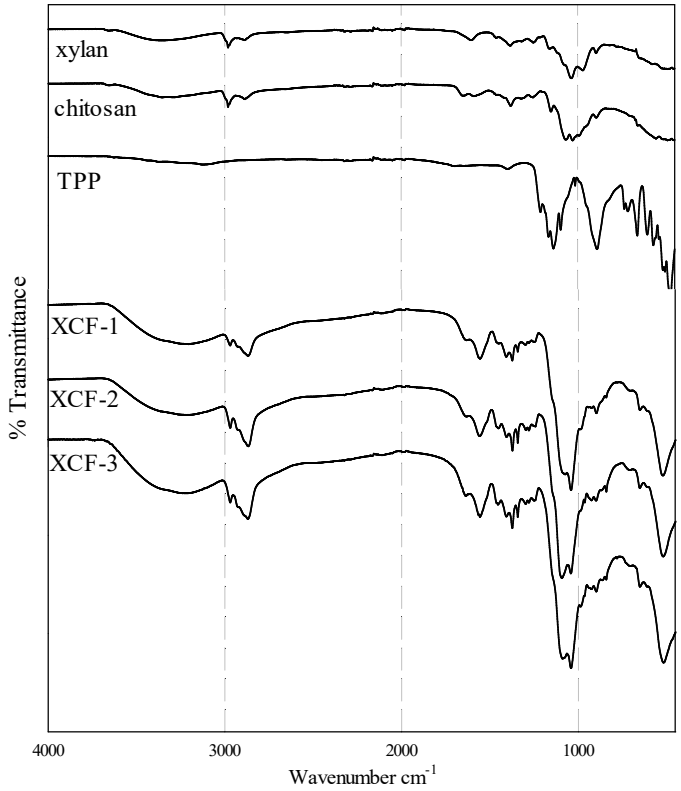

Figure 6.6. FTIR specturum of pure mateails and composite biofoams crosslinked with TPP.

The curcumin release from composite biofoams is presented in Figure 6.7. Since XCF-1 was quite brittle, it could not be included in the relase studies. XCF-2 and XCF-3 released around 20% of curcumin in the first 4 h. Although the xylan biofoams dispersed within the first 6 h, the composite biofoams were intact throughout the incubation. The biofoams in the phosphate buffer can be seen in the figure.

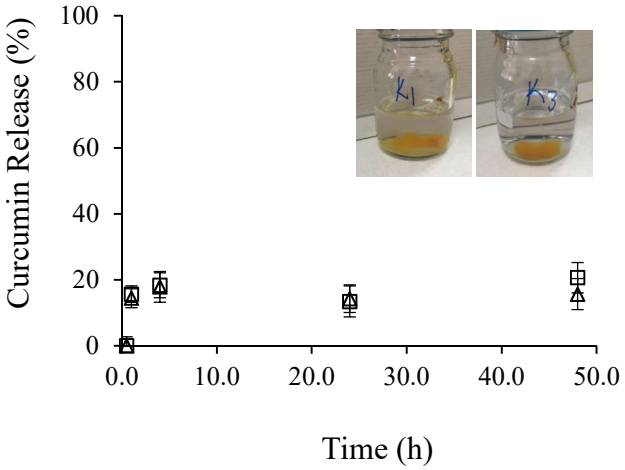

Figure 6.7. Curcumin release from composite biofoams crosslinked with TPP. (sqaure: XCF-1; triangle: XCF-3).

6.3.2.2. Cross-linking with TPP and SDS

Composite biofoams were more stable under physiological conditions than xylan biofoams. However, composite biofoams showed a rather brittle structure and did not have sufficient mechanical strength as a scaffold. Besides the nature of the polymers, the crosslinking agent quite affects the strength of scaffolds. Since TPP has caused brittleness in biofoams, an alternative crosslinking agent SDS was added to the system. As in the previous composite biofoams, the relationship between polymers was still utilized. Moreover, SDS has a negative charge like TPP and it can crosslink chitosan to form a 3D network. In this section, the effect of SDS on the system was examined. Also, the effect of polymer ratios on biofoams was investigated. The composition and physiochemical properties of composite biofoams contained 0.3 mM curcumin is given in Table 6.3. While keeping the chitosan concentration constant, the xylan concentration was gradually increased. The physical appearances are shown in Figure 6.8.

Table 6.3. The composition of composite biofoams.

Code	Xylan (%)	Chitosan (%)	TPP (%)	SDS (mM)
XCF-4	0.5	2.0	2.5	10
XCF-5	1.0	2.0	3.0	10
XCF-6	2.0	2.0	4.0	10
XCF-7	3.0	2.0	3.0	10

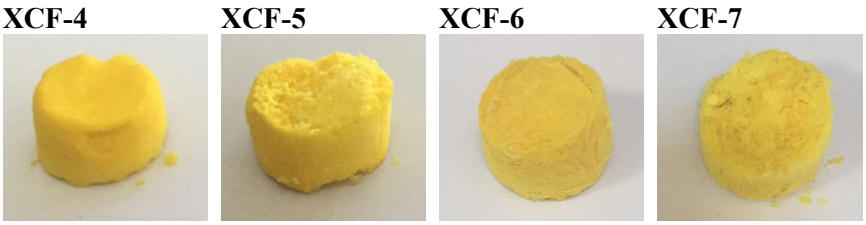

Figure 6.8. Curcumin loaded composite biofoams cross-linked with TPP and SDS.

The morphological characterization of the curcumin loaded composite biofoams were characterized by SEM and presented in Figure 6.9. Composite biofoams have a highly porous structure. In addition to the large pores around 150 µm, there were smaller pores of around 20-30 µm. Pore diameters are very important for cell attachment and proliferation. The optimal pore size of scaffolds is dependent on the type of tissue (Kramschuster and Turng 2012). Although the optimum pore size has been most studied for bone regeneration, it is still a controversial. For example, different studies have suggested optimal pore sizes for bone tissue between 50-710 µm and 150-350 µm (Agrawal and Ray 2001; Yang et al. 2001; Karande, Ong, and Agrawal 2004). Pores of 200 to 300 µm are required for growth of fibrocartilaginous tissue and 5 µm for neovascularization (Kramschuster and Turng 2012; Yang et al. 2001). Although no consensus regarding the optimal pore size in scaffolds, it is generally assumed that pores below 10 µm are small for cells (Zhong et al. 2011). However, smaller pores in scaffolds can generate interconnectivity and transport nutrients, oxygen or waste products. Thus, the macro and micro porous structure can provide the optimum environment for cells to grow.

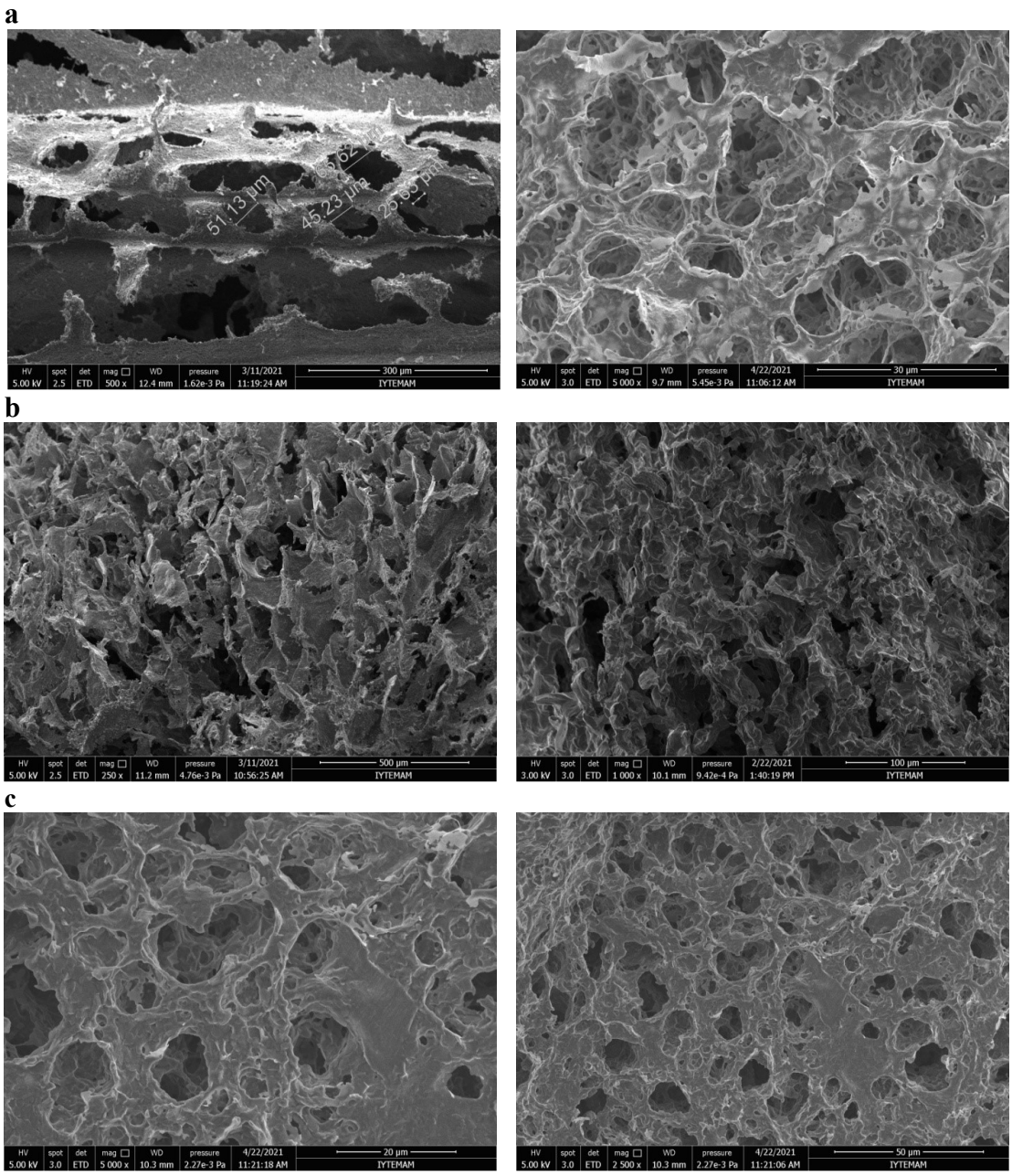

Figure 6.9. SEM images of composite biofoam cross-linked with SDS and TPP. a) XCF-4, b) XCF-7, and c) XCF-6.

The FT-IR spectra of pure materials and composite biofoams are shown in Figure 6.10. The characteristic bands of chitosan, xylan, and TPP have been described in detail in the previous section. In the spectra of chitosan/xylan composite biofoams, the absorption bands of O–H and N–H became wider and stronger, and they shifted to the lower wavenumbers. It indicating that there might be strong hydrogen bonds and

electrostatic interactions between the chitosan and xylan (Umemura and Kawai 2008). The bands at 2882–2988 cm^{-1} were also sharper which could be based on the presence of more number of C–H groups in the biofoams. In the composite biofoams, shifting was observed at the characteristic bands of chitosan because of the potential interaction of protonated amine and/or amide groups and a negatively charged cross-linking agent. The amine band at 1588 cm^{-1} shifted to 1545 cm^{-1} and similarly, the amide band shifted from 1648 cm to 1637 cm^{-1}. Since, the entrapment of curcumin in micelles, the characteristic bands of curcumin at 1605 cm^{-1} (stretching vibrations of benzene ring), 1502 cm^{-1} (C=O and C–C vibrations), and 1285 cm^{-1} (aromatic C–O stretching vibration) (See Fig. 3.8) were hardly seen in biofoams (Butt et al. 2012; Zhang et al. 2011; Anitha et al. 2012). In addition, bands in the 2850-2950 cm^{-1} band for the characteristic C-H stretch of SDS were also appeared in biofoams crosslinked with SDS. All these facts suggest composite biofoams were successfully obtained.

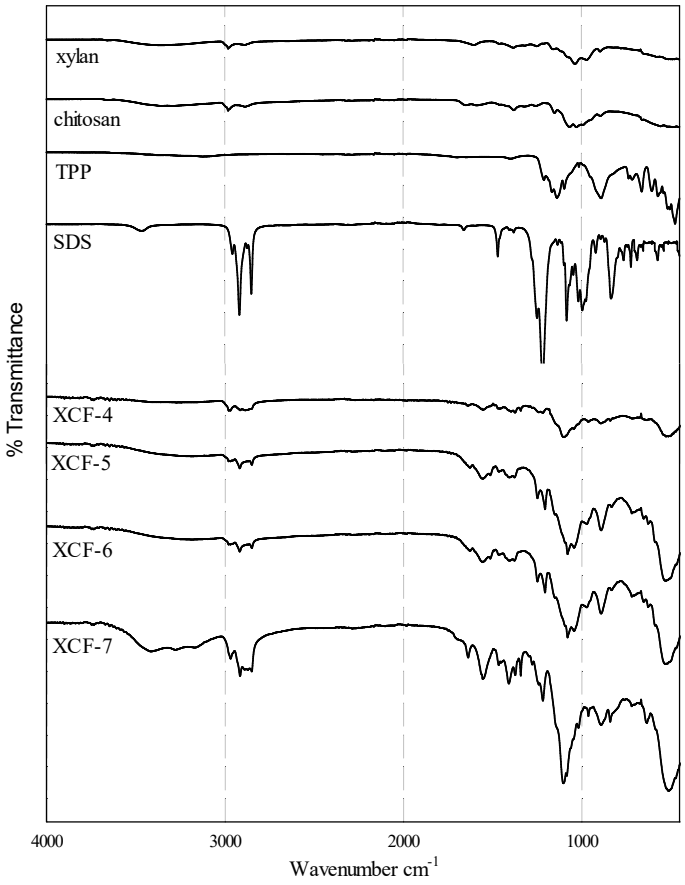

Figure 6.10. FTIR specturum of pure materials and composite biofoams crossllinked with SDS and TPP.

The swelling ability of scaffolds is very important for the absorption of body fluid and transfer of cell nutrients and metabolites. The degree of scaffold swelling is highly dependent on the pore size, interconnectivity conditions, and higher values result in a larger surface area to volume ratio. It facilitates the infusion of cells into the scaffolds, allowing the cells to utilize the maximum inner surface of the scaffolds (Olad and Azhar, 2014). The swelling ratios of the biofoams were calculated at 4 and 24 h and they reached their maximum values in 4h. Figure 6.11a and b shows the swelling ratios and structural apparence after swelling of composite biofoams crosslinked with TPP and SDS. They showed approximately 4-5 times swelling.

Porosity, one of the important parameters in scaffold production, is shown in Figure 6.11c. The porosity of the composite biofoams reached to 90%. The change of polymer ratios did not cause a significant difference in porosity. Composite biofoams have a more porous structure than xylan biofoams. This may be due to the formation of additional smaller pores in the structure, which can also be seen in SEM images. As a result, composite biofoams produced with SDS and TPP as crosslinkers met the porosity criteria for scaffolds.

The compressive strength of the composite biofoams are given in Fig. 6.11d. The brittle structure caused by TPP was not observed in composite biofoams produced with SDS and TPP. Moreover, composite biofoams with SDS have higher mechanical strength than xylan biofoams (See Fig. 6.2d).

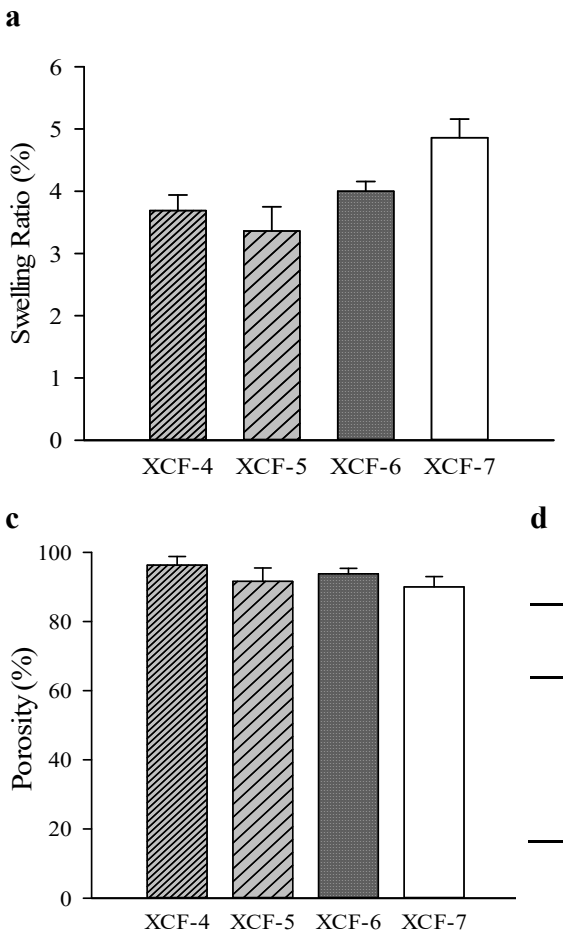

d

Code	Compressive Strenght (KPa)
XCF-4	11.67 ± 1.26
XCF-5	23.0 ± 3.51
XCF-6	15.2 ± 1.20
XCF-7	8.33 ± 0.69

Figure 6.11. Physiochemical characterization of composite biofoams. a) Swelling ratio; b) Physical apperance after swelling; c) Porosity; d) Mechanical properties.

The curcumin release from composite biofoams is presented in Figure 6.12. A significant amounts of curcumin released from the biofoams occurred with burst release within the first 4 h in pH 7.4. The rapid diffusion of curcumin localized on the surface of the biofoams into the phosphate buffer might have caused a burst release of curcumin. Curcumin release continued for up to 48 hours and then remained stable thorough the incubation. The curcumin release in phosphate buffer was reached max 24.9%. It can be clearly seen that as the xylan concentrations of the biofoams increase, the release of curcumin increases in parallel.

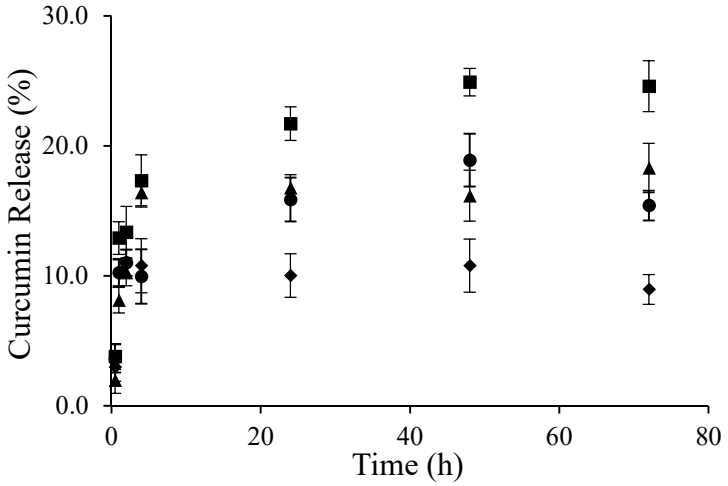

Figure 6. 12. Curcumin release from composite biofoams.
(diamond: XCF-4; triangle: XCF-5; circle: XCF-6; square: XCF-7).

6.3.2.3. Cross-linking with SDS

As a result of the positive effect of SDS on the biofoams, only SDS was used as crosslinking agent. Due to the negative charge of SDS, it can create ionic strength between them with positively charged chitosan. In addition, SDS molecules can be in hydrophobic interactions with hydrophobic tail portions so that polymers can form a more connected structure. As in the previous composite biofoams, the relationship between polymers was still utilized. The composition of composite biofoams contained 0.3 mM curcumin is given in Table 6.4. The physical appearances of the composite biofoams are shown in Figure 6.13.

Table 6.4. The composition of composite biofoams.

Code	Xylan (%)	Chitosan (%)	SDS (mM)
XCF-8	0.5	2.0	10.0
XCF-9	1.0	2.0	10.0
XCF-10	2.0	2.0	10.0
XCF-11	3.0	2.0	10.0
XCF-12	4.0	2.0	10.0
XCF-13	5.0	2.0	10.0
XCF-14	4.0	4. 0	10.0

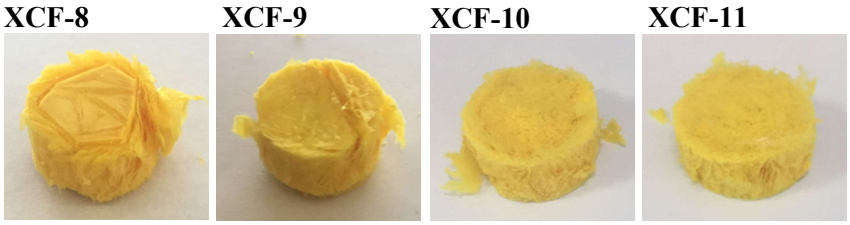

Figure 6.13. Curcumin loaded composite biofoams crosslinked with SDS.

The morphological characterization of the curcumin loaded composite biofoams were characterized by SEM and presented in Figure 6.14. Composite biofoams had a highly porous structure. In addition to the large pores around 100-200 µm, there were smaller pores of around 20-30 µm. As mentioned earlier, porosity and pore diameters are very important for cell attachment and proliferation. The smaller pores in addition larger ones in scaffolds can generate interconnectivity and transport nutrients, oxygen or waste products. The porous structure of composite biofoams can provide the optimum environment for cells to grow.

a

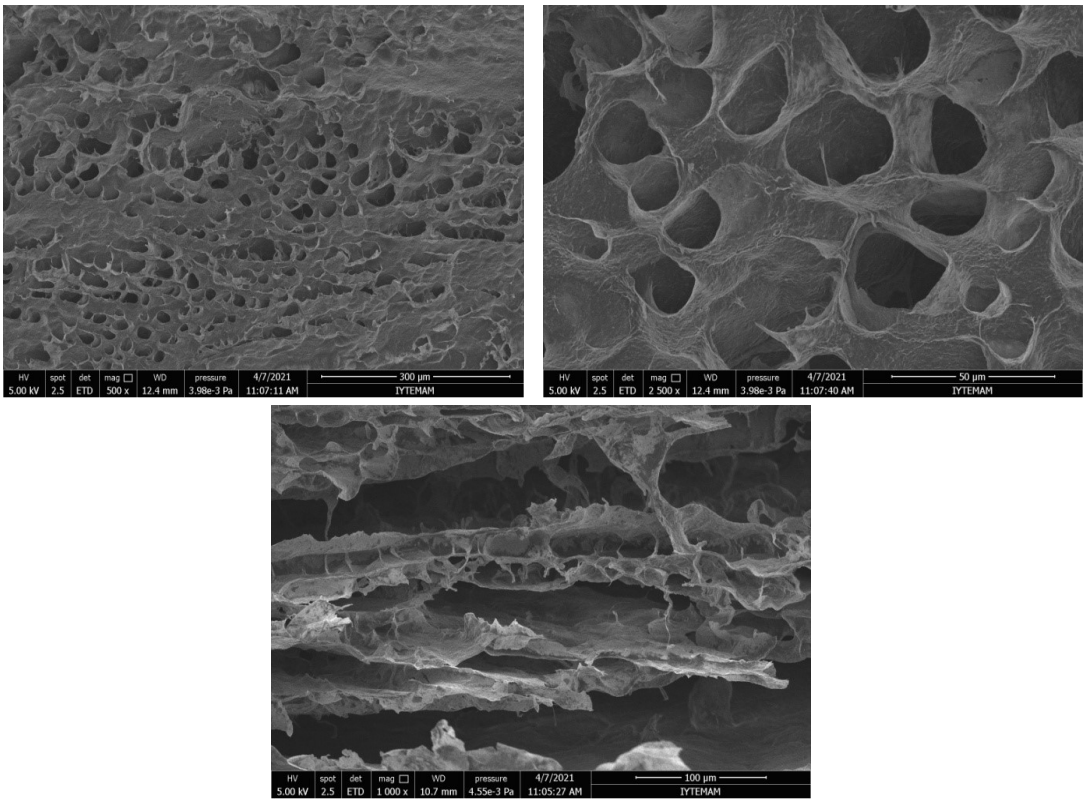

b

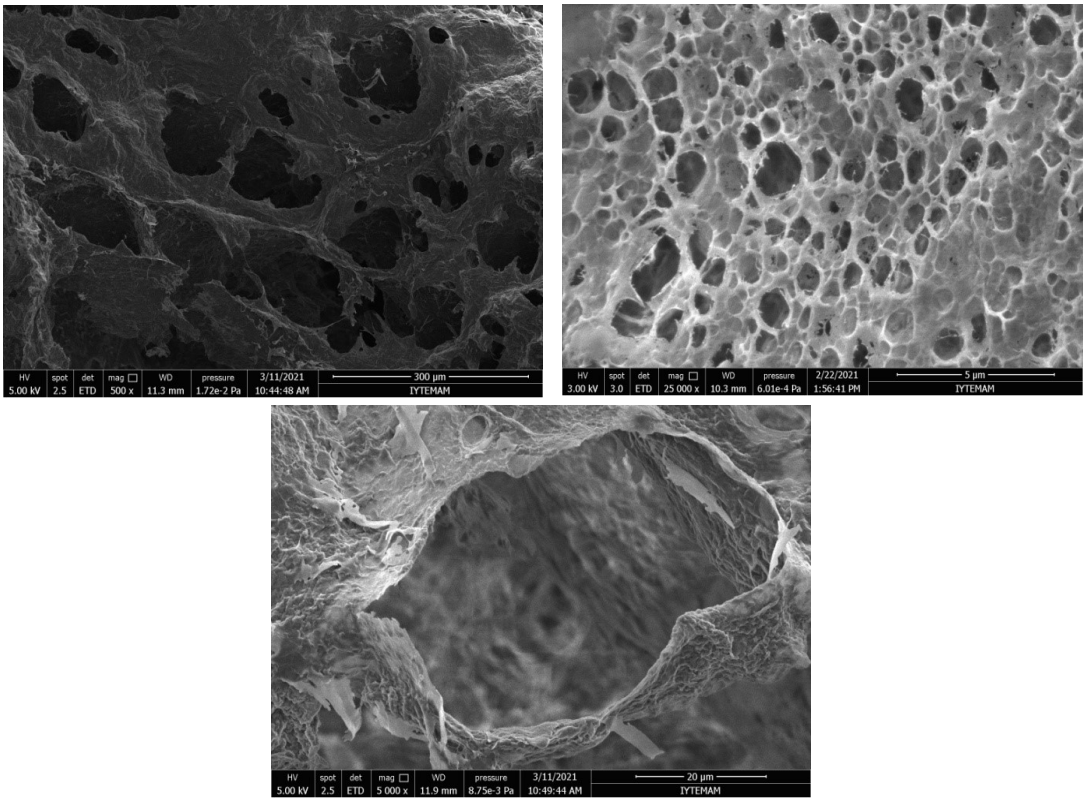

Figure 6.14. SEM images of composite biofoam cross-linked with SDS. a) XCF-8 and b) XCF-11.

The FT-IR spectra of composite biofoams are shown in Figure 6.15. The characteristic bands of chitosan, xylan, and SDS have been described in detail in the previous section. In the spectra of composite biofoams, the absorption bands of O–H and N–H became wider and stronger, and they shifted to the lower wavenumbers (Umemura and Kawai 2008). The bands at 2882–2988 cm^{-1} were also sharper which could be based on the presence of more number of C–H groups in the biofoams. In addition, bands in the 2850-2950 cm^{-1} band for the characteristic C-H stretch of SDS were also appeared in biofoams crosslinked with SDS. Since, the entrapment of curcumin in micelles, the characteristic bands of curcumin at 1605 cm^{-1}, 1502 cm^{-1}, and 1285 cm^{-1} (See Fig. 3.8) were hardly seen in biofoams (Butt et al. 2012; Zhang et al. 2011; Anitha et al. 2012). All these facts suggest composite biofoams were successfully obtained.

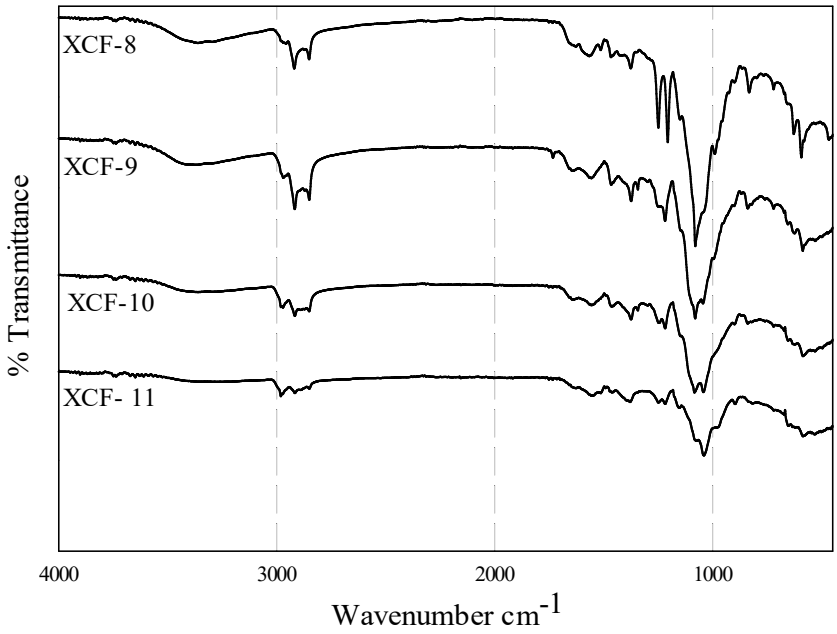

Figure 6. 15. FTIR spectrum of composite biofoams crosslinked with SDS.

The swelling ratios of the biofoams were calculated at 4 and 24 h and they reached their maximum values in 4h. Figure 6.16a and b shows the swelling ratios and structural apparence after swelling of composite biofoams crosslinked with SDS. The biofoams XCF 8-11 showed high swelling capacity around 15-18%. The high swelling capacity of biofoams facilitates the infusion of cells, allowing to utilize the maximum inner surface

(Olad and Azha 2014). When compared to biofoams XCF 4-7 that crosslinked with TPP+SDS (See Fig. 6.11a), XCF 8-11 had 3-4 times higher swelling capacity. The lower swelling in XCF 4-7 might be originated from more cross-linking chains formed by TPP and SDS. At high crosslinker concentrations, polymer chains grow to form high network density. It prevents the movement of the polymeric chain or does not allow water to enter the network, and so reduces the water holding capacity. Another parameter affecting the swelling ratio is the chemical structure of polymers. Those with hydrophobic groups show more swelling. Both TPP and SDS might have reduced the hydrophilicity of the polymers by grafting more hydrophilic NH_2 or OH groups. On the other hand, XCF 12-14 had higher xylan content and it had 10% swelling ratio. The decreasing swelling ratio with increasing xylan concentration can be attributed to the decreased mechanical strength of the pore walls. The inadequate strength of the pore walls may cause them to be unable to retain water. As can be seen in Figure 6.16d, the increase of xylan content in biofoams caused a lower mechanical strength. The biofoams XCF 8-11 had nearly 10 times more mechanical strength than TPP crosslinked foams (XCF 4-7), under the same condition. The mechanical strength has an inversely proportional relationship to the porosity of foams. In the TPP contaning group, both the relatively higher porosity and their cross-linking with TPP might have caused the structural strength values to be lower.

In addition to observing the porous structure with SEM analysis, the porosity was also examined with the liquid displacement method (Fig. 6.16c). The porosity of the composite biofoams was around 85-90%. Increasing xylan content in biofoams (XCF12-14) caused a relative increase in porosity. The lower mechanical strength might have resulted from their higher porosity. Because these two physiochemical properties are inversely proportional to each other.

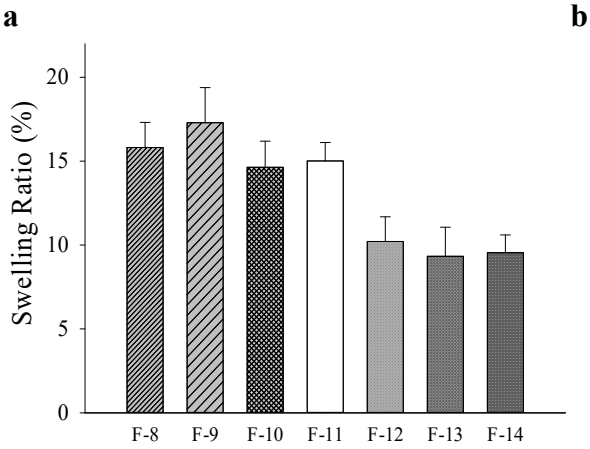

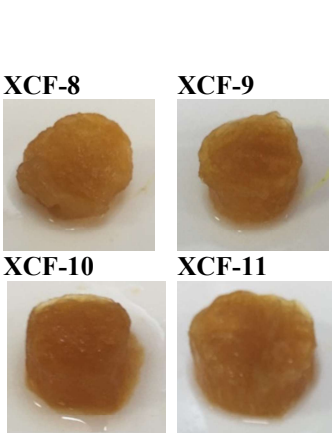

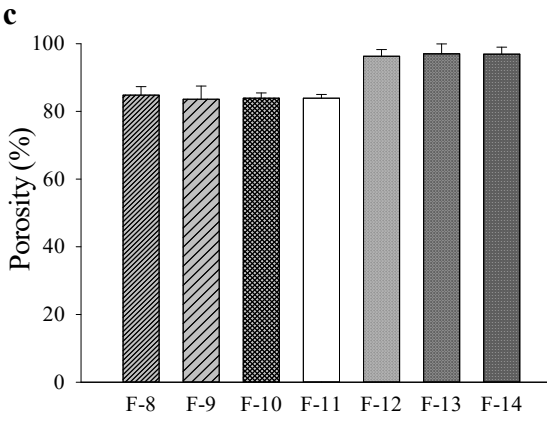

d

Code	Compressive Strenght (KPa)
XCF-8	73.75 ± 2.41
XCF-9	131.0 ± 5.70
XCF-10	99.25 ± 5.45
XCF-11	216.67 ± 19.19
XCF-12	47.0 ± 12.12
XCF-13	37.33 ± 6.65
XCF-14	60.33 ± 17.21

Figure 6.16. Physiochemical properties of composite biofoams. a) Swelling ratio; b) Physical apperance after swelling; c) Porosity; d) Mechanical properties.
Sample names (XCF) were abbreviated as "F" in the a and c.

The N_2 adsorption isotherms are shown in Figure 6.17a. The presence of a sharp adsorption step in the P / P_0 region between 0.9 and 1.00 indicates that the materials process a well-defined and regular array of mesoporous (Wang et al. 2012). The specific surface area and the pore volume were computed using Brunauer-Emmett-Teller (BET) method (Fig. 6.17b).

a

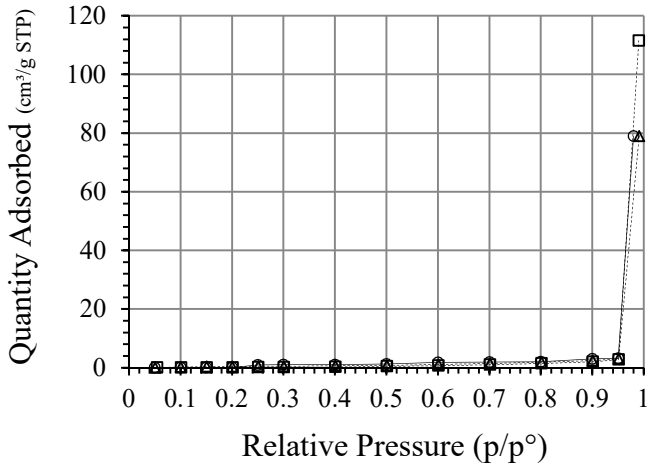

b

Code	Surface area (m^2/g)	Pore-volume (cm^3/g)
XCF-8	2.249	0.122
XCF-9	1.501	0.33
XCF-11	3.317	0.909

Figure 6.17. BET analysis of composite biofoams. a) N_2 adsorption isotherm; b) The surface area, pore volume, and pore size.

The curcumin release from composite biofoams is presented in Figure 6.18. The curcumin release can be characterized as a two-phase: immediate release within the first 4 h and relatively slow release within 48 h. The significant initial burst release might have resulted from the diffusion of curcumin into the phosphate buffer on the surface of the biofoams. After the first phase, curcumin micelles localized in the interior of the biofoams showed a slower release. The maximum curcumin releasing was achieved in the highest xylan-containing biofoams (75.6%). It can be clearly seen that the increase in the xylan/chitosan ratio in biofoams affects the release of curcumin.

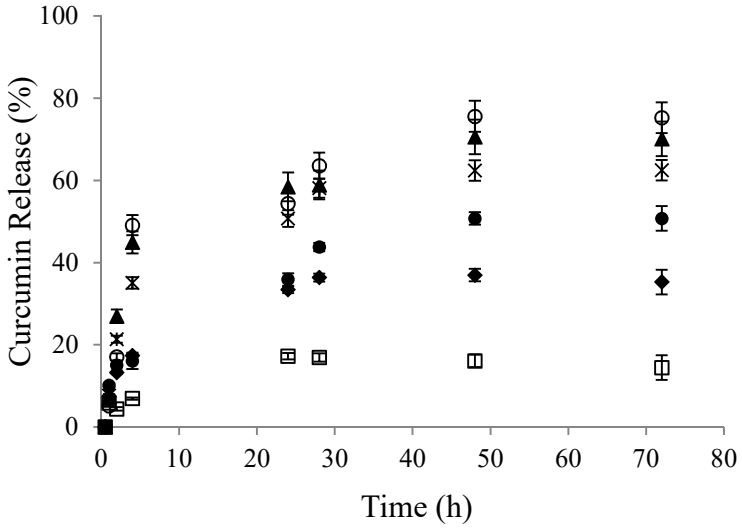

Figure 6.18. Curcumin release from composite biofoams. (open square: XCF-8; diamond: XCF-10; closed circle: XCF-11; star: XCF-12; triangle: XCF-13; open circle: XCF-14.

In order to the observation of cell adhesion on the biofoams, 3T3 fibroblast cell line was used. The spindle-shaped morphology of 3T3 cells under the light microscope can be seen in Figure 6.19.

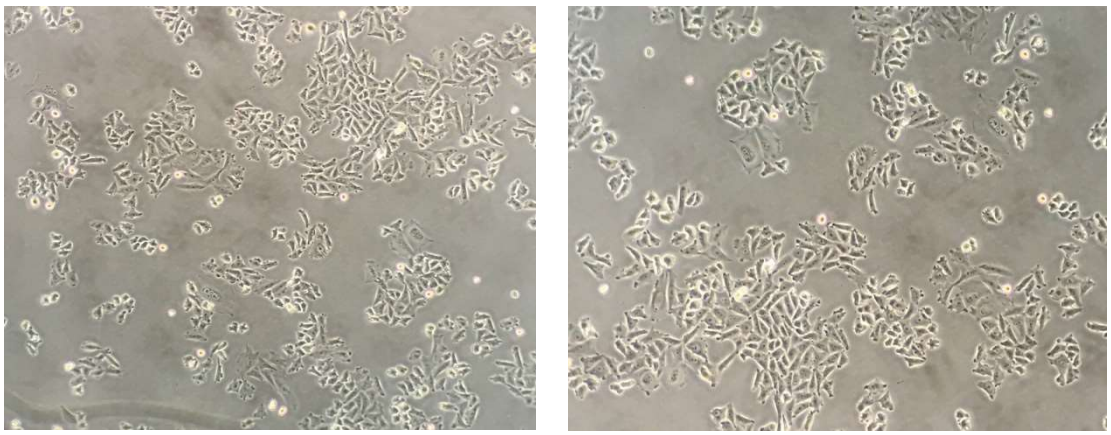

Figure 6.19. Morphology of 3T3 fibroblast cell on light microscope.

Biofoam which did not seed with cells but applied whole cell culture and SEM procedures can be seen in Figure 6.20a. It was used as a control for the comparison of the biofoam surface. Figure 6.20b, showed the morphology of fibroblast cells on the inner

surface of the XCF-10 composite biofoam after 24 h cultivation. When the cells come into contact with the surface, they first adhere loosely. At this initial stage, they have a relatively smooth round shape. Then, the spreading of the cell body begins, forming a type of body extension to form adhesion complexes. The polygonal morphology typical for cell differentiation can be seen in SEM images.

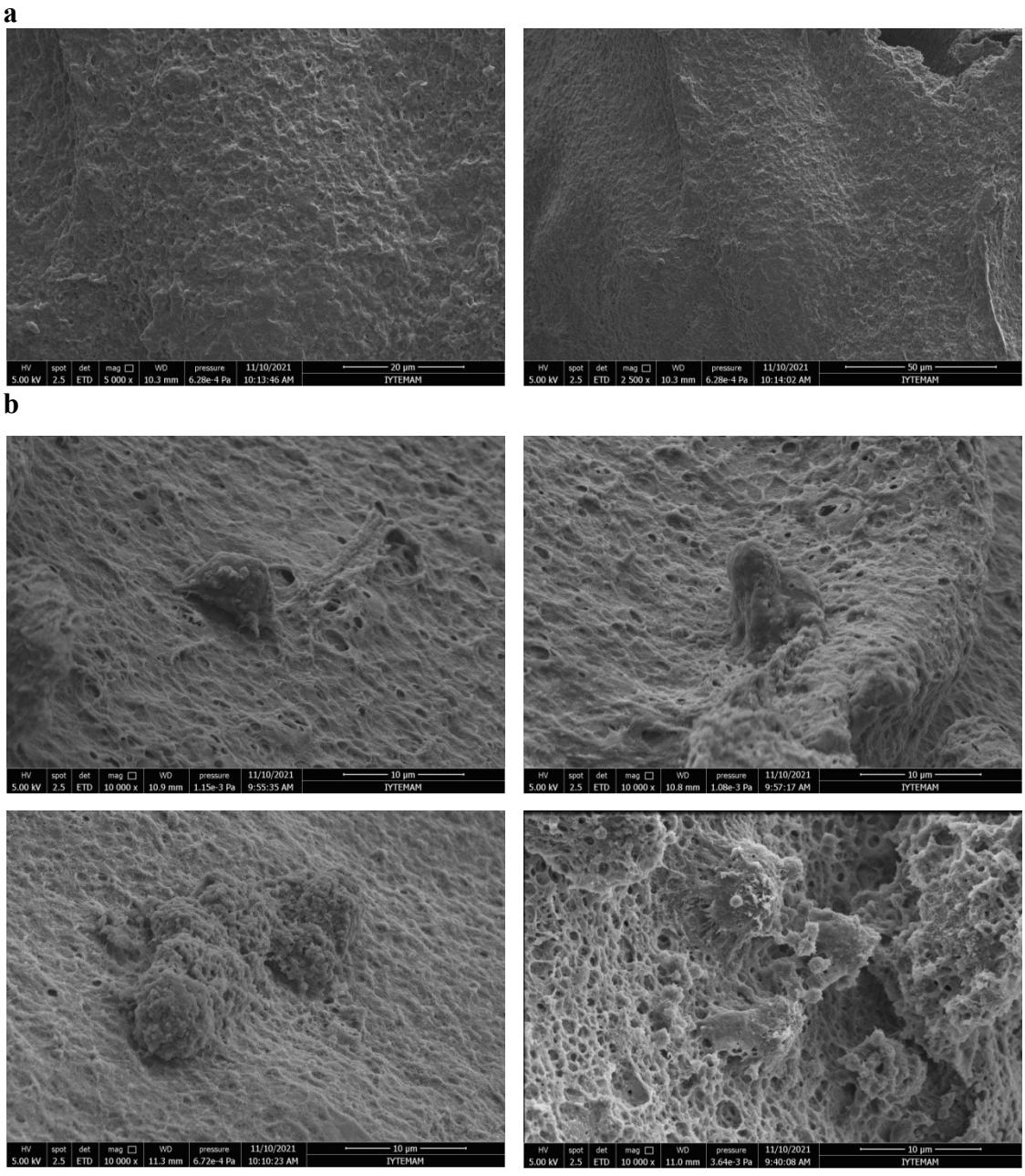

Figure 6. 20. SEM images of attached 3T3 fibroblast cell on composite biofoam XCF-10 after 24 h incubation.

As a result of observation of attached cells on the surface of composite biofoams and the beginning of cell differentiation, it can be assumed that the morphology, interconnectivity, and physicochemical properties of biofoams were convenient for cell adhesion. Composite biofoams have a great potential to provide suitable matrices for cells. They can allow nutrient and gas exchange; help cell migration and vascularisation.

7.4. Conclusions

In summary, this study demonstrated a facile and simple strategy to fabricate xylan-based crosslinked biofoams for use in tissue engineering applications. Curcumin-loaded biofoams were synthesized with thin-film hydration coupled with oil in water emulsion methods. The effect of cross-linking agents on the considerable characteristics of the scaffold such as stability, swelling ability, and mechanical strength of polymers has been clearly demonstrated. The porosity, mechanical strength, and swelling ability are important properties of scaffolds. The xylan biofoams that crosslinked with CTAB had a highly porous structure but did not provide sufficient biostability. The xylan biofoams may be applied for alternative applications that degrade in a shorter time in physiological environments. On the other hand, xylan-based composite biofoams crosslinked with SDS provided convenient porosity, mechanical strength, and swelling ability. The bioactive molecules loaded scaffolds can accelerate tissue healing, cells adhesion, proliferation; and can prevent infections. The curcumin loaded composite xylan based biofoams produced by utilizing the synergistic effect of drug delivery and scaffold system is promising for developing a more effective tissue therapy. The adhesion and differentiation of 3T3 cells on composite biofoams clearly supported that the physicochemical properties of composite biofoams provided a satisfactory framework and can assist new tissue formation.

The results of this study suggest that the development of xylan-based biofoams can provide new approaches for the development of natural and cost-effective biomedical materials that can be used in tissue engineering applications.

CHAPTER 7

SUMMARY AND CONCLUSIONS

Polysaccharides can be presenting important roles in versatile biomedical platforms including drug delivery and tissue regeneration. Polysaccharides are being extensively researched for developing functional biomaterials due to their unique properties like biocompatibility, biodegradability, and structural diversity. In this study, a natural polysaccharide, xylan, was utilized to produce novel smart functional systems to achieve their widespread use in biomedical applications were examined.

In the first part of the study, xylan-based colon-targeted oral drug delivery systems were developed. Xylan degradability by hydrolysis of glycosidic bonds by colonic microbiota was utilized as a trigger mechanism of drug release in colon. Two different approaches were used for the delivery of hydrophobic molecules to the colon by oral administration. Firstly, xylan based composite nanoparticles with polymeric micellar core were produced. In this system, the model hydrophobic molecule, curcumin, was encapsulated in the core of P-123 micelles by thin-film hydration method in order to increase the absorption and bioavailability, transport large amounts of drugs into a cell, and provide separated functionality. To protect the curcumin-loaded micelles from the external environment, they were coated with xylan to form a shell. The electrostatic interaction of xylan and chitosan was used for coating of the micelles, and chitosan was cross-linked with TPP to increase the stability of nanoparticles. The mucoadhesive property of chitosan also increases drug permeability in the colon by providing a prolonged residence time on mucosal surfaces. The xylan based composite nanoparticles which had high curcumin loading capacity minimized the drug loss in the upper GIT, and released the curcumin as a result of xylan degradation by *Bact. ovatus*. Polymer ratios and crosslinking agent concentration were affective on the curcumin release behaviors of composite nanoparticles. These two impontant parameters should be considered when designing a colon-targeted drug carrier. Besides the drug delivery, xylan can improve the

colon health of the host by inducing the proliferation of beneficial bacteria. The health-promoting effects of prebiotic substrates are generally attributed to the induction of beneficial species and the production of SCFA. The increase in the number of *B. lactis* and SCFA production showed that the degradation of xylan could potentially contribute to colon health through prebiotic action. The in vitro cytocompatibility was investigated and the results indicate the xylan and chitosan that cross-linked with TPP provide a non-toxic coating on the P-123 micelles. Secondly, xylan/chitosan coated silica nanoparticles were investigated for another microbially activated colon targeted oral drug delivery system. Mesoporous silica nanoparticles (MSNs) have been well-recognized drug carriers due to their hydrophilicity, biocompatibility, adjustable pore diameter, and modifiable surface properties. Although they show excellent properties for enhancing the oral bioavailability of drugs, premature release is one of the well-documented disadvantages. MSNs were produced by using a cationic surfactant, CTAB, micelles as templates and loaded with curcumin that was made water soluble with a nonionic surfactant TX-100. Then, they were coated with xylan/chitosan to protect them from the upper GIT conditions and to be activated microbiologically in the colon. The stability test demonstrated the significant effect of the xylan/chitosan coating of MSNs in inhibiting drug loss at the upper GIT pH. The polymer-coated MSN released curcumin owing to the saccharolytic activity of *Bact. ovatus*. It has been observed that both nanocarrier systems released curcumin as a result of xylan degradation by colon bacteria *Bact. ovatus*. However, the in-vivo performance of nanoparticles should be investigated more extensively in clinical studies. Similar to the xylan based composite nanoparticles with polymeric micellar core, xylan degradation demonstrated that they had the potential to improve colon health through prebiotic action. The in vitro cytocompatibility was investigated and the results indicate the MSNs and xylan/chitosan-coated MSNs did not show any significant cytotoxic effect.

In the second part of the study, the suitability of a xylan-based biofoam as a scaffold was examined. Bioactive molecules-loaded frameworks can be developed as a more effective technique for tissue therapy. To investigate the hydrophobic molecule and biofoam interaction and release behavior of biofoams, curcumin was used. Curcumin-loaded xylan based biofoams were synthesized by thin-film hydration coupled with oil in water emulsion methods. The effect of cross-linking agents on the considerable physiochemical and mechanical characteristics of the biofoams has been clearly demonstrated. Crosslinking the polymeric chains of xylan with CTAB to form a 3D

network did not provide adequate biostability and could not withstand the physiological environment to allow cell differentiation. Therefore, xylan was combined with chitosan to produce more durable xylan-based biofoams. Composite foams containing xylan and chitosan were produced using TPP and/or SDS as the crosslinking agent. Composite foams produced with TPP exhibited a very brittle structure. For that, SDS was added to the system as a cross-linking agent and it was observed that SDS provided mechanical strength to biofoams. The composite biofoams cross-linked with SDS demonstrated highly porous structure and swelling ability. Although all types biofoams had high loading capacity, SDS crosslinked biofoams showed the highest curcumin release. In order to investigate the adhesion and differentiation of cells on composite biofoams, 3T3 fibroblast cells were used. The morphological examination of attached cells supported that the physicochemical properties of composite biofoams provided a satisfactory framework and can assist new tissue formation.

In conclusion, xylan-based nanocarriers and biofoams provided promising approaches for microbially activated colon targeted drug delivery and tissue engineering applications, respectively. These xylan-based functional materials can provide important insights into xylan utilization in such fields. The findings of this thesis study are a good agreement with the current perspective; xylan is an encouraging, natural, and safe material for the biomedical area.

REFERENCES

Aggarwal, B. Bharata, Kumar Anushree, and Bharti Alok C. 2003. “Anticancer potential of curcumin: preclinical and clinical studies”. *Anticancer research* 23 (1/A): 363-398.

Aggarwal, Bharata, and Harikumar, Kuzhuvelil B. 2009. “Potential therapeutic effects of curcumin, the anti-inflammatory agent, against neurodegenerative, cardiovascular, pulmonary, metabolic, autoimmune and neoplastic diseases”. *The international journal of biochemistry & cell biology* 41 (1): 40-59.

Agrawal, C. Mauli, and Robert B. Ray. 2001. "Biodegradable Polymeric Scaffolds for Musculoskeletal Tissue Engineering". *Journal of Biomedical Materials Research* 55 (2): 141-150. doi:10.1002/1097-4636.

Ahmed, Shakeel, Annu, Akbar Ali, and Javed Sheikh. 2018. "A Review On Chitosan Centred Scaffolds and Their Applications in Tissue Engineering". *International Journal of Biological Macromolecules* 116: 849-862. doi:10.1016/j.ijbiomac.2018.04.176.

Ai, Jiayi, Kai Li, Jianbin Li, Fei Yu, and Jie Ma. 2021. "Super Flexible, Fatigue Resistant, Self-Healing PVA/Xylan/Borax Hydrogel with Dual-Crosslinked Network". *International Journal of Biological Macromolecules* 172: 66-73. doi:10.1016/j.ijbiomac.2021.01.038.

Al Zaki, Ajlan, Daniel Joh, Zhiliang Cheng, André Luís Branco De Barros, Gary Kao, Jay Dorsey, and Andrew Tsourkas. 2014. "Gold-Loaded Polymeric Micelles for Computed Tomography-Guided Radiation Therapy Treatment and Radiosensitization". *ACS Nano* 8 (1): 104-112. doi:10.1021/nn405701q

Alexandridis, Paschalis, and T Alan Hatton. 1995. "Poly(Ethylene Oxide)□Poly(Propylene Oxide)□Poly(Ethylene Oxide) Block Copolymer Surfactants In Aqueous Solutions And At Interfaces: Thermodynamics, Structure, Dynamics, And Modeling". *Colloids and Surfaces A: Physicochemical and Engineering Aspects* 96 (1-2): 1-46. doi:10.1016/0927-7757(94)03028-x.

Alexandridis, Paschalis. 1997. “Poly (ethylene oxide)/poly (propylene oxide) block copolymer surfactants”. *Current opinion in colloid & interface science 2* (5): 478-489.

Ali, Akbar, and Shakeel Ahmed. 2018. "A Review On Chitosan and Its Nanocomposites in Drug Delivery". *International Journal of Biological Macromolecules* 109: 273-286.

doi:10.1016/j.ijbiomac.2017.12.078.

Ali, Asif, Abshar Hasan, and Yuvraj Singh Negi. 2022. "Effect of Carbon Based Fillers On Xylan/Chitosan/Nano-Hap Composite Matrix for Bone Tissue Engineering Application". *International Journal of Biological Macromolecules* 197: 1-11. doi:10.1016/j.ijbiomac.2021.12.012.

Ali, Asif, Saleheen Bano, Satish S. Poojary, Dhruv Kumar, and Yuvraj Singh Negi. 2019. "Effect of Incorporation Of Montmorillonite On Xylan/Chitosan Conjugate Scaffold". *Colloids and Surfaces B: Biointerfaces* 180: 75-82. doi:10.1016/j.colsurfb.2019.04.032.

Allen, Theresa M., and Pieter R. Cullis. 2004. "Drug Delivery Systems: Entering The Mainstream". Science 303 (5665): 1818-1822.

Al-Saidan, S., Y. Krishnaiah, V. Satyanarayana, and G. Rao. 2005. "In Vitro and In Vivo Evaluation Of Guar Gum-Based Matrix Tablets Of Rofecoxib For Colonic Drug Delivery". *Current Drug Delivery* 2 (2): 155-163. doi:10.2174/1567201053586010.

Álvarez, I., C. Gutiérrez, J.F. Rodríguez, A. de Lucas, and M.T. García. 2020. "Production of Drug-Releasing Biodegradable Microporous Scaffold Impregnated with Gemcitabine Using A CO2 Foaming Process". *Journal of CO2 Utilization* 41: 101227. doi:10.1016/j.jcou.2020.101227.

Amidon, Seth, Jack E. Brown, and Vivek S. Dave. 2015. "Colon-Targeted Oral Drug Delivery Systems: Design Trends and Approaches". *AAPS Pharmscitech* 16 (4): 731-741. doi:10.1208/s12249-015-0350-9.

Amri, Faisal, Salmah Husseinsyah, and Kamarudin Hussin. 2011. "Effect of Sodium Dodecyl Sulfate On Mechanical and Thermal Properties of Polypropylene/Chitosan Composites". *Journal of Thermoplastic Composite Materials* 26 (7): 878-892. doi:10.1177/0892705711430430.

Anand, Preetha, Ajaikumar B. Kunnumakkara, Robert A. Newman, and Bharat B. Aggarwal. 2007. "Bioavailability of Curcumin: Problems and Promises". *Molecular Pharmaceutics* 4 (6): 807-818. doi:10.1021/mp700113r.

Andreani, Tatiana, Ana Luiza R. de Souza, Charlene P. Kiill, Esteban N. Lorenzón, Joana F. Fangueiro, Ana Cristina Calpena, and Marco V. Chaud et al. 2014. "Preparation and Characterization of PEG-Coated Silica Nanoparticles for Oral Insulin Delivery". *International Journal of Pharmaceutics* 473 (1-2): 627-635. doi:10.1016/j.ijpharm.2014.07.049.

Anitha, A., S. Maya, N. Deepa, K.P. Chennazhi, S.V. Nair, and R. Jayakumar. 2012. "Curcumin-Loaded, O-Carboxymethyl Chitosan Nanoparticles for Cancer Drug

Delivery". *Journal of Biomaterials Science, Polymer Edition* 23 (11): 1381-1400. doi:10.1163/092050611x581534.

Anna, Isakova, and Novakovic Katarina. 2018. "Correction: Pulsatile Release from A Flat Self-Oscillating Chitosan Macrogel". *Journal of Materials Chemistry B* 6 (32): 5314-5314. doi:10.1039/c8tb90111b.

Antunes, B.P., A.F. Moreira, V.M. Gaspar, and I.J. Correia. 2015. "Chitosan/Arginine–Chitosan Polymer Blends for Assembly of Nanofibrous Membranes for Wound Regeneration". *Carbohydrate Polymers* 130: 104-112. doi:10.1016/j.carbpol.2015.04.072.

Araújo, Francisca, Neha Shrestha, Pedro L Granja, Jouni Hirvonen, Hélder A Santos, and Bruno Sarmento. 2015. "Safety and Toxicity Concerns of Orally Delivered Nanoparticles as Drug Carriers". *Expert Opinion On Drug Metabolism & Toxicology* 11 (3): 381-393. doi:10.1517/17425255.2015.992781.

Argyo, Christian, Veronika Weiss, Christoph Braeuchle, and Thomas Bein. 2014. "Cheminform Abstract: Multifunctional Mesoporous Silica Nanoparticles as A Universal Platform for Drug Delivery". *Cheminform* 45 (11): no-no. doi:10.1002/chin.201411272.

Atala, Anthony. 2004. "Tissue Engineering and Regenerative Medicine: Concepts for Clinical Application". *Rejuvenation Research* 7 (1): 15-31. doi:10.1089/154916804323105053.

Avadi, Mohammad Reza, Assal Mir Mohammad Sadeghi, Nasser Mohammadpour, Saideh Abedin, Fatemeh Atyabi, Rassoul Dinarvand, and Morteza Rafiee-Tehrani. 2010. "Preparation and Characterization of Insulin Nanoparticles Using Chitosan And Arabic Gum With Ionic Gelation Method". *Nanomedicine: Nanotechnology, Biology and Medicine* 6 (1): 58-63. doi:10.1016/j.nano.2009.04.007.

Awad, Atheer, Christine M. Madla, Laura E. McCoubrey, Fabiana Ferraro, Francesca K.H. Gavins, Asma Buanz, and Simon Gaisford et al. 2022. "Clinical Translation of Advanced Colonic Drug Delivery Technologies". *Advanced Drug Delivery Reviews* 181: 114076. doi:10.1016/j.addr.2021.114076.

Azhary, S. Y., Purnama, D., Florena, F. F., Vanitha, M., Panatarani, C., Joni, I. M. July 2019. 1Synthesis and characterization of chitosan: SiO_2 nanocomposite by ultrasonic spray drying". In IOP Conference Series: Materials Science and Engineering (550): No. 1, p. 012037, IOP Publishing.

Aznar, Elena, Ma Dolores Marcos, Ramón Martínez-Máñez, Félix Sancenón, Juan Soto, Pedro Amorós, and Carmen Guillem. 2009. "Ph- And Photo-Switched Release of Guest Molecules from Mesoporous Silica Supports". *Journal of The American Chemical Society* 131 (19): 6833-6843.

doi:10.1021/ja810011p.

Baeza, Alejandro, Montserrat Colilla, and María Vallet-Regí. 2014. "Advances in Mesoporous Silica Nanoparticles for Targeted Stimuli-Responsive Drug Delivery". *Expert Opinion on Drug Delivery* 12 (2): 319-337. doi:10.1517/17425247.2014.953051.

Bansal, Kuldeep K., Deepak K. Mishra, Ari Rosling, and Jessica M. Rosenholm. 2020. "Therapeutic Potential of Polymer-Coated Mesoporous Silica Nanoparticles". *Applied Sciences* 10 (1): 289. doi:10.3390/app10010289.

Barroso, Telma, Raquel Viveiros, Teresa Casimiro, and Ana Aguiar-Ricardo. 2014. "Development of Dual-Responsive Chitosan–Collagen Scaffolds for Pulsatile Release of Bioactive Molecules". *The Journal of Supercritical Fluids* 94: 102-112. doi:10.1016/j.supflu.2014.07.005.

Bartis D. and Pongrácz J. 2011. Three dimensional tissue cultures and tissue engineering. University of Pécs, Hungary.

Basit, Abdul W., Michael D. Short, and Emma L. McConnell. 2009. "Microbiota-Triggered Colonic Delivery: Robustness of The Polysaccharide Approach in The Fed State in Man". *Journal of Drug Targeting* 17 (1): 64-71. doi:10.1080/10611860802455805.

Batrakova, Elena V., Alexander V. Kabanov. 2008. “Pluronic block copolymers: evolution of drug delivery concept from inert nanocarriers to biological response modifiers”. *Journal of Control Release* 130 (2): 98e106. doi:10.1016/j.jconrel.2008.04.013

Berridge, Michael V., Patries M. Herst, and An S. Tan. 2005. “Tetrazolium Dyes as Tools in Cell Biology: New Insights into their Cellular Reduction”. *Biotechnology annual review* 11: 127-152. doi:10.1016/S1387-2656(05)11004-7

Bidkar, Anil Parsram, Pallab Sanpui, and Siddhartha Sankar Ghosh. 2017. "Efficient Induction of Apoptosis in Cancer Cells by Paclitaxel-Loaded Selenium Nanoparticles". *Nanomedicine* 12 (21): 2641-2651. doi:10.2217/nnm-2017-0189.

Bisht, Savita, Georg Feldmann, Sheetal Soni, Rajani Ravi, Collins Karikar, Amarnath Maitra, and Anirban Maitra. 2007. "Polymeric Nanoparticle-Encapsulated Curcumin ("Nanocurcumin"): A Novel Strategy for Human Cancer Therapy". *Journal of Nanobiotechnology* 5 (1). doi:10.1186/1477-3155-5-3.

Boccardi, E., A. Philippart, J. A. Juhasz-Bortuzzo, G. Novajra, C. Vitale-Brovarone, and A. R. Boccaccini. 2015. "Characterisation of Bioglass Based Foams

Developed Via Replication of Natural Marine Sponges". *Advances in Applied Ceramics* 114 (sup1): S56-S62. doi:10.1179/1743676115y.0000000036.

Bratten, Jason, and Michael P. Jones. 2006. "New Directions in The Assessment of Gastric Function: Clinical Applications of Physiologic Measurements". *Digestive Diseases* 24 (3-4): 252-259. doi:10.1159/000092878.

Brewster, Marcus E., and Thorsteinn Loftsson. 2007. "Cyclodextrins as Pharmaceutical Solubilizers". *Advanced Drug Delivery Reviews* 59 (7): 645-666. doi:10.1016/j.addr.2007.05.012.

Briquez P.S., Hubbell J.A. 2020. “Morphogenesis and tissue engineering. In: Lanza R et al (ed) Principles of Tissue Engineering” 5th edn. p 133-144, Academic Press,

Brunton, L. L., Knollmann, B. C., and Hilal-Dandan, R. 2018. “Goodman & Gilman"s: The Pharmacological Basis of Therapeutics”. 13th edn, New York: McGraw-Hill Education.

Bruschi, Marcos. L., Fernanda Borghi-Pangoni, Mariana Junqueira, and Sabrina de Souza Ferreira. 2017. “Nanostructured therapeutic systems with bioadhesive and thermoresponsive properties”. *Nanostructures for novel therapy*. p.313-342. Elsevier. doi:10.1016/B978-0-323-46142-9.00012-8

Bush, Joshua R., Haixiang Liang, Molly Dickinson, and Edward A. Botchwey. 2016. "Xylan Hemicellulose Improves Chitosan Hydrogel for Bone Tissue Regeneration". *Polymers for Advanced Technologies* 27 (8): 1050-1055. doi:10.1002/pat.3767.

Butt, Adeel Masood, Mohd Cairul Iqbal Mohd Amin, Haliza Katas, Narong Sarisuta, Wasu Witoonsaridsilp, and Ruthairat Benjakul. 2012. "In Vitro Characterization of Pluronic F127 and D-Tocopheryl Polyethylene Glycol 1000 Succinate Mixed Micelles as Nanocarriers for Targeted Anticancer-Drug Delivery". *Journal of Nanomaterials* 2012: 1-11. doi:10.1155/2012/916573.

Calori, Italo Rodrigo, Gustavo Braga, Priscila da Costa Carvalhode Jesus, Hong Bi, Antonio Claudio Tedesco. 2020. “Polymer scaffolds as drug delivery systems”. *European Polymer Journal* 129: 109621 doi:10.1016/j.eurpolymj.2020.109621.

Cao, Xuefei, Xinwen Peng, Linxin Zhong, and Runcang Sun. 2014. "Multiresponsive Hydrogels Based on Xylan-Type Hemicelluloses and Photoisomerized Azobenzene Copolymer as Drug Delivery Carrier". *Journal of Agricultural and Food Chemistry* 62 (41): 10000-10007. doi:10.1021/jf504040s.

Caraballo, Isidoro. 2010. "Factors Affecting Drug Release from Hydroxypropyl Methylcellulose Matrix Systems in The Light Of Classical And Percolation

Theories". *Expert Opinion On Drug Delivery* 7 (11): 1291-1301. doi:10.1517/17425247.2010.528199.

Cartaxo da Costa Urtiga, Silvana, Camilla Aquino Azevedo de Lucena Gabi, Giovanna Rodrigues de Araújo Eleamen, Bartolomeu Santos Souza, Hilzeth de Luna Freire Pessôa, Henrique Rodrigues Marcelino, Elisângela Afonso de Moura Mendonça, Eryvaldo Sócrates Tabosa do Egito, and Elquio Eleamen Oliveira. 2017. "Preparation and Characterization of Safe Microparticles Based On Xylan". *Drug Development and Industrial Pharmacy* 43 (10): 1601-1609. doi:10.1080/03639045.2017.1326932.

Cartaxo da Costa Urtiga, Silvana, Henrique Rodrigues Marcelino, Eryvaldo Sócrates Tabosa do Egito, and Elquio Eleamen Oliveira. 2020. "Xylan In Drug Delivery: A Review Of Its Engineered Structures And Biomedical Applications". *European Journal Of Pharmaceutics And Biopharmaceutics* 151: 199-208. doi:10.1016/j.ejpb.2020.04.016.

Causa, Filippo, Paolo A. Netti, and Luigi Ambrosio. 2007. "A Multi-Functional Scaffold for Tissue Regeneration: The Need to Engineer A Tissue Analogue". *Biomaterials* 28 (34): 5093-5099. doi:10.1016/j.biomaterials.2007.07.030.

Celikkin, Nehar, Chiara Rinoldi, Marco Costantini, Marcella Trombetta, Alberto Rainer, and Wojciech Święszkowski. 2017. "Naturally Derived Proteins And Glycosaminoglycan Scaffolds For Tissue Engineering Applications". *Materials Science And Engineering: C* 78: 1277-1299. doi:10.1016/j.msec.2017.04.016.

Chassard, C., E. Delmas, P. A. Lawson, and A. Bernalier-Donadille. 2008. "Bacteroides Xylanisolvens Sp. Nov., A Xylan-Degrading Bacterium Isolated from Human Faeces". *International Journal of Systematic and Evolutionary Microbiology* 58 (4): 1008-1013. doi:10.1099/ijs.0.65504-0.

Chaudhary, Anil, Neha Tiwari, Vikas Jain, and Ranjit Singh. 2011. "Microporous Bilayer Osmotic Tablet for Colon-Specific Delivery". *European Journal of Pharmaceutics and Biopharmaceutics* 78 (1): 134-140. doi:10.1016/j.ejpb.2011.01.004.

Chen, Yu, Hangrong Chen, and Jianlin Shi. 2013. "In Vivo Bio-Safety Evaluations and Diagnostic/Therapeutic Applications of Chemically Designed Mesoporous Silica Nanoparticles". *Advanced Materials* 25 (23): 3144-3176. doi:10.1002/adma.201205292.

Cheng, Woei Ping, Alexander I. Gray, Laurence Tetley, Thi Le Bich Hang, Andreas G. Schätzlein, and Ijeoma F. Uchegbu. 2006. "Polyelectrolyte Nanoparticles with High Drug Loading Enhance the Oral Uptake of Hydrophobic Compounds". *Biomacromolecules* 7 (5): 1509-1520. doi:10.1021/bm060130l.

Cholkar, Kishore, Ashaben Patel, Aswani Dutt Vadlapudi, and Ashim K. Mitra. 2012. "Novel Nanomicellar Formulation Approaches for Anterior and Posterior Segment Ocular Drug Delivery". *Recent Patents on Nanomedicinee* 2 (2): 82-95. doi:10.2174/1877912311202020082.

Chourasia, M. K., and S. K. Jain. 2004. "Polysaccharides for Colon Targeted Drug Delivery". *Drug Delivery* 11 (2): 129-148. doi:10.1080/10717540490280778.

Cihan, Esra, Mehmet Polat, and Hurriyet Polat. 2017. "Designing of Spherical Chitosan Nano-Shells with Micellar Cores for Solvation and Safeguarded Delivery of Strongly Lipophilic Drugs". *Colloids and Surfaces A: Physicochemical and Engineering Aspects* 529: 815-823. doi:10.1016/j.colsurfa.2017.06.074.

Coco, Régis, Laurence Plapied, Vincent Pourcelle, Christine Jérôme, David J. Brayden, Yves-Jacques Schneider, and Véronique Préat. 2013. "Drug Delivery to Inflamed Colon by Nanoparticles: Comparison of Different Strategies". *International Journal of Pharmaceutics* 440 (1): 3-12. doi:10.1016/j.ijpharm.2012.07.017.

Coll, Carmen, Laura Mondragón, Ramón Martínez-Máñez, Félix Sancenón, M. Dolores Marcos, Juan Soto, Pedro Amorós, and Enrique Pérez-Payá. 2011. "Enzyme-Mediated Controlled Release Systems by Anchoring Peptide Sequences on Mesoporous Silica Supports". *Angewandte Chemie* 123 (9): 2186-2188. doi:10.1002/ange.201004133.

Cormode, David P., Pratap C. Naha, and Zahi A. Fayad. 2014. "Nanoparticle Contrast Agents for Computed Tomography: A Focus On Micelles". *Contrast Media & Molecular Imaging* 9 (1): 37-52. doi:10.1002/cmmi.1551.

Coughlan, D.C., F.P. Quilty, and O.I. Corrigan. 2004. "Effect of Drug Physicochemical Properties on Swelling/Deswelling Kinetics and Pulsatile Drug Release from Thermoresponsive Poly(N-Isopropylacrylamide) Hydrogels". *Journal of Controlled Release* 98 (1): 97-114. doi:10.1016/j.jconrel.2004.04.014.

Croisier, Florence, and Jérôme Christine. 2013. “Chitosan-based biomaterials for tissue engineering”. *European polymer journal* 49 (4): 780-792. doi: 10.1016/j.eurpolymj.2012.12.009.

Daus, Stephan, and Thomas Heinze. 2010. "Xylan-Based Nanoparticles: Prodrugs for Ibuprofen Release". *Macromolecular Bioscience* 10 (2): 211-220. doi:10.1002/mabi.200900201.

Davoodi, Pooya, Lai Yeng Lee, Qingxing Xu, Vishnu Sunil, Yajuan Sun, Siowling Soh, and Chi-Hwa Wang. 2018. "Drug Delivery Systems for Programmed and On-Demand Release". *Advanced Drug Delivery Reviews* 132: 104-138. doi:10.1016/j.addr.2018.07.002.

Declercq, Heidi A., Tim Desmet, Peter Dubruel, and Maria J. Cornelissen. 2014. "The Role of Scaffold Architecture and Composition on The Bone Formation by Adipose-Derived Stem Cells". *Tissue Engineering Part A* 20 (1-2): 434-444. doi:10.1089/ten.tea.2013.0179.

DeMuth, Peter, Matthew Hurley, Chunwei Wu, Stephanie Galanie, Michael R. Zachariah, and Philip DeShong. 2011. "Mesoscale Porous Silica as Drug Delivery Vehicles: Synthesis, Characterization, And Ph-Sensitive Release Profiles". *Microporous and Mesoporous Materials* 141 (1-3): 128-134. doi:10.1016/j.micromeso.2010.10.035.

Deshmukh, Anand S., Pratik N. Chauhan, Malleshappa N. Noolvi, Kiran Chaturvedi, Kuntal Ganguly, Shyam S. Shukla, Mallikarjuna N. Nadagouda, and Tejraj M. Aminabhavi. 2017. "Polymeric Micelles: Basic Research to Clinical Practice". *International Journal of Pharmaceutics* 532 (1): 249-268. doi:10.1016/j.ijpharm.2017.09.005.

Dhandayuthapani, Brahatheeswaran, Yasuhiko Yoshida, Toru Maekawa, and D. Sakthi Kumar. 2011. "Polymeric Scaffolds in Tissue Engineering Application: A Review". *International Journal of Polymer Science* 2011: 1-19. doi:10.1155/2011/290602.

Dulbecco, Pietro, and V. Savarino. 2013. "Therapeutic Potential of Curcumin in Digestive Diseases". *World Journal of Gastroenterology* 19 (48): 9256. doi:10.3748/wjg.v19.i48.9256.

Dumortier, Gilles, Jean Louis Grossiord, Florence Agnely, and Jean Claude Chaumeil. 2006. "A Review of Poloxamer 407 Pharmaceutical and Pharmacological Characteristics". *Pharmaceutical Research* 23 (12): 2709-2728. doi:10.1007/s11095-006-9104-4.

Ebringerová, Anna, and Thomas Heinze. 2000. "Xylan and Xylan Derivatives - Biopolymers With Valuable Properties, 1. Naturally Occurring Xylans Structures, Isolation Procedures And Properties". *Macromolecular Rapid Communications* 21 (9): 542-556. doi:10.1002/1521-3927.

Ebringerová, Anna. 2005. "Structural Diversity and Application Potential of Hemicelluloses". *Macromolecular Symposia* 232 (1): 1-12. doi:10.1002/masy.200551401.

Eltom, Abdalla, Gaoyan Zhong, and Ameen Muhammad. 2019. "Scaffold Techniques And Designs In Tissue Engineering Functions and Purposes: A Review". *Advances in Materials Science and Engineering* 2019: 1-13. doi:10.1155/2019/3429527.

Falony, Gwen, Thomas Calmeyn, Frédéric Leroy, and Luc De Vuyst. 2009. "Coculture Fermentations Of Bifidobacterium Species And Bacteroides Thetaiotaomicron Reveal A Mechanistic Insight Into The Prebiotic Effect Of Inulin-Type Fructans".

Applied And Environmental Microbiology 75 (8): 2312-2319. doi:10.1128/aem.02649-08.

Fang, Xiaoling, Chen, Xianyi Sha, Jiang, Yanzuo Chen, and Ren. 2013. "Pluronic P105/F127 Mixed Micelles for The Delivery of Docetaxel Against Taxol-Resistant Non-Small Cell Lung Cancer: Optimization and In Vitro, In Vivo Evaluation". *International Journal of Nanomedicine*, 73. doi:10.2147/ijn.s38221.

Fishman, Jay A., Linda Scobie, and Yasuhiro Takeuchi. 2012. "Xenotransplantation-Associated Infectious Risk: A WHO Consultation". *Xenotransplantation* 19 (2): 72-81. doi:10.1111/j.1399-3089.2012.00693.x.

Flint, Harry J., Karen P. Scott, Sylvia H. Duncan, Petra Louis, and Evelyne Forano. 2012. "Microbial Degradation of Complex Carbohydrates in The Gut". *Gut Microbes* 3 (4): 289-306. doi:10.4161/gmic.19897.

Foster, Beth, Terence Cosgrove, and Boualem Hammouda. 2009. "Pluronic Triblock Copolymer Systems and Their Interactions with Ibuprofen". *Langmuir* 25 (12): 6760-6766. doi:10.1021/la900298m.

Gabrielii, I, P Gatenholm, W.G Glasser, R.K Jain, and L Kenne. 2000. "Separation, Characterization and Hydrogel-Formation of Hemicellulose from Aspen Wood". *Carbohydrate Polymers* 43 (4): 367-374. doi:10.1016/s0144-8617(00)00181-8.

Gabrielii, I., and P. Gatenholm. 1998. "Preparation and Properties Of Hydrogels Based On Hemicellulose". *Journal of Applied Polymer Science* 69 (8): 1661-1667. doi:10.1002/(sici)1097-4628.

Ganguly, R., A. Kunwar, B. Dutta, S. Kumar, K.C. Barick, A. Ballal, V.K. Aswal, and P.A. Hassan. 2017. "Heat-Induced Solubilization of Curcumin In Kinetically Stable Pluronic P123 Micelles And Vesicles: An Exploit Of Slow Dynamics Of The Micellar Restructuring Processes In The Aqueous Pluronic System". *Colloids and Surfaces B: Biointerfaces* 152: 176-182. doi:10.1016/j.colsurfb.2017.01.023.

Gao, Cundian, Junli Ren, Cui Zhao, Weiqing Kong, Qingqing Dai, Qifeng Chen, Chuanfu Liu, and Runcang Sun. 2016. "Xylan-Based Temperature/Ph Sensitive Hydrogels For Drug Controlled Release". *Carbohydrate Polymers* 151: 189-197. doi:10.1016/j.carbpol.2016.05.075.

Gaoa, Hailong, Liua Na, Nib Shuzhen, Lina Haixia, and Fua Yingjuan. 2017 "Xylan/Chitosan Composites Prepared by an Ionic Liquid System With Unique Antioxidant Properties". *Journal of Bioresources and Bioproducts* 2 (3). doi:10.21967/jbb.v2i3.83.

Garcia, B.Rosângela, Toshiyuki. Nagashima-Jr, Ana K.C. Praxedes, Fernanda.N. Raffin, Tulio.F.A. Moura, E.Socrates.T. Egito. 2001. “Preparation of micro and nanoparticles from corn cobs xylan”. *Polymer Bulletin.* 46: 371-379.

García-Uriostegui, L., E. Delgado, H. Iván Meléndez-Ortiz, T.A. Camacho-Villegas, H. Esquivel-Solís, P. Gatenholm, and G. Toriz. 2018. "Spruce Xylan/HEMA-SBA15 Hybrid Hydrogels As A Potential Scaffold For Fibroblast Growth And Attachment". *Carbohydrate Polymers* 201: 490-499. doi:10.1016/j.carbpol.2018.08.066.

Gazzaniga, Andrea, Alessandra Maroni, Maria Edvige Sangalli, and Lucia Zema. 2006. "Time-Controlled Oral Delivery Systems for Colon Targeting". *Expert Opinion On Drug Delivery* 3 (5): 583-597. doi:10.1517/17425247.3.5.583.

Ge, Yazhong, Shahid Ahmed, Wanzi Yao, Lijun You, Jianxian Zheng, and Kseniya Hileuskaya. 2020. "Regulation Effects of Indigestible Dietary Polysaccharides on Intestinal Microflora: An Overview". *Journal of Food Biochemistry* 45 (1). doi:10.1111/jfbc.13564.

Gradauer, K., J. Barthelmes, C. Vonach, G. Almer, H. Mangge, B. Teubl, and E. Roblegg et al. 2013. "Liposomes Coated with Thiolated Chitosan Enhance Oral Peptide Delivery to Rats". *Journal of Controlled Release* 172 (3): 872-878. doi:10.1016/j.jconrel.2013.10.011.

Grün, Michael, Iris Lauer, and Klaus K. Unger. 1997. "The Synthesis of Micrometer- And Submicrometer-Size Spheres of Ordered Mesoporous Oxide MCM-41". Advanced Materials 9 (3): 254-257. doi:10.1002/adma.19970090317.

Gundloori, Rathna V., Amarnath Singam, and Naresh Killi. 2019. “Nanobased intravenous and transdermal drug delivery systems”. In *Applications of Targeted Nano Drugs and Delivery Systems*. p. 551-594, Elsevier. doi:10.1016/B978-0-12-814029-1.00019-3

Han, Hyo Kyung, Hyun Jae Shin, and Dong Hoon Ha. 2012. “Improved oral bioavailability of alendronate via the mucoadhesive liposomal delivery system”. *European journal of pharmaceutical sciences* 46 (5): 500-507. doi:10.1016/j.ejps.2012.04.002

Hanai, Hiroyuki, Iida TakayukiIida, Takeuchi Ken, Watanabe Fumitoshi, Maruyama Yasuhiko, Andoh Akira, Tsujikawa Tomoyuki, Fujiyama Yosihihide, Mitsuyama Keiichi, Sata Michio, Koide Yukio. 2006. “Curcumin maintenance therapy for ulcerative colitis: randomized, multicenter, double-blind, placebo-controlled trial”. *Clinical Gastroenterology and Hepatology*, *4* (12): 1502-1506. doi: 10.1016/j.cgh.2006.08.008

Hansen, Natanya M. L., and David Plackett. 2008. "Sustainable Films and Coatings from Hemicelluloses: A Review". *Biomacromolecules* 9 (6): 1493-1505. doi:10.1021/bm800053z.

Hatcher, H., R. Planalp, J. Cho, F. M. Torti, and S. V. Torti. 2008. "Curcumin: From Ancient Medicine to Current Clinical Trials". *Cellular and Molecular Life Sciences* 65 (11): 1631-1652. doi:10.1007/s00018-008-7452-4.

He, Zhiqi, and Paschalis Alexandridis. 2017. "Micellization Thermodynamics of Pluronic P123 (EO20PO70EO20) Amphiphilic Block Copolymer in Aqueous Ethylammonium Nitrate (EAN) Solutions". *Polymers* 10 (1): 32. doi:10.3390/polym10010032.

Hodges, L.A., S.M. Connolly, J. Band, B. O'Mahony, T. Ugurlu, M. Turkoglu, C.G. Wilson, and H.N.E. Stevens. 2009. "Scintigraphic Evaluation of Colon Targeting Pectin–HPMC Tablets in Healthy Volunteers". *International Journal of Pharmaceutics* 370 (1-2): 144-150. doi:10.1016/j.ijpharm.2008.12.002.

Hollister, Scott J. 2005. "Porous Scaffold Design for Tissue Engineering". *Nature Materials* 4 (7): 518-524. doi:10.1038/nmat1421.

Homayun, Bahman, Xueting Lin, and Hyo-Jick Choi. 2019. "Challenges and Recent Progress in Oral Drug Delivery Systems for Biopharmaceuticals". *Pharmaceutics* 11 (3): 129.

Hopkins, Mark J., Hans N. Englyst, Sandra Macfarlane, Elizabeth Furrie, George T. Macfarlane, and Andrew J. McBain. 2003. "Degradation of Cross-Linked and Non-Cross-Linked Arabinoxylans by The Intestinal Microbiota In Children". *Applied and Environmental Microbiology* 69 (11): 6354-6360. doi:10.1128/aem.69.11.6354-6360.2003.

Hoseinifar, S.H., A. Mirvaghefi, M.A. Amoozegar, D.L. Merrifield, and E. Ringø. 2015. "In Vitroselection of A Synbiotic Andin Vivoevaluation On Intestinal Microbiota, Performance And Physiological Response Of Rainbow Trout (Oncorhynchus Mykiss) Fingerlings". *Aquaculture Nutrition* 23 (1): 111-118. doi:10.1111/anu.12373.

Howard, Daniel, Lee D. Buttery, Kevin M. Shakesheff, and Scott J. Roberts. 2008. "Tissue Engineering: Strategies, Stem Cells And Scaffolds". *Journal Of Anatomy* 213 (1): 66-72. doi:10.1111/j.1469-7580.2008.00878.x.

Hsu, Hao-jui, Yanxiao Han, Michael Cheong, Petr Král, and Seungpyo Hong. 2018. "Dendritic PEG Outer Shells Enhance Serum Stability of Polymeric Micelles". *Nanomedicine: Nanotechnology, Biology and Medicine* 14 (6): 1879-1889. doi:10.1016/j.nano.2018.05.010.

Hu, Yang, Yang Li, and Fu-Jian Xu. 2017. "Versatile Functionalization Of Polysaccharides Via Polymer Grafts: From Design To Biomedical

Applications". *Accounts Of Chemical Research* 50 (2): 281-292. doi:10.1021/acs.accounts.6b00477.

Hua, Susan, Ellen Marks, Jennifer J. Schneider, and Simon Keely. 2015. "Advances In Oral Nano-Delivery Systems for Colon Targeted Drug Delivery In Inflammatory Bowel Disease: Selective Targeting to Diseased Versus Healthy Tissue". *Nanomedicine: Nanotechnology, Biology and Medicine* 11 (5): 1117-1132. doi:10.1016/j.nano.2015.02.018.

Hua, Susan. 2020. "Advances in Oral Drug Delivery for Regional Targeting In The Gastrointestinal Tract - Influence Of Physiological, Pathophysiological And Pharmaceutical Factors". *Frontiers in Pharmacology* 11. doi:10.3389/fphar.2020.00524.

Hughes, S. A., P. R. Shewry, L. Li, G. R. Gibson, M. L. Sanz, and R. A. Rastall. 2007. "In Vitro Fermentation by Human Fecal Microflora of Wheat Arabinoxylans". *Journal of Agricultural and Food Chemistry* 55 (11): 4589-4595. doi:10.1021/jf070293g.

Hussain, M. Delwar, and Saxena. 2012. "Poloxamer 407/TPGS Mixed Micelles for Delivery of Gambogic Acid to Breast and Multidrug-Resistant Cancer". *International Journal of Nanomedicine*, 713. doi:10.2147/ijn.s28745.

Hutmacher, Dietmar W. 2000. "Scaffolds in Tissue Engineering Bone and Cartilage". *Biomaterials* 21 (24): 2529-2543. doi:10.1016/s0142-9612(00)00121-6.

Ibekwe, Valentine C., Hala M. Fadda, Emma L. McConnell, Mandeep K. Khela, David F. Evans, and Abdul W. Basit. 2008. "Interplay Between Intestinal Ph, Transit Time and Feed Status On the In Vivo Performance Of Ph Responsive Ileo-Colonic Release Systems". *Pharmaceutical Research* 25 (8): 1828-1835. doi:10.1007/s11095-008-9580-9.

Ikada, Yoshito. 2006. Challenges in tissue engineering. *Journal of the Royal Society Interface* 3 (10): 589-601. doi:10.1098/rsif.2006.0124

Ikeda, Takeshi, Kahori Ikeda, Kouhei Yamamoto, Hidetaka Ishizaki, Yuu Yoshizawa, Kajiro Yanagiguchi, Shizuka Yamada, and Yoshihiko Hayashi. 2014. "Fabrication and Characteristics of Chitosan Sponge as A Tissue Engineering Scaffold". *Biomed Research International* 2014: 1-8. doi:10.1155/2014/786892.

Inamuddin, Abdullah Asiri and Ali Mohammad. 2018. “Applications of nanocomposite materials in drug delivery”. Cambridge, UK, Woodhead Publishing.

Izydorczyk, Marta S., and Costas G. Biliaderis. 1992. "Effect of Molecular Size On Physical Properties of Wheat Arabinoxylan". *Journal of Agricultural and Food Chemistry* 40 (4): 561-568. doi:10.1021/jf00016a006.

Jafari, Samira, Hossein Derakhshankhah, Loghman Alaei, Ali Fattahi, Behrang Shiri Varnamkhasti, and Ali Akbar Saboury. 2019. "Mesoporous Silica Nanoparticles for Therapeutic/Diagnostic Applications". *Biomedicine & Pharmacotherapy* 109: 1100-1111. doi:10.1016/j.biopha.2018.10.167.

Jagannathan, Ramya, Priya Mary Abraham, and Pankaj Poddar. 2012. "Temperature-Dependent Spectroscopic Evidences of Curcumin in Aqueous Medium: A Mechanistic Study of Its Solubility and Stability". *The Journal of Physical Chemistry B* 116 (50): 14533-14540. doi:10.1021/jp3050516.

Jagur-Grodzinski, Joseph. 2009. "Polymeric Gels And Hydrogels For Biomedical and Pharmaceutical Applications". *Polymers for Advanced Technologies* 21 (1): 27-47. doi:10.1002/pat.1504.

Jeong, Young-Il, Tomoya Ohno, Zhaopeng Hu, Yukako Yoshikawa, Nobuhito Shibata, Shunji Nagata, and Kanji Takada. 2001. "Evaluation of An Intestinal Pressure-Controlled Colon Delivery Capsules Prepared By A Dipping Method". *Journal Of Controlled Release* 71 (2): 175-182. doi:10.1016/s0168-3659(01)00211-5.

Johansson, Malin E. V., Henrik Sjövall, and Gunnar C. Hansson. 2013. "The Gastrointestinal Mucus System in Health and Disease". *Nature Reviews Gastroenterology & Hepatology* 10 (6): 352-361. doi:10.1038/nrgastro.2013.35.

Jurenka, S. Julie. 2009. “Anti-inflammatory properties of curcumin, a major constituent of Curcuma longa: a review of preclinical and clinical research”, *Alternative medicine review 14* (2).

Kabanov, Alexander V, Elena V Batrakova, and Valery Yu Alakhov. 2002. "Pluronic® Block Copolymers as Novel Polymer Therapeutics for Drug and Gene Delivery". *Journal of Controlled Release* 82 (2-3): 189-212. doi:10.1016/s0168-3659(02)00009-3.

Kagan, Leonid, and Amnon Hoffman. 2008. "Systems for Region Selective Drug Delivery in The Gastrointestinal Tract: Biopharmaceutical Considerations". *Expert Opinion on Drug Delivery* 5 (6): 681-692. doi:10.1517/17425247.5.6.681.

Kang, Yunqing, and Jia Chang. 2018. "Channels in A Porous Scaffold: A New Player for Vascularization". *Regenerative Medicine* 13 (6): 705-715. doi:10.2217/rme-2018-0022.

Kankala, Ranjith Kumar, Ya-Hui Han, Jongbeom Na, Chia-Hung Lee, Ziqi Sun, Shi-Bin Wang, and Tatsuo Kimura et al. 2020. "Nanoarchitectured Structure and Surface Biofunctionality of Mesoporous Silica Nanoparticles". *Advanced Materials* 32 (23): 1907035. doi:10.1002/adma.201907035.

Kannan, Marikani, Nesakumari Maliga, Rajarathinam K., and Singh A. J. A. Ranjit. 2010. “Production and characterization of mushroom chitosan under solid-state fermentation conditions”. *Advances in Biological Research* 4 (1): 10-13.

Kapse, Anuja, Neelima Anup, Vruti Patel, Gaurav K. Saraogi, Dinesh Kumar Mishral, Rakesh K. Tekade. 2020. Polymeric micelles: a ray of hope among new drug delivery systems. Drug Delivery Systems A volume in *Advances in Pharmaceutical Product Development and Research*. p. 235-289, Academic Press. doi:10.1016/B978-0-12-814487-9.00006-5

Karande, Tejas S., Joo L. Ong, and C. Mauli Agrawal. 2004. "Diffusion in Musculoskeletal Tissue Engineering Scaffolds: Design Issues Related to Porosity, Permeability, Architecture, And Nutrient Mixing". *Annals of Biomedical Engineering* 32 (12): 1728-1743. doi:10.1007/s10439-004-7825-2.

Katti, Dhirendra, Rajesh Vasita, and Kirubanandan Shanmugam. 2008. "Improved Biomaterials for Tissue Engineering Applications: Surface Modification of Polymers". *Current Topics in Medicinal Chemistry* 8 (4): 341-353. doi:10.2174/156802608783790893.

Kaviani, Alireza, Seyed Mojtaba Zebarjad, Sirus Javadpour, Maryam Ayatollahi, and Reza Bazargan-Lari. 2019. "Fabrication and Characterization of Low-Cost Freeze-Gelated Chitosan/Collagen/Hydroxyapatite Hydrogel Nanocomposite Scaffold". *International Journal of Polymer Analysis and Characterization* 24 (3): 191-203. doi:10.1080/1023666x.2018.1562477.

Kayser, O., C. Olbricha, V. Yardley, A.F. Kiderlen, S.L. Croft. 2003. "Formulation of Amphotericin B as Nanosuspension for Oral Administration". *International Journal of Pharmaceutics* 254 (1): 73-75. doi:10.1016/s0378-5173(02)00686-5.

Kesisoglou, Filippos, Santipharp Panmai, and Yunhui Wu. 2007. "Nanosizing — Oral Formulation Development and Biopharmaceutical Evaluation". *Advanced Drug Delivery Reviews* 59 (7): 631-644. doi:10.1016/j.addr.2007.05.003.

Kikuchi, A., Okano, T., 2005. “Hydrogels-stimuli sensitive hydrogels”. *Polymeric drug delivery systems*. Taylor & Francis Group, pp. 275–322.

Kohane, Daniel S., and Robert Langer. 2010. "Biocompatibility and Drug Delivery Systems". Journal of *Chemical Science* 1 (4): 441-446. doi:10.1039/c0sc00203h.

Köhnke, Tobias, Thomas Elder, Hans Theliander, and Arthur J. Ragauskas. 2014. "Ice Templated and Cross-Linked Xylan/Nanocrystalline Cellulose Hydrogels". *Carbohydrate Polymers* 100: 24-30. doi:10.1016/j.carbpol.2013.03.060.

Kramschuster, A. and Turng, L.S. 2012. "Fabrication of tissue engineering scaffolds". *Handbook of Biopolymers and Biodegradable Plastics: Properties, Processing and Applications*, 427, Elsevier.

Krishnaiah, Y.S.R, P Veer Raju, B Dinesh Kumar, V Satyanarayana, R.S Karthikeyan, and P Bhaskar. 2003. "Pharmacokinetic Evaluation of Guar Gum-Based Colon-Targeted Drug Delivery Systems of Mebendazole in Healthy Volunteers". *Journal of Controlled Release* 88 (1): 95-103. doi:10.1016/s0168-3659(02)00483-2.

Krishnaiah, Y.S.R., Y. Indira Muzib, and P. Bhaskar. 2003. "In Vivo Evaluation of Guar Gum-Based Colon-Targeted Drug Delivery Systems of Ornidazole in Healthy Human Volunteers". *Journal of Drug Targeting* 11 (2): 109-115. doi:10.1080/1061186031000138614.

Krishnan, R., R. Rajeswari, J. Venugopal, S. Sundarrajan, R. Sridhar, M. Shayanti, and S. Ramakrishna. 2012. "Polysaccharide Nanofibrous Scaffolds as A Model for In Vitro Skin Tissue Regeneration". *Journal of Materials Science: Materials in Medicine* 23 (6): 1511-1519. doi:10.1007/s10856-012-4630-6.

Kumar, S. Uday, Vinay Kumar, Ruchir Priyadarshi, P. Gopinath, and Yuvraj Singh Negi. 2018. "Ph-Responsive Prodrug Nanoparticles Based On Xylan-Curcumin Conjugate For The Efficient Delivery Of Curcumin In Cancer Therapy". *Carbohydrate Polymers* 188: 252-259.

Kumar, Samit, and Negi, Yuvraj Singh. 2012a. "Corn cob xylan-based nanoparticles: Ester prodrug of 5-aminosalicylic acid for possible targeted delivery of drug". *Journal of Pharmaceutical Sciences and Research*, 4 (12): 1995.

Kumar, Samit, and Yuvraj Singh Negi. 2012b. "Nanoparticles Synthesis from Corn Cob (Xylan) And Their Potential Application as Colon-Specific Drug Carrier". *Macromolecular Symposia* 320 (1): 75-80. doi:10.1002/masy.201251010.

Kunwar, Amit, Atanu Barik, Ruchi Pandey, and K. Indira Priyadarsini. 2006. "Transport of Liposomal and Albumin Loaded Curcumin to Living Cells: An Absorption and Fluorescence Spectroscopic Study". *Biochimica Et Biophysica Acta (BBA) - General Subjects* 1760 (10): 1513-1520. doi:10.1016/j.bbagen.2006.06.012.

Kuo, Chang-Yi, Chih-Hao Chen, Chien-Yu Hsiao, and Jyh-Ping Chen. 2015. "Incorporation of Chitosan in Biomimetic Gelatin/Chondroitin-6-Sulfate/Hyaluronan Cryogel For Cartilage Tissue Engineering". *Carbohydrate Polymers* 117: 722-730. doi:10.1016/j.carbpol.2014.10.056.

Lestari, Maria L. and Gunawan Indrayanto. 2014. "Curcumin". In *Profiles of drug substances, excipients and related methodology*. (39) p. 113-204, Academic Press. doi:10.1016/B978-0-12-800173-8.00003-9

Li, Ruixiang, Zhiqing Pang, Huining He, Seungjin Lee, Jing Qin, Jian Wu, Liang Pang, Jianxin Wang, and Victor C. Yang. 2017. "Drug Depot-Anchoring Hydrogel: A Self-Assembling Scaffold for Localized Drug Release and Enhanced Stem Cell Differentiation". *Journal of Controlled Release* 261: 234-245. doi:10.1016/j.jconrel.2017.07.008.

Li, Tao, Xiongbo Song, Changmei Weng, Xin Wang, Liling Gu, Xiaoyuan Gong, Quanfang Wei, Xiaojun Duan, Liu Yang, and Cheng Chen. 2019. "Silk Fibroin/Carboxymethyl Chitosan Hydrogel with Tunable Biomechanical Properties Has Application Potential As Cartilage Scaffold". *International Journal of Biological Macromolecules* 137: 382-391. doi:10.1016/j.ijbiomac.2019.06.245.

Li, Xiaoming, Rongrong Cui, Lianwen Sun, Katerina E. Aifantis, Yubo Fan, Qingling Feng, Fuzhai Cui, and Fumio Watari. 2014. "3D-Printed Biopolymers for Tissue Engineering Application". *International Journal of Polymer Science* 2014: 1-13. doi:10.1155/2014/829145.

Li, Xiaoxia, Xiaowen Shi, Miao Wang, and Yumin Du. 2011. "Xylan Chitosan Conjugate - A Potential Food Preservative". *Food Chemistry* 126 (2): 520-525. doi:10.1016/j.foodchem.2010.11.037.

Lindner, Lars H., Martin Hossann, Michael Vogeser, Nicole Teichert, Kirsten Wachholz, Hansjoerg Eibl, Wolfgang Hiddemann, and Rolf D. Issels. 2008. "Dual Role of Hexadecylphosphocholine (Miltefosine) In Thermosensitive Liposomes: Active Ingredient and Mediator Of Drug Release". *Journal of Controlled Release* 125 (2): 112-120. doi:10.1016/j.jconrel.2007.10.009.

Liu, Xinxin, Minmin Chang, Bei He, Ling Meng, Xiaohui Wang, Runcang Sun, Junli Ren, and Fangong Kong. 2019. "A One-Pot Strategy For Preparation Of High-Strength Carboxymethyl Xylan-G-Poly(Acrylic Acid) Hydrogels With Shape Memory Property". *Journal of Colloid and Interface Science* 538: 507-518. doi:10.1016/j.jcis.2018.12.023.

Loh, Qiu Li, and Cleo Choong. 2013. "Three-Dimensional Scaffolds for Tissue Engineering Applications: Role of Porosity And Pore Size". *Tissue Engineering Part B: Reviews* 19 (6): 485-502. doi:10.1089/ten.teb.2012.0437.

Louis, Petra, and Harry J. Flint. 2009. "Diversity, Metabolism and Microbial Ecology of Butyrate-Producing Bacteria From The Human Large Intestine". *FEMS Microbiology Letters* 294 (1): 1-8. doi:10.1111/j.1574-6968.2009.01514.x.

Loutfy, Samah A, Hanaa M Alam El-Din, Mostafa H Elberry, Nanis G Allam, M T M Hasanin, and Ahmed M Abdellah. 2016. "Synthesis, Characterization and Cytotoxic Evaluation of Chitosan Nanoparticles: In Vitro Liver Cancer Model". *Advances in Natural Sciences: Nanoscience And Nanotechnology* 7 (3): 035008. doi:10.1088/2043-6262/7/3/035008.

Luo, Yuqiong, Xingqiang Pan, Yunzhi Ling, Xiaoying Wang, and Runcang Sun. 2014. "Facile Fabrication of Chitosan Active Film with Xylan Via Direct Immersion". *Cellulose* 21 (3): 1873-1883. doi:10.1007/s10570-013-0156-4.

Mabrouk, Mostafa, Hanan H. Beherei, and Diganta B. Das. 2020. "Recent Progress in The Fabrication Techniques Of 3D Scaffolds For Tissue Engineering". *Materials Science and Engineering: C* 110: 110716. doi:10.1016/j.msec.2020.110716.

Macfarlane, Sandra, and George T. Macfarlane. 2003. "Regulation of Short-Chain Fatty Acid Production". *Proceedings of The Nutrition Society* 62 (1): 67-72. doi:10.1079/pns2002207.

Macleod, Graeme S, John T Fell, John H Collett, Harbans L Sharma, and Anne-Marie Smith. 1999. "Selective Drug Delivery To The Colon Using Pectin:Chitosan:Hydroxypropyl Methylcellulose Film Coated Tablets". *International Journal of Pharmaceutics* 187 (2): 251-257. doi:10.1016/s0378-5173(99)00196-9.

Maheshwari, Radha K., Anoop K. Singh, Jaya Gaddipati, and Rikhab C. Srimal. 2006. "Multiple Biological Activities of Curcumin: A Short Review". *Life Sciences* 78 (18): 2081-2087. doi:10.1016/j.lfs.2005.12.007.

Mansouri, Negar, and SamiraBagheri. 2016. "The Influence of Topography On Tissue Engineering Perspective". *Materials Science and Engineering: C* 61: 906-921. doi:10.1016/j.msec.2015.12.094.

Manzano, Miguel, and Vallet-Regí Maria. 2020. “Mesoporous silica nanoparticles for drug delivery”. *Advanced functional materials*, 30 (2): 1902634. doi: 10.1002/adfm.201902634.

Marcelino, Henrique, Acarília da Silva, Monique Gomes, Elquio Oliveira, Toshiyuki Nagashima-Junior, Gardênia Pinheiro, and Acarízia da Silva et al. 2015. "Leads from Physical, Chemical, And Thermal Characterization On Cytotoxic Effects of Xylan-Based Microparticles". *Polymers* 7 (11): 2304-2315. doi:10.3390/polym7111515.

Martinez, Marilyn N., and Gordon L. Amidon. 2002. "A Mechanistic Approach to Understanding the Factors Affecting Drug Absorption: A Review of Fundamentals". *The Journal of Clinical Pharmacology* 42 (6): 620-643. doi:10.1177/00970002042006005.

Martínez-López, A.L., E. Carvajal-Millan, N. Sotelo-Cruz, V. Micard, A. Rascón-Chu, Y.L. López-Franco, J. Lizardi-Mendoza, and R. Canett-Romero. 2019. "Enzymatically Cross-Linked Arabinoxylan Microspheres as Oral Insulin Delivery System". *International Journal of Biological Macromolecules* 126: 952-959. doi:10.1016/j.ijbiomac.2018.12.192.

Mathias, Neil R., and Munir A. Hussain. 2010. "Non-Invasive Systemic Drug Delivery: Developability Considerations for Alternate Routes of Administration". Journal of Pharmaceutical Sciences 99 (1): 1-20. doi:10.1002/jps.21793.

Mayol, L, F Quaglia, A Borzacchiello, L Ambrosio, and M Rotonda. 2008. "A Novel Poloxamers/Hyaluronic Acid in Situ Forming Hydrogel for Drug Delivery: Rheological, Mucoadhesive and In Vitro Release Properties". *European Journal of Pharmaceutics and Biopharmaceutics* 70 (1): 199-206. doi:10.1016/j.ejpb.2008.04.025.

McConnell, Emma L., Juned Tutas, Mohamed A. M. Mohamed, Douglas Banning, and Abdul W. Basit. 2006. "Colonic Drug Delivery Using Amylose Films: The Role of Aqueous Ethylcellulose Dispersions in Controlling Drug Release". *Cellulose* 14 (1): 25-34. doi:10.1007/s10570-006-9078-8.

McConnell, Emma L., Michael D. Short, and Abdul W. Basit. 2008. "An in Vivo Comparison of Intestinal Ph And Bacteria As Physiological Trigger Mechanisms For Colonic Targeting In Man". *Journal of Controlled Release* 130 (2): 154-160. doi:10.1016/j.jconrel.2008.05.022.

McConnell, Emma L., Sudaxshina Murdan, and Abdul W. Basit. 2008. "An Investigation into The Digestion of Chitosan (Noncrosslinked and Crosslinked) By Human Colonic Bacteria". *Journal of Pharmaceutical Sciences* 97 (9): 3820-3829. doi:10.1002/jps.21271.

Meena, Ramavatar, Ralph Lehnen, and Bodo Saake. 2013. "Microwave-Assisted Synthesis of Kc/Xylan/PVP-Based Blend Hydrogel Materials: Physicochemical and Rheological Studies". *Cellulose* 21 (1): 553-568. doi:10.1007/s10570-013-0155-5.

Melo-Silveira, Raniere Fagundes, Gabriel Pereira Fidelis, Mariana Santana Santos Pereira Costa, Cinthia Beatrice Silva Telles, Nednaldo Dantas-Santos, Susana de Oliveira Elias, and Vanessa Bley Ribeiro et al. 2012. "In Vitro Antioxidant, Anticoagulant And Antimicrobial Activity And In Inhibition Of Cancer Cell Proliferation By Xylan Extracted From Corn Cobs". *International Journal Of Molecular Sciences* 13 (1): 409-426. doi:10.3390/ijms13010409.

Metaxa, Aikaterini-Foteini, Eleni Vrontaki, Eleni K. Efthimiadou, Thomas Mavromoustakos. 2021. “Drug Delivery Systems Based on Modified Polysaccharides: Synthesis and Characterization”. In *Supramolecules in Drug Discovery and Drug Delivery* p. 151-161, Springer, New York.

Miri, Abdolhossein, Majid Darroudi, and Mina Sarani. 2019. "Biosynthesis of Cerium Oxide Nanoparticles and Its Cytotoxicity Survey Against Colon Cancer Cell Line". *Applied Organometallic Chemistry* 34 (1). doi:10.1002/aoc.5308

Mocchiutti, Paulina, Carla N. Schnell, Gerardo D. Rossi, María S. Peresin, Miguel A. Zanuttini, and María V. Galván. 2016. "Cationic and Anionic Polyelectrolyte Complexes of Xylan and Chitosan. Interaction with Lignocellulosic Surfaces". *Carbohydrate Polymers* 150: 89-98. doi:10.1016/j.carbpol.2016.04.111.

Mondon, Karine, Robert Gurny, and Michael Möller. 2008. "Colloidal Drug Delivery Systems – Recent Advances with Polymeric Micelles". *CHIMIA International Journal for Chemistry* 62 (10): 832-840. doi:10.2533/chimia.2008.832.

Moradi Kashkooli, Farshad, M. Soltani, and Mohammad Souri. 2020. "Controlled Anti-Cancer Drug Release Through Advanced Nano-Drug Delivery Systems: Static and Dynamic Targeting Strategies". *Journal of Controlled Release* 327: 316-349. doi:10.1016/j.jconrel.2020.08.012.

Mourya, V. K., Inamdar, N., Nawale, R. B., and Kulthe, S. S. 2011. "Polymeric micelles: general considerations and their applications". *Indian Journal Pharmaceutical Education and Research*, *45* (2): 128-38.

Movassaghian, Sara, Olivia M. Merkel, and Vladimir P. Torchilin. 2015. "Applications of Polymer Micelles for Imaging and Drug Delivery". *Wiley Interdisciplinary Reviews: Nanomedicine and Nanobiotechnology* 7 (5): 691-707. doi:10.1002/wnan.1332.

Muhammad, Faheem, Mingyi Guo, Wenxiu Qi, Fuxing Sun, Aifei Wang, Yingjie Guo, and Guangshan Zhu. 2011. "Ph-Triggered Controlled Drug Release from Mesoporous Silica Nanoparticles Via Intracelluar Dissolution of Zno Nanolids". *Journal of The American Chemical Society* 133 (23): 8778-8781. doi:10.1021/ja200328s.

Naahidi, Sheva, Mousa Jafari, Megan Logan, Yujie Wang, Yongfang Yuan, Hojae Bae, Brian Dixon, and P. Chen. 2017. "Biocompatibility of Hydrogel-Based Scaffolds for Tissue Engineering Applications". *Biotechnology Advances* 35 (5): 530-544. doi:10.1016/j.biotechadv.2017.05.006.

Nagashima, Toshiyuki, Elquio Eleamen Oliveira, Acarília Eduardo da Silva, Henrique Rodrigues Marcelino, Monique Christine Salgado Gomes, Larissa Muratori Aguiar, Ivonete Batista de Araújo, Luiz Alberto Lira Soares, Anselmo Gomes de Oliveira, and E. Sócrates Tabosa do Egito. 2008. "Influence Of The Lipophilic

External Phase Composition On The Preparation And Characterization Of Xylan Microcapsules—A Technical Note". *AAPS Pharmscitech* 9 (3): 814-817. doi:10.1208/s12249-008-9115-z.

Neyrinck, Audrey M., Sam Possemiers, Céline Druart, Tom Van de Wiele, Fabienne De Backer, Patrice D. Cani, Yvan Larondelle, and Nathalie M. Delzenne. 2011. "Prebiotic Effects of Wheat Arabinoxylan Related to The Increase in Bifidobacteria, Roseburia And Bacteroides/Prevotella In Diet-Induced Obese Mice". *Plos ONE* 6 (6): e20944. doi:10.1371/journal.pone.0020944.

Niculescu, Violeta-Carolina. 2020. "Mesoporous Silica Nanoparticles for Bio-Applications". *Frontiers in Materials* 7. doi:10.3389/fmats.2020.00036.

Nielsen, Tina S., Helle N. Lærke, Peter K. Theil, Jens F. Sørensen, Markku Saarinen, Sofia Forssten, and Knud E. Bach Knudsen. 2014. "Diets High in Resistant Starch and Arabinoxylan Modulate Digestion Processes and SCFA Pool Size In The Large Intestine And Faecal Microbial Composition In Pigs". *British Journal of Nutrition* 112 (11): 1837-1849. doi:10.1017/s000711451400302x.

Nishiyama, Tozo, Tatsumasa Mae, Hideyuki Kishida, Misuzu Tsukagawa, Yoshihiro Mimaki, Minpei Kuroda, and Yutaka Sashida et al. 2005. "Curcuminoids and Sesquiterpenoids in Turmeric (Curcuma Longa L.) Suppress an Increase in Blood Glucose Level In Type 2 Diabetic KK-Ay Mice". *Journal of Agricultural and Food Chemistry* 53 (4): 959-963. doi:10.1021/jf0483873.

Noaman, Eman, Nariman K. Badr El-Din, Mona A. Bibars, Ahlam A. Abou Mossallam, and Mamdooh Ghoneum. 2008. "Antioxidant Potential By Arabinoxylan Rice Bran, MGN-3/Biobran, Represents A Mechanism For Its Oncostatic Effect Against Murine Solid Ehrlich Carcinoma". *Cancer Letters* 268 (2): 348-359. doi:10.1016/j.canlet.2008.04.012.

Notarbartolo, Monica, Paola Poma, Daniela Perri, Luisa Dusonchet, Melchiorre Cervello, and Natale D'Alessandro. 2005. "Antitumor Effects of Curcumin, Alone or in Combination with Cisplatin or Doxorubicin, On Human Hepatic Cancer Cells. Analysis of Their Possible Relationship to Changes in NF-Kb Activation Levels and in IAP Gene Expression". *Cancer Letters* 224 (1): 53-65. doi:10.1016/j.canlet.2004.10.051.

Nugent, S. G., Kumar, D., Rampton, D. S., and Evans, D. F. 2001. "Intestinal luminal pH in inflammatory bowel disease: possible determinants and implications for therapy with aminosalicylates and other drugs". *Gut*, *48*(4), 571-577. doi:10.1136/gut.48.4.571

Obayemi, J.D., S.M. Jusu, A.A. Salifu, S. Ghahremani, M. Tadesse, V.O. Uzonwanne, and W.O. Soboyejo. 2020. "Degradable Porous Drug-Loaded Polymer Scaffolds for Localized Cancer Drug Delivery and Breast Cell/Tissue Growth". *Materials*

Science and Engineering: C 112: 110794. doi:10.1016/j.msec.2020.110794.

O'brien, Fergal J. 2011. "Biomaterials & scaffolds for tissue engineering". *Materials Today* 14: 88-95. doi:10.1016/S1369-7021(11)70058-X

Ofori-Kwakye, Kwabena, John T Fell, Harbans L Sharma, and Anne-Marie Smith. 2004. "Gamma Scintigraphic Evaluation of Film-Coated Tablets Intended for Colonic Or Biphasic Release". *International Journal of Pharmaceutics* 270 (1-2): 307-313. doi:10.1016/j.ijpharm.2003.11.009.

Olad, Ali, and Fahimeh Farshi Azhar. 2014. "The Synergetic Effect of Bioactive Ceramic and Nanoclay On The Properties Of Chitosan–Gelatin/Nanohydroxyapatite–Montmorillonite Scaffold For Bone Tissue Engineering". *Ceramics International* 40 (7): 10061-10072. doi:10.1016/j.ceramint.2014.04.010.

Oliveira, Elquio Eleamen, Acarília Eduardo Silva, Toshiyuki Nagashima Júnior, Monique Christine Salgado Gomes, Larissa Muratori Aguiar, Henrique Rodrigues Marcelino, Ivonete Batista Araújo, Marc P. Bayer, Nágila M.P.S. Ricardo, and Anselmo Gomes Oliveira. 2010. "Xylan From Corn Cobs, A Promising Polymer For Drug Delivery: Production And Characterization". *Bioresource Technology* 101 (14): 5402-5406. doi:10.1016/j.biortech.2010.01.137.

Ong, Yi Xian Jolene, Lai Yeng Lee, Pooya Davoodi, and Chi-Hwa Wang. 2018. "Production of Drug-Releasing Biodegradable Microporous Scaffold Using a Two-Step Micro-Encapsulation/Supercritical Foaming Process". *The Journal of Supercritical Fluids* 133: 263-269. doi:10.1016/j.supflu.2017.10.018.

Owen, Shawn C., Dianna P.Y. Chan, and Molly S. Shoichet. 2012. "Polymeric Micelle Stability". *Nano Today* 7 (1): 53-65. doi:10.1016/j.nantod.2012.01.002.

Paharia, Amol, Awesh K. Yadav, Gopal Rai, Sunil K. Jain, Shyam S. Pancholi, and Govind P. Agrawal. 2007. "Eudragit-Coated Pectin Microspheres of 5-Fluorouracil For Colon Targeting". *AAPS Pharmscitech* 8 (1): E87-E93. doi:10.1208/pt0801012.

Palframan, Richard J., Gibson Gleen R., and Rastall Robert A. 2003. “Carbohydrate preferences of Bifidobacterium species isolated from the human gut”. *Current Issues in Intestinal Microbiology* 4: 71-75.

Park, Jun-Hwan, Young-Ho Lee, and Seong-Geun Oh. 2007. "Preparation of Thermosensitive Pnipam-Grafted Mesoporous Silica Particles". *Macromolecular Chemistry and Physics* 208 (22): 2419-2427. doi:10.1002/macp.200700247.

Peng, Xin-wen, Jun-li Ren, Lin-xin Zhong, and Run-cang Sun. 2011. "Nanocomposite Films Based On Xylan-Rich Hemicelluloses And Cellulose Nanofibers With Enhanced Mechanical Properties". *Biomacromolecules* 12 (9): 3321-3329. doi:10.1021/bm2008795.

Perumal, Ramesh Kannan, Sathiamurthi Perumal, Ramar Thangam, Arun Gopinath, Satiesh Kumar Ramadass, Balaraman Madhan, and Srinivasan Sivasubramanian. 2018. "Collagen-Fucoidan Blend Film with The Potential to Induce Fibroblast Proliferation For Regenerative Applications". *International Journal of Biological Macromolecules* 106: 1032-1040. doi:10.1016/j.ijbiomac.2017.08.111.

Petrov, Petar, Jiayin Yuan, Krassimira Yoncheva, Axel H. E. Müller, and Christo B. Tsvetanov. 2008. "Wormlike Morphology Formation and Stabilization of "Pluronic P123" Micelles by Solubilization Of Pentaerythritol Tetraacrylate". *The Journal of Physical Chemistry B* 112 (30): 8879-8883. doi:10.1021/jp8008767.

Philip, Anil, and Betty Philip. 2010. "Colon Targeted Drug Delivery Systems: A Review On Primary and Novel Approaches". *Oman Medical Journal* 25 (2): 70-78. doi:10.5001/omj.2010.24.

Pierce, Mark W. 2010. "Transdermal Delivery of Sumatriptan for The Treatment of Acute Migraine". *Neurotherapeutics* 7 (2): 159-163. doi:10.1016/j.nurt.2010.03.005.

Pirmoradi, Fatemeh Nazly, John K. Jackson, Helen M. Burt, and Mu Chiao. 2011. "On-Demand Controlled Release of Docetaxel from A Battery-Less MEMS Drug Delivery Device". *Lab On a Chip* 11 (16): 2744. doi:10.1039/c1lc20134d.

Polat Mehmet, Hurriyet Polat. 2020. "Recent Advances of Chitosan-Based Systems for Delivery of Anticancer Drugs". In: Jana S, Jana S (eds*) Functional Chitosan: Drug Delivery And Biomedical Applications*. p 191-228, Springer Nature. doi:10.1007/978-981-15-0263-7_7

Pollet, Annick, Valerie Van Craeyveld, Tom Van de Wiele, Willy Verstraete, Jan A. Delcour, and Christophe M. Courtin. 2012. "In Vitro Fermentation of Arabinoxylan Oligosaccharides and Low Molecular Mass Arabinoxylans with Different Structural Properties From Wheat (Triticum Aestivum L.) Bran And Psyllium (Plantago Ovata Forsk) Seed Husk". *Journal of Agricultural and Food Chemistry* 60 (4): 946-954. doi:10.1021/jf203820j.

Popat, Amirali, Jian Liu, Qiuhong Hu, Michael Kennedy, Brenton Peters, Gao Qing (Max) Lu, and Shi Zhang Qiao. 2012. "Adsorption and Release of Biocides with Mesoporous Silica Nanoparticles". *Nanoscale* 4 (3): 970-975. doi:10.1039/c2nr11691j.

Popat, Amirali, Sandy Budi Hartono, Frances Stahr, Jian Liu, Shi Zhang Qiao, and Gao Qing (Max) Lu. 2011. "Mesoporous Silica Nanoparticles for Bioadsorption, Enzyme Immobilisation, And Delivery Carriers". *Nanoscale* 3 (7): 2801. doi:10.1039/c1nr10224a.

Prabaharan, M., and R. Jayakumar. 2009. "Chitosan-Graft-B-Cyclodextrin Scaffolds with Controlled Drug Release Capability for Tissue Engineering Applications". *International Journal of Biological Macromolecules* 44 (4): 320-325. doi:10.1016/j.ijbiomac.2009.01.005.

Prabaharan, M., M. A. Rodriguez-Perez, J. A. de Saja, and J. F. Mano. 2007. "Preparation And Characterization Of Poly(L-Lactic Acid)-Chitosan Hybrid Scaffolds With Drug Release Capability". *Journal of Biomedical Materials Research Part B: Applied Biomaterials* 81B (2): 427-434. doi:10.1002/jbm.b.30680.

Prasher, Parteek, Mousmee Sharma, Meenu Mehta, Saurabh Satija, Alaa A. Aljabali, Murtaza M. Tambuwala, and Krishnan Anand et al. 2021. "Current-Status And Applications Of Polysaccharides In Drug Delivery Systems". *Colloid And Interface Science Communications* 42: 100418. doi:10.1016/j.colcom.2021.100418.

Raghavan, Chellan Vijaya, Chithambaram Muthulingam, Joseph Amaladoss Josephine Leno Jenita, and Thengungal Kochupapy Ravi. 2002. "An In Vitro And In Vivo Investigation Into The Suitability Of Bacterially Triggered Delivery System For Colon Targeting.". *Chemical and Pharmaceutical Bulletin* 50 (7): 892-895. doi:10.1248/cpb.50.892.

Ram, Arjun, Moumita Das, and Balaram Ghosh. 2003. "Curcumin Attenuates Allergen-Induced Airway Hyperresponsiveness in Sensitized Guinea Pigs". *Biological and Pharmaceutical Bulletin* 26 (7): 1021-1024. doi:10.1248/bpb.26.1021.

Ramos Berger, Lúcia Raquel, Thayza Christina Montenegro Stamford, Kataryne Árabe Rimá de Oliveira, Adjane de Miranda Pereira Pessoa, Marcos Antonio Barbosa de Lima, Maria Manuela Estevez Pintado, Marcos Paz Saraiva Câmara, Luciana de Oliveira Franco, Marciane Magnani, and Evandro Leite de Souza. 2018. "Chitosan Produced from Mucorales Fungi Using Agroindustrial By-Products and Its Efficacy to Inhibit Colletotrichum Species". *International Journal of Biological Macromolecules* 108: 635-641. doi:10.1016/j.ijbiomac.2017.11.178.

Rao, K A. 2004. "Objective Evaluation of Small Bowel and Colonic Transit Time Using Ph Telemetry In Athletes With Gastrointestinal Symptoms". British Journal of Sports Medicine 38 (4): 482-487. doi:10.1136/bjsm.2003.006825.

Ravindranath, Vijayalaksmi, and Nanajundiah Chandrasekhara. 1981. "Metabolism Of Curcumn-Studies With [3H]Curcumin". *Toxicology* 22 (4): 337-344. doi:10.1016/0300-483x(81)90027-5.

Reinus, John. F. and Douglas Simon. 2014. "*Gastrointestinal anatomy and physiology: The Essentials*". John Wiley & Sons.

Ren, Xiaofei, and Yongmin Zhang. 2020. "Switching Pickering Emulsion Stabilized by Chitosan-SDS Complexes Through Ion Competition". *Colloids and Surfaces A: Physicochemical and Engineering Aspects* 587: 124316. doi:10.1016/j.colsurfa.2019.124316.

Rosa-Sibakov, Natalia, Terhi K. Hakala, Nesli Sözer, Emilia Nordlund, Kaisa Poutanen, and Anna-Marja Aura. 2016. "Birch Pulp Xylan Works as a Food Hydrocolloid In Acid Milk Gels And Is Fermented Slowly In Vitro". *Carbohydrate Polymers* 154: 305-312. doi:10.1016/j.carbpol.2016.06.028.

Rose, Devin J, George E Inglett, and Sean X. Liu. 2010. "Utilisation of Corn (Zea Mays) Bran and Corn Fiber In The Production Of Food Components". *Journal of The Science of Food and Agriculture* 90 (6): 915-924. doi:10.1002/jsfa.3915.

Rosenholm, Jessica, Cecilia Sahlgren, and Mika Linden. 2011. "Multifunctional Mesoporous Silica Nanoparticles for Combined Therapeutic, Diagnostic and Targeted Action In Cancer Treatment". *Current Drug Targets* 12 (8): 1166-1186. doi:10.2174/138945011795906624.

Sami El-banna, Fatma, Magdy Elsayed Mahfouz, Stefano Leporatti, Maged El-Kemary, and Nemany A. N. Hanafy. 2019. "Chitosan as A Natural Copolymer with Unique Properties for The Development Of Hydrogels". *Applied Sciences* 9 (11): 2193. doi:10.3390/app9112193.

Sang, Xinxin, Qiyi Yang, Gang Shi, Liping Zhang, Dawei Wang, and Caihua Ni. 2018. "Preparation of Ph/Redox Dual Responsive Polymeric Micelles with Enhanced Stability and Drug Controlled Release". *Materials Science and Engineering: C* 91: 727-733. doi:10.1016/j.msec.2018.06.012.

Santos, M. S., F. W. Tavares, and E. C. Biscaia Jr. 2016. "Molecular Thermodynamics of Micellization: Micelle Size Distributions and Geometry Transitions". *Brazilian Journal of Chemical Engineering* 33 (3): 515-523. doi:10.1590/0104-6632.20160333s20150129.

Sanyakamdhorn, Sriwanna, Daniel Agudelo, and Heidar-Ali Tajmir-Riahi. 2013. "Encapsulation of Antitumor Drug Doxorubicin and Its Analogue by Chitosan Nanoparticles". *Biomacromolecules* 14 (2): 557-563. doi:10.1021/bm3018577.

Sastry, Srikonda Venkateswara, Janaki Ram Nyshadham, and Joseph A. Fix. 2000. "Recent Technological Advances In Oral Drug Delivery – A Review". *Pharmaceutical Science & Technology Today* 3 (4): 138-145. doi:10.1016/s1461-5347(00)00247-9.

Sauraj, S. Uday Kumar, P. Gopinath, and Yuvraj Singh Negi. 2017. "Synthesis and Bio-Evaluation of Xylan-5-Fluorouracil-1-Acetic Acid Conjugates As Prodrugs For Colon Cancer Treatment". *Carbohydrate Polymers* 157: 1442-1450. doi:10.1016/j.carbpol.2016.09.096.

Sauraj, Vinay Kumar, Bijender Kumar, Farha Deeba, Saleheen Bano, Anurag Kulshreshtha, P. Gopinath, and Yuvraj Singh Negi. 2019. "Lipophilic 5-Fluorouracil Prodrug Encapsulated Xylan-Stearic Acid Conjugates Nanoparticles for Colon Cancer Therapy". *International Journal of Biological Macromolecules* 128: 204-213. doi:10.1016/j.ijbiomac.2019.01.101.

Sauraj, Vinay kumar, Bijender Kumar, Ruchir Priyadarshi, Farha Deeba, Anurag Kulshreshtha, Anuj Kumar, Garima Agrawal, P. Gopinath, and Yuvraj Singh Negi. 2020. "Redox Responsive Xylan-SS-Curcumin Prodrug Nanoparticles for Dual Drug Delivery In Cancer Therapy". *Materials Science and Engineering: C* 107: 110356. doi:10.1016/j.msec.2019.110356.

Saxena, Vipin, and Muhammad Delwar Hussain. 2013. "Polymeric Mixed Micelles for Delivery Of Curcumin To Multidrug Resistant Ovarian Cancer". *Journal of Biomedical Nanotechnology* 9 (7): 1146-1154. doi:10.1166/jbn.2013.1632.

Scheller, Henrik Vibe, and Ulvskov Peter. 2010. “Hemicelluloses”. *Annual review of plant biology* 61: 263-289. doi: 10.1146/annurev-arplant-042809-112315.

Schneider, Galen B., Anthony English, Matthew Abraham, Rebecca Zaharias, Clark Stanford, and John Keller. 2004. "The Effect Of Hydrogel Charge Density On Cell Attachment". *Biomaterials* 25 (15): 3023-3028. doi:10.1016/j.biomaterials.2003.09.084

Sharma, Ricky A., Stephanie A. Euden, Sharon L. Platton, Darren N. Cooke, Aisha Shafayat, Heather R. Hewitt, and Timothy H. Marczylo et al. 2004. "Phase I Clinical Trial Of Oral Curcumin". *Clinical Cancer Research* 10 (20): 6847-6854. doi:10.1158/1078-0432.ccr-04-0744.

She, Zhending, Bofeng Zhang, Chenrui Jin, Qingling Feng, and Yingxin Xu. 2008. "Preparation And In Vitro Degradation Of Porous Three-Dimensional Silk Fibroin/Chitosan Scaffold". Polymer Degradation and Stability 93 (7): 1316-1322. doi:10.1016/j.polymdegradstab.2008.04.001.

Shen, Zhi-Sen, Xiang Cui, Rui-Xia Hou, Qun Li, Hong-Xia Deng, and Jun Fu. 2015. "Tough Biodegradable Chitosan–Gelatin Hydrogels Via In Situ Precipitation For

Potential Cartilage Tissue Engineering". *RSC Advances* 5 (69): 55640-55647. doi:10.1039/c5ra06835e.

Shimono, Norihito, Toshihito Takatori, Masumi Ueda, Masaaki Mori, Yutaka Higashi, and Yasuhiko Nakamura. 2002. "Chitosan Dispersed System For Colon-Specific Drug Delivery". *International Journal Of Pharmaceutics* 245 (1-2): 45-54. doi:10.1016/s0378-5173(02)00344-7.

Siew, Adeline, Hang Le, Marion Thiovolet, Paul Gellert, Andreas Schatzlein, and Ijeoma Uchegbu. 2011. "Enhanced Oral Absorption Of Hydrophobic And Hydrophilic Drugs Using Quaternary Ammonium Palmitoyl Glycol Chitosan Nanoparticles". *Molecular Pharmaceutics* 9 (1): 14-28. doi:10.1021/mp200469a.

Silva, A, E Dasilva, E Oliveria, T Nagashimajr, L Soares, A Medeiros, J Araujo, I Araujo, A Carrico, and E Egito. 2007. "Synthesis And Characterization Of Xylan-Coated Magnetite Microparticles". *International Journal Of Pharmaceutics* 334 (1-2): 42-47. doi:10.1016/j.ijpharm.2006.10.019.

Silva, Acarilia Eduardo, Elquio Eleamen Oliveira, Monique C. Salgado Gomes, Henrique Rodrigues Marcelino, Karen C. Holanda Silva, Bartolomeu Santos Souza, Toshiyuki Nagashima, Alejandro Pedro Ayala, Anselmo Gomes Oliveira, and Eryvaldo Sócrates Tabosa do Egito. 2013. "Producing Xylan/Eudragit® S100-Based Microparticles by Chemical And Physico-Mechanical Approaches as Carriers For 5-Aminosalicylic Acid". *Journal of Microencapsulation* 30 (8): 787-795. doi:10.3109/02652048.2013.788087.

Silverstein, Michael S. 2014. "Emulsion-Templated Porous Polymers: A Retrospective Perspective". *Polymer* 55 (1): 304-320. doi:10.1016/j.polymer.2013.08.068.

Singh MR, Patel S, and Singh D. 2016. "Natural polymer-based hydrogels as scaffolds for tissue engineering*". Nanobiomaterials in Soft Tissue Engineering. Applications of Nanobiomaterials*, (5), p. 231-260, Elsevier.

Singh, V., Malviya, T., Gupta, S., Dwivedi, L. M., Baranwal, K., and Prabha, M. 2020. *"*Polysaccharide-based nanoparticles: nanocarriers for sustained delivery of drugs*". Advanced Biopolymeric Systems for Drug Delivery,* p. 151-181, Springer.

Sinha, V.R., and Rachna Kumria. 2001. "Polysaccharides In Colon-Specific Drug Delivery". *International Journal of Pharmaceutics* 224 (1-2): 19-38. doi:10.1016/s0378-5173(01)00720-7.

Siretli, Cagrı. 2012. "Synthesis of silica nano particles with custom-made morphology for controlled drug delivery", MSc Thesis, IZTECH.

Sneddon, Gregor, Alexey Y. Ganin, and Humphrey H. P. Yiu. 2015. "Sustainable CO 2 Adsorbents Prepared by Coating Chitosan onto Mesoporous Silicas for Large-

Scale Carbon Capture Technology". *Energy Technology* 3 (3): 249-258. doi:10.1002/ente.201402211.

Sood, Ankur, Aastha Gupta, and Garima Agrawal. 2021. "Recent Advances In Polysaccharides Based Biomaterials For Drug Delivery And Tissue Engineering Applications". *Carbohydrate Polymer Technologies And Applications* 2: 100067. doi:10.1016/j.carpta.2021.100067.

Sornalatha, Jesuvathy, Murugakoothan, P. 2013. “Room temperature synthesis of ZnO nanostructures using CTAB assisted sol-gel method for application in solar cells”. *International journal of emerging technology and advanced engineering*, 3 (9): 414-418.

Sou, Keitaro, Shunsuke Inenaga, Shinji Takeoka, and Eishun Tsuchida. 2008. "Loading of Curcumin into Macrophages Using Lipid-Based Nanoparticles". *International Journal of Pharmaceutics* 352 (1-2): 287-293. doi:10.1016/j.ijpharm.2007.10.033.

Sriamornsak, Pornsak, Jurairat Nunthanid, Kamonrak Cheewatanakornkool, and Somkamol Manchun. 2010. "Effect of Drug Loading Method On Drug Content And Drug Release From Calcium Pectinate Gel Beads". *AAPS Pharmscitech* 11 (3): 1315-1319. doi:10.1208/s12249-010-9513-x.

Stella, Valentino J., and Kwame W. Nti-Addae. 2007. "Prodrug Strategies to Overcome Poor Water Solubility". *Advanced Drug Delivery Reviews* 59 (7): 677-694. doi:10.1016/j.addr.2007.05.013.

Stöber, Werner, Fink Arthur, and Bohn Ernst. 1968. “Controlled growth of monodisperse silica spheres in the micron size range”. *Journal of colloid and interface science* 26 (1): 62-69. doi: 10.1016/0021-9797(68)90272-5.

Subramanian, Anuradha, David Vu, Gustavo F. Larsen, and Hsin-Yi Lin. 2005. "Preparation and Evaluation of the Electrospun Chitosan/PEO Fibers for Potential Applications In Cartilage Tissue Engineering". *Journal of Biomaterials Science, Polymer Edition* 16 (7): 861-873. doi:10.1163/1568562054255682.

Sun, Xiao-Feng, Hai-hong Wang, Zhan-xin Jing, and Rajaratnam Mohanathas. 2013. "Hemicellulose-Based Ph-Sensitive And Biodegradable Hydrogel For Controlled Drug Delivery". *Carbohydrate Polymers* 92 (2): 1357-1366. doi:10.1016/j.carbpol.2012.10.032.

Sun, Yanzhen, Xiaodong Jing, Xiaoli Ma, Yinglong Feng, and Hao Hu. 2020. "Versatile Types of Polysaccharide-Based Drug Delivery Systems: From Strategic Design to Cancer Therapy". *International Journal of Molecular Sciences* 21 (23): 9159. doi:10.3390/ijms21239159.

Szejtli, Jozsef. 2005. "Past, Present, And Future of Cyclodextrin Research". *Cheminform* 36 (17). doi:10.1002/chin.200517261.

Takeuchi, Hirofumi, Hiromitsu Yamamoto, and Yoshiaki Kawashima. 2001. "Mucoadhesive Nanoparticulate Systems for Peptide Drug Delivery". *Advanced Drug Delivery Reviews* 47 (1): 39-54. doi:10.1016/s0169-409x(00)00120-4.

Tandya, Andrian, Fariba Dehghani, and Neil R. Foster. 2006. "Micronization of Cyclosporine Using Dense Gas Techniques". *The Journal of Supercritical Fluids* 37 (3): 272-278. doi:10.1016/j.supflu.2005.10.004.

Tang, Chuan, Yi-Xin Guan, Shan-Jing Yao, and Zi-Qiang Zhu. 2014. "Preparation of Ibuprofen-Loaded Chitosan Films for Oral Mucosal Drug Delivery Using Supercritical Solution Impregnation". *International Journal Of Pharmaceutics* 473 (1-2): 434-441. doi:10.1016/j.ijpharm.2014.07.039.

Tejada, G., G.N. Piccirilli, M. Sortino, C.J. Salomón, M.C. Lamas, and D. Leonardi. 2017. "Formulation And In-Vitro Efficacy Of Antifungal Mucoadhesive Polymeric Matrices For The Delivery Of Miconazole Nitrate". *Materials Science And Engineering: C* 79: 140-150. doi:10.1016/j.msec.2017.05.034.

Thommes, M., Kaneko, K., Neimark, A. V., Olivier, J. P., Rodriguez-Reinoso, F., Rouquerol, J., & Sing, K. S. 2015. "Physisorption of Gases, With Special Reference to The Evaluation Of Surface Area And Pore Size Distribution (IUPAC Technical Report)". *Pure and applied chemistry* 87 (910): 1051-1069. doi:10.1515/ci.2011.33.2.22a.

Tiwari, Gaurav, Tiwari Ruchi, Sriwastawa Birendra, Bhati L., Pandey S., Pandey P., and Bannerjee S.K. 2012. “Drug delivery systems: An updated review”. *International Journal of Pharmaceutical Investigation*, 2 (1): 2. doi:10.4103/2230-973X.96920.

Tiyaboonchai, Waree, Watcharaphorn Tungpradit, and Pinyupa Plianbangchang. 2007. "Formulation and Characterization of Curcuminoids Loaded Solid Lipid Nanoparticles". *International Journal of Pharmaceutics* 337 (1-2): 299-306. doi:10.1016/j.ijpharm.2006.12.043.

Tønnesen, Hanne Hjorth, Már Másson, and Thorsteinn Loftsson. 2002. "Studies of Curcumin and Curcuminoids. XXVII. Cyclodextrin Complexation: Solubility, Chemical and Photochemical Stability". *International Journal of Pharmaceutics* 244 (1-2): 127-135. doi:10.1016/s0378-5173(02)00323-x.

Torchilin Vladimir P. 1999. "Polychelating amphiphilic polymers to optimize the concentrations of contrast agents used in medical diagnostic imaging" *Chemtech* 29 (11): 27-34.

Torchilin, Vladimir P. 2002. "PEG-Based Micelles as Carriers of Contrast Agents For Different Imaging Modalities". *Advanced Drug Delivery Reviews* 54 (2): 235-252. doi:10.1016/s0169-409x(02)00019-4.

Trivedi, Ruchit, and Uday B Kompella. 2010. "Nanomicellar Formulations for Sustained Drug Delivery: Strategies and Underlying Principles". *Nanomedicine* 5 (3): 485-505. doi:10.2217/nnm.10.10.

Trubetskoy, Vladimir S., Maria D. Frank-Kamenetsky, Kathleen R. Whiteman, Gerald L. Wolf, and Vladimir P. Torchilin. 1996. "Stable Polymeric Micelles: Lymphangiographic Contrast Media for Gamma Scintigraphy and Magnetic Resonance Imaging". *Academic Radiology* 3 (3): 232-238. doi:10.1016/s1076-6332(96)80448-x.

Tuleu, C., A. W. Basit, W. A. Waddington, P. J. Ell, and J. M. Newton. 2002. "Colonic Delivery of 4-Aminosalicylic Acid Using Amylose-Ethylcellulose-Coated Hydroxypropylmethylcellulose Capsules". *Alimentary Pharmacology & Therapeutics* 16 (10): 1771-1779. doi:10.1046/j.1365-2036.2002.01327.x.

Ukil, A, S Maity, S Karmakar, N Datta, J R Vedasiromoni, and Pijush K Das. 2003. "Curcumin, The Major Component of Food Flavour Turmeric, Reduces Mucosal Injury in Trinitrobenzene Sulphonic Acid-Induced Colitis". *British Journal of Pharmacology* 139 (2): 209-218. doi:10.1038/sj.bjp.0705241.

Umemura, Kenji, and Kawai Shuichi. 2008. “Preparation and characterization of Maillard reacted chitosan films with hemicellulose model compounds”. *Journal of Applied Polymer Science* 108 (4): 2481-2487. doi: 10.1002/app.27842

Vallet-Regí, Maria, Balas Francisco, Arcos Daniel. 2007. “Mesoporous materials for drug delivery”. *Angewandte Chemie International Edition* 46 doi: 10.1002/anie.200604488.

Vallet-Regí, María, Montserrat Colilla, Isabel Izquierdo-Barba, and Miguel Manzano. 2018. "Mesoporous Silica Nanoparticles for Drug Delivery: Current Insights". Molecules 23 (1): 47. doi:10.3390/molecules23010047.

Van den Abbeele, Pieter, Philippe Gérard, Sylvie Rabot, Aurélia Bruneau, Sahar El Aidy, Muriel Derrien, and Michiel Kleerebezem et al. 2011. "Arabinoxylans and Inulin Differentially Modulate the Mucosal And Luminal Gut Microbiota And Mucin-Degradation In Humanized Rats". *Environmental Microbiology* 13 (10): 2667-2680. doi:10.1111/j.1462-2920.2011.02533.x.

Vemula, Praveen Kumar, Jun Li, and George John. 2006. "Enzyme Catalysis: Tool to Make and Break Amygdalin Hydrogelators from Renewable Resources: A Delivery Model for Hydrophobic Drugs". *Journal of The American Chemical Society* 128 (27): 8932-8938. doi:10.1021/ja062650u.

Venugopal, J., R. Rajeswari, M. Shayanti, R. Sridhar, S. Sundarrajan, R. Balamurugan, and S. Ramakrishna. 2013. "Xylan Polysaccharides Fabricated into Nanofibrous Substrate for Myocardial Infarction". *Materials Science and Engineering: C* 33 (3): 1325-1331. doi:10.1016/j.msec.2012.12.032.

Vivero-Escoto, Juan L., Igor I. Slowing, Chian-Wen Wu, and Victor S.-Y. Lin. 2009. "Photoinduced Intracellular Controlled Release Drug Delivery in Human Cells by Gold-Capped Mesoporous Silica Nanosphere". *Journal of The American Chemical Society* 131 (10): 3462-3463. doi:10.1021/ja900025f.

Wang Chong, Wei Huang, Yu Zhou, Libing He, Zhi He, Ziling Chen, Xiao He, Shuo Tian, Jiaming Liao, Bingheng Lu, Yen Weid, Min Wang. 2020. "3D printing of bone tissue engineering scaffolds". *Bioactive Materials* 5:82-91. doi:10.1016/j.jconrel.2008.04.013

Wang, Ming-Jun, Yu-Liang Xie, Qiao-Dong Zheng, and Shan-Jing Yao. 2009. "A Novel, Potential Microflora-Activated Carrier for A Colon-Specific Drug Delivery System And Its Characteristics". *Industrial & Engineering Chemistry Research* 48 (11): 5276-5284. doi:10.1021/ie801295y.

Wei, Xiaoyue, Chunyang Liu, Zhiyong Wang, and Yongxiang Luo. 2020. "3D Printed Core-Shell Hydrogel Fiber Scaffolds with NIR-Triggered Drug Release For Localized Therapy Of Breast Cancer". *International Journal of Pharmaceutics* 580: 119219. doi:10.1016/j.ijpharm.2020.119219.

Wei, Zhang, Junguo Hao, Shi Yuan, Yajuan Li, Wu Juan, Xianyi Sha, and Xiaoling Fang. 2009. "Paclitaxel-Loaded Pluronic P123/F127 Mixed Polymeric Micelles: Formulation, Optimization and In Vitro Characterization". *International Journal of Pharmaceutics* 376 (1-2): 176-185. doi:10.1016/j.ijpharm.2009.04.030.

Wong, S.M., I.W. Kellaway, and S. Murdan. 2006. "Enhancement of The Dissolution Rate And Oral Absorption Of A Poorly Water Soluble Drug By Formation Of Surfactant-Containing Microparticles". *International Journal of Pharmaceutics* 317 (1): 61-68. doi:10.1016/j.ijpharm.2006.03.001.

Xiong, Sijia, HuiChang Gao, Lanfeng Qin, Yong-Guang Jia, and Li Ren. 2019. "Engineering Topography: Effects On Corneal Cell Behavior and Integration Into

Corneal Tissue Engineering". *Bioactive Materials* 4: 293-302. doi:10.1016/j.bioactmat.2019.10.001.

Xu, Jing, Tian-Duo Li, Xiao-Long Tang, Cong-De Qiao, and Qing-Wei Jiang. 2012. "Effect of Aggregation Behavior Of Gelatin In Aqueous Solution On The Grafting Density of Gelatin Modified With Glycidol". *Colloids and Surfaces B: Biointerfaces* 95: 201-207. doi:10.1016/j.colsurfb.2012.02.041.

Xu, Wei, Peixue Ling, and Tianmin Zhang. 2013. "Polymeric Micelles, A Promising Drug Delivery System to Enhance Bioavailability Of Poorly Water-Soluble Drugs". *Journal of Drug Delivery* 2013: 1-15. doi:10.1155/2013/340315.

Yang, Chen, Nicholas Thomas Blum, Jing Lin, Junle Qu, and Peng Huang. 2020. "Biomaterial Scaffold-Based Local Drug Delivery Systems for Cancer Immunotherapy". *Science Bulletin* 65 (17): 1489-1504. doi:10.1016/j.scib.2020.04.012.

Yang, Kuo-Yi, Lei-Chwen Lin, Ting-Yu Tseng, Shau-Chun Wang, and Tung-Hu Tsai. 2007. "Oral Bioavailability of Curcumin In Rat And The Herbal Analysis From Curcuma Longa By LC–MS/MS". *Journal of Chromatography B* 853 (1-2): 183-189. doi:10.1016/j.jchromb.2007.03.010.

Yang, Lei, Yongsan Li, Yanzi Gou, Xing Wang, Xinming Zhao, and Lei Tao. 2017. "Improving Tumor Chemotherapy Effect Using an Injectable Self-Healing Hydrogel as Drug Carrier". *Polymer Chemistry* 8 (34): 5071-5076. doi:10.1039/c7py00112f.

Yang, Shoufeng, Kah-Fai Leong, Zhaohui Du, and Chee-Kai Chua. 2001. "The Design of Scaffolds For Use In Tissue Engineering. Part I. Traditional Factors". *Tissue Engineering* 7 (6): 679-689. doi:10.1089/107632701753337645.

Zahouani, H., C. Pailler-Mattei, B. Sohm, R. Vargiolu, V. Cenizo, and R. Debret. 2009. "Characterization of The Mechanical Properties Of A Dermal Equivalent Compared With Human Skinin Vivoby Indentation And Static Friction Tests". *Skin Research And Technology* 15 (1): 68-76. doi:10.1111/j.1600-0846.2008.00329.x.

Zeybek, Nuket, Robert A. Rastall, and Ali Oguz Buyukkileci. 2020. "Utilization of Xylan-Type Polysaccharides In Co-Culture Fermentations Of Bifidobacterium And Bacteroides Species". *Carbohydrate Polymers* 236: 116076. doi:10.1016/j.carbpol.2020.116076.

Zhang, Qiang, Yingchun Li, Zhi Yuan (William) Lin, Kenneth K.Y. Wong, Min Lin, Lara Yildirimer, and Xin Zhao. 2017. "Electrospun Polymeric Micro/Nanofibrous Scaffolds for Long-Term Drug Release and Their Biomedical Applications". *Drug Discovery Today* 22 (9): 1351-1366.

doi:10.1016/j.drudis.2017.05.007.

Zhang, Ruiyun, and Peter X. Ma. 1999. "Porous Poly(L-Lactic Acid)/Apatite Composites Created By Biomimetic Process". *Journal of Biomedical Materials Research* 45 (4): 285-293. doi:10.1002/(sici)1097-4636(19990615)

Zhang, Wei, Yuan Shi, Yanzuo Chen, Junguo Hao, Xianyi Sha, and Xiaoling Fang. 2011. "The Potential of Pluronic Polymeric Micelles Encapsulated With Paclitaxel For The Treatment of Melanoma Using Subcutaneous And Pulmonary Metastatic Mice Models". *Biomaterials* 32 (25): 5934-5944. doi:10.1016/j.biomaterials.2011.04.075.

Zhang, Wei, Yuan Shi, Yanzuo Chen, Shuangyin Yu, Junguo Hao, Jieqi Luo, Xianyi Sha, and Xiaoling Fang. 2010. "Enhanced Antitumor Efficacy by Paclitaxel-Loaded Pluronic P123/F127 Mixed Micelles Against Non-Small Cell Lung Cancer Based On Passive Tumor Targeting And Modulation Of Drug Resistance". *European Journal of Pharmaceutics and Biopharmaceutics* 75 (3): 341-353. doi:10.1016/j.ejpb.2010.04.017.

Zheng, Yu, Qingxuan Xie, Hong Wang, Yanjun Hu, Bo Ren, and Xiaofang Li. 2020. "Recent Advances In Plant Polysaccharide-Mediated Nano Drug Delivery Systems". *International Journal of Biological Macromolecules* 165: 2668-2683. doi:10.1016/j.ijbiomac.2020.10.173.

Zhong, Xia, Chengdong Ji, Andrew K. L. Chan, Sergei G. Kazarian, Andrew Ruys, and Fariba Dehghani. 2011. "Fabrication Of Chitosan/Poly(E-Caprolactone) Composite Hydrogels For Tissue Engineering Applications". *Journal of Materials Science: Materials in Medicine* 22 (2): 279-288. doi:10.1007/s10856-010-4194-2.

Zhu, Jing-jing, Xin-xin Zhang, Yun-qiu Miao, Shu-fang He, Dan-mei Tian, Xin-sheng Yao, Jin-shan Tang, and Yong Gan. 2016. "Delivery of Acetylthevetin B, An Antitumor Cardiac Glycoside, Using Polymeric Micelles For Enhanced Therapeutic Efficacy Against Lung Cancer Cells". *Acta Pharmacologica Sinica* 38 (2): 290-300. doi:10.1038/aps.2016.113.

Zhu, Qiang, and Shirui Mao. 2019. "Enhanced Drug Loading Efficiency of Contact Lenses Via Salt-Induced Modulation". *Asian Journal of Pharmaceutical Sciences* 14 (2): 204-215. doi:10.1016/j.ajps.2018.05.002.

APPENDICES

APPENDIX A. MEDIA COMPOSITION

Table A.1. Composition of Wilkins-Chalgren Anaerobe Broth.

Component	Concentration g/L
Tryptone	10.0
Gelatine peptone	10.0
Yeast Extract	5.0
Glucose	1.0
Sodium chloride	5.0
L-arginine	1.0
Sodium pyruvate	1.0
Menadione	0.0005
Haemin	0.005

Table A.2. Composition of Reinforced Clostiridial Medium.

Component	Concentration g/L
Peptone	10.0
Yeast extract	13.0
Sodium chloride	5.0
Glucose	5.0
Soluble starch	1.0
Sodium acetate	3.0
Cysteine hydrochloride	0.5
Agar	0.5

Table A. 3. Composition of Basal Medium

Component	**Concentration g/L**
Peptone water	2.0
Yeast extract	2.0
Sodium chloride	0.1
Potassium phosphate dibasic	0.04
Potassium phosphate monobasic	0.04
Magnesium sulfate heptahydrate	0.01
Calcium chloride hexahydrate	0.01
Sodium bicarbonate	2.0
Tween 80	2 µl
Haemin	0.005
Vitamin k1	10 µl
Resazurin	0.001
Bile salt	0.5

APPENDIX B

STANDARD CALIBRATION GRAPH FOR XYLOSE

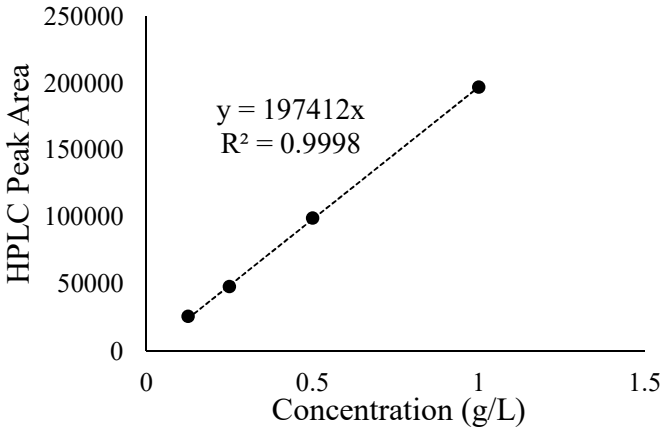

Figure B.1. Xylose standard curve for HPLC

APPENDIX C

STANDARD CALIBRATION GRAPH FOR ORGANIC ACIDS

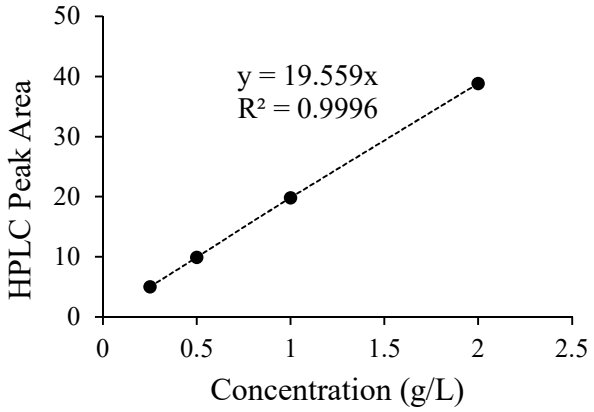

Figure C.1. Lactate standard curve for HPLC

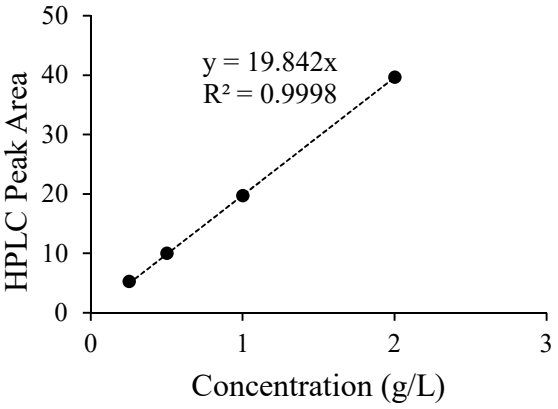

Figure C.2. Acetate standard curve for HPLC

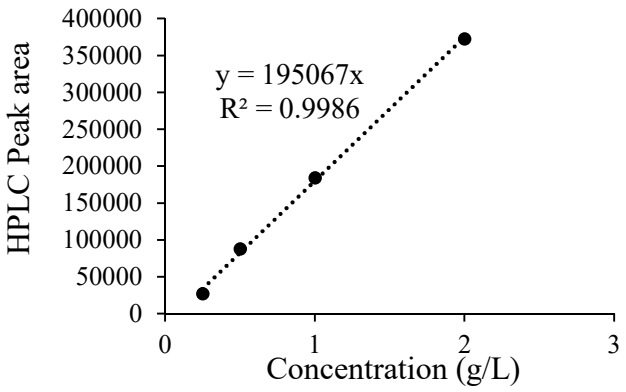

Figure C.3. Succinate standard curve for HPLC.

APPENDIX D

STANDARD CALIBRATION GRAPH FOR CURCUMIN

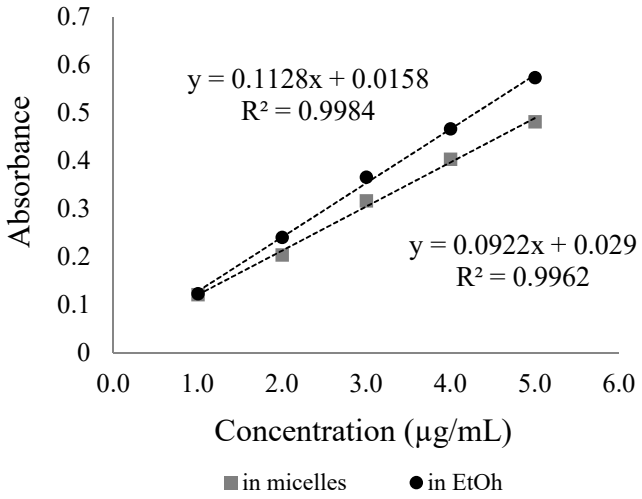

Figure D.1. Standard calibration curve of free curcumin and cur-P123 micelles.

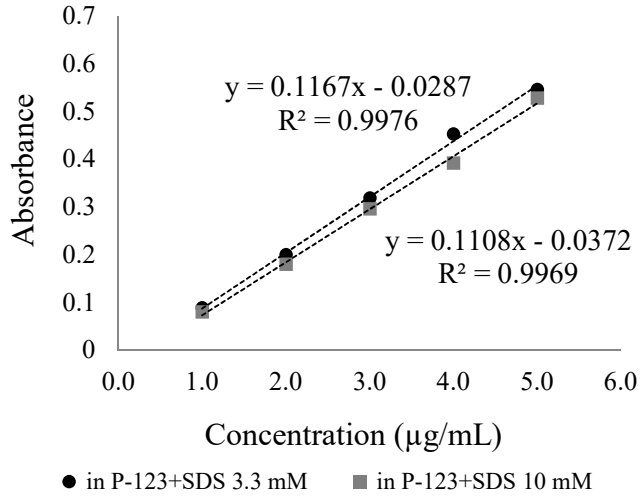

Figure D.2. Standard calibration curve of SDS modified cur-P123 micelles.

VITA

Nüket ZEYBEK

Education:

2017-2022: Ph.D. Biotechnology and Bioenginerring Department, Bioengineering PhD Program, Izmir, Turkey.
Thesis Title: Xylan Based Composite Nanoparticles and Biofoams for Drug Delivery and Tissue Engineering
2014-2017: M.Sc. Izmir Institute of Technology, Biotechnology and Bioenginerring Department, Biotechnology Master's Program, Izmir, Turkey.
Thesis Title: Xylan Degradation Mechanism of Human Intestinal Bacteria.
2009-2014: B.Sc. Ege University, Science Faculty, Biology Department, Biology Majored in Fundamental and Industrial Microbiology, Izmir, Turkey.
Thesis Title: Characterization of Halophilic Fungus.

Scholarship:

YOK 100/2000 PhD Scholarship Program, 2017-2021

Publications/ Presentations

Polat M., **Zeybek N.**, Polat H. (2022) Biopolymeric Micelles in Drug Delivery Applications, Design and Use, Biopolymer Science and Technology-Applications in Pharma & Cosmetics, Jana S, Jana S (eds.), Wiley.

Polat H., **Zeybek N.**, Polat M. (2021) Tissue Engineering Application of Marine Based Materials, Marine Biomaterials Drug Delivery and Therapeutic Applications, Jana S, Jana S (eds.), Springer Nature.

Zeybek, N., Rastall, R.A., Buyukkileci, A.O. (2020). Utilization of xylan-type polysaccharides in co-culture fermentations of Bifidobacterium and Bacteroides species. Carbohydrate polymers, 236, 116076.

Zeybek N., Polat M., Polat H. (2019). Synthesis of Curcumin Loaded Xylan-Chitosan Composite Nanoparticles. In: Yelken G, Polat M, Tanoglu M (eds) The Proceedings of the 4th International Porous and Powder Materials Symposium and Exhibition 2019, pp 46-50.

Polat N., Büyükkileci AO. (2018). Xylan Degradation of Colonic Bacteria. COST Action FP1306 Annual Workshop & MC meeting, and 4th Workshop of COST Action FP1306, Thessaloniki, Greece (Oral Presentation).

Gökduran H., **Polat N.**, Polat H. (2018). Encapsulation of Therapeutic Agents within Xylan Nanoparticles for Colon Specific Delivery: Polymeric Micelle Templated Method, IZTECH, Turkey (Poster).

Türker Y., **Zeybek N.**, Polat H. (2018). Encapsulation of Therapeutic Agents within Xylan Nanoparticles for Colon Specific Delivery: Water in Oil Emulsion Method, IZTECH, Turkey (Poster).